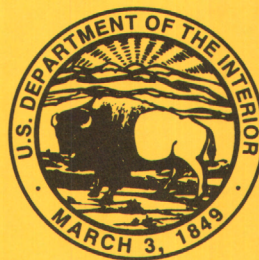


# EFFECTS OF SIMULATED GROUND-WATER PUMPING AND RECHARGE ON GROUND-WATER FLOW IN CAPE COD, MARTHA'S VINEYARD, AND NANTUCKET ISLAND BASINS, MASSACHUSETTS

---

U.S. GEOLOGICAL SURVEY  
Open-File Report 94-316

Prepared in cooperation with the  
MASSACHUSETTS DEPARTMENT OF ENVIRONMENTAL  
MANAGEMENT, OFFICE OF WATER RESOURCES



3 1822 0000719 5



USGS LAFAYETTE BRANCH LIBRARY  
700 CAJUNDOME BLVD  
LAFAYETTE LA 70506-3152



# EFFECTS OF SIMULATED GROUND-WATER PUMPING AND RECHARGE ON GROUND-WATER FLOW IN CAPE COD, MARTHA'S VINEYARD, AND NANTUCKET ISLAND BASINS, MASSACHUSETTS

By JOHN P. MASTERSON and PAUL M. BARLOW

---

U.S. GEOLOGICAL SURVEY  
Open-File Report 94-316

Prepared in cooperation with the  
MASSACHUSETTS DEPARTMENT OF ENVIRONMENTAL  
MANAGEMENT, OFFICE OF WATER RESOURCES



Marlborough, Massachusetts  
1994

USGS LAFAYETTE BRANCH LIBRARY  
700 CAJUNDOME BLVD  
LAFAYETTE LA 70506-3152



**U.S. DEPARTMENT OF THE INTERIOR**  
**BRUCE BABBITT, Secretary**

U.S. GEOLOGICAL SURVEY  
Gordon P. Eaton, Director

---

For additional information write to:

Chief, Massachusetts-Rhode Island District  
U.S. Geological Survey  
Water Resources Division  
28 Lord Road, Suite 280  
Marlborough, MA 01752

Copies of this report can be  
purchased from:

U.S. Geological Survey  
Earth Science Information Center  
Open-File Reports Section  
Box 25286, MS 517  
Federal Center  
Denver, CO 80225



# CONTENTS

Abstract .....	1
Introduction .....	2
Purpose and Scope .....	2
Approach.....	5
Previous Investigations .....	6
Acknowledgments .....	6
Hydrogeologic Setting.....	7
Cape Cod Basin .....	7
Geologic Setting .....	7
Hydrologic System .....	8
Aquifer Hydraulic Properties .....	9
Ground-Water Pumping.....	12
Martha's Vineyard Basin.....	22
Nantucket Island Basin .....	25
Effects of Simulated Ground-Water Pumping and Recharge on Ground-Water Flow in Cape Cod Basin .....	25
West Cape and East Cape Flow Cells .....	26
Modeling Approach.....	28
Description of Models .....	28
Grids.....	28
Hydraulic Properties .....	30
Boundary Conditions .....	31
Freshwater-Saltwater Flow Models.....	31
Freshwater Flow Models .....	31
Stresses and Stress Periods .....	32
Calibration.....	34
Response of the Freshwater-Saltwater Interface to Simulated Ground-Water Pumping and Recharge .....	44
Response of the Freshwater Flow Systems to Simulated Ground-Water Pumping and Recharge .....	48
Truro Flow Cell.....	53
Description of Model.....	55
Grid .....	55
Hydraulic Properties .....	55
Boundary Conditions .....	55
Stresses and Stress Periods .....	56
Calibration.....	56
Response of the Freshwater-Saltwater Flow System to Simulated Ground-Water Pumping and Recharge .....	60
Eastham and Wellfleet Flow Cells .....	64
Description of Models .....	65
Grids.....	65
Hydraulic Properties .....	65
Boundary Conditions .....	65
Stresses and Stress Periods .....	68
Calibration.....	68
Simulation of the Freshwater Flow Systems.....	68
Limitations of the Numerical Modeling Analyses for the Cape Cod Basin .....	71



# CONTENTS--Continued

Effects of Simulated Ground-Water Pumping and Recharge on Martha's Vineyard and Nantucket Island Basins.....	74
Summary and Conclusions.....	76
References Cited .....	79

## PLATE

[Plate is in pocket at back of report]

1. Hydrogeologic sections of glacial drift for the Cape Cod Basin, Massachusetts, 1994.

## FIGURES

1,2. Maps showing:	
1. Location of Cape Cod, Martha's Vineyard, and Nantucket Island Basins, Massachusetts .....	3
2. Location of flow cells, model boundaries, and water-table configuration on May 25-27, 1976, Cape Cod Basin, Massachusetts.....	4
3. Schematic diagram illustrating ice recession and lobe formation in southeastern Massachusetts .....	7
4,5. Maps showing existing and proposed public-supply wells in the:	
4. West Cape flow cell, Cape Cod Basin, Massachusetts .....	20
5. East Cape flow cell, Cape Cod Basin, Massachusetts.....	21
6,7. Maps showing:	
6. Water-table configuration on October 28-30, 1991, surficial geology, and location of modeled area, Martha's Vineyard Basin, Massachusetts.....	23
7. Water-table configuration on August 10-22, 1989, surficial geology, and location of modeled area, Nantucket Island Basin, Massachusetts.....	26
8,9. Maps showing grid and boundary conditions for the:	
8. West Cape flow cell, Cape Cod Basin, Massachusetts .....	27
9. East Cape flow cell, Cape Cod Basin, Massachusetts.....	29
10. Schematic section illustrating incorporation of hydraulic dynamics along the freshwater-saltwater boundary as represented in the SHARP model (A) into the MODFLOW model (B) for the West Cape and East Cape flow cells, Cape Cod Basin, Massachusetts.....	32
11,12. Maps showing model-calculated water-table configuration for the:	
11. West Cape flow cell, Cape Cod Basin, Massachusetts, 1989 .....	35
12. East Cape flow cell, Cape Cod Basin, Massachusetts, 1989.....	36
13. Sections showing measured chloride concentrations and model-calculated freshwater and saltwater zones at selected observation wells in the (A) West Cape and (B) East Cape flow cells, Cape Cod Basin, Massachusetts .....	37
14. Hydrogeologic section showing steady-state location of the model-calculated freshwater-saltwater interface for predevelopment and projected 2020 stress conditions for (A) column 84 of the West Cape flow model and (B) column 40 of the East Cape flow model, Cape Cod Basin, Massachusetts .....	45
15,16. Maps showing model-calculated location of fresh water overlying salt water and fresh water extending to bedrock for the:	
15. West Cape flow cell, Cape Cod Basin, Massachusetts .....	46
16. East Cape flow cell, Cape Cod Basin, Massachusetts.....	47
17-20. Maps showing model-calculated change in the altitude of the water-table configuration in the:	
17. West Cape flow cell from predevelopment to 1989, Cape Cod Basin, Massachusetts.....	49
18. West Cape flow cell from 1989 to 2020, Cape Cod Basin, Massachusetts .....	50

# CONTENTS--Continued

19.	East Cape flow cell from predevelopment to 1989, Cape Cod Basin, Massachusetts.....	51
20.	East Cape flow cell from 1989 to 2020, Cape Cod Basin, Massachusetts.....	52
21,22.	Maps showing:	
21.	Grid and boundary conditions for the Truro flow cell, Cape Cod Basin, Massachusetts .....	54
22.	Model-calculated water-table configuration for the Truro flow cell, Cape Cod Basin, Massachusetts, 1989.....	57
23.	Sections showing measured chloride concentrations and model-calculated freshwater and saltwater zones at selected observation wells in the Truro flow cell, Cape Cod Basin, Massachusetts .....	59
24,25.	Maps showing model-calculated change in the altitude of the water-table configuration in the Truro flow cell from:	
24.	Predevelopment to 1989, Cape Cod Basin, Massachusetts.....	61
25.	1989 to 2020, Cape Cod Basin, Massachusetts.....	62
26.	Section showing model-calculated position of the freshwater-saltwater interface along section <i>L-L'</i> in the Truro flow cell for predevelopment, 1975, 1989, and projected 2020 pumping and recharge rates, Cape Cod Basin, Massachusetts .....	63
27.	Graph showing model-calculated water-table altitude and position of the freshwater-saltwater interface at observation well TSW-89 for average recharge conditions and for simulation of a 5-year drought and 1989 pumping rates, Cape Cod Basin, Massachusetts .....	64
28,29.	Maps showing grid and boundary conditions for the:	
28.	Eastham flow cell, Cape Cod Basin, Massachusetts.....	66
29.	Wellfleet flow cell, Cape Cod Basin, Massachusetts.....	67
30,31.	Maps showing model-calculated steady-state water-table configuration for the:	
30.	Eastham flow cell, Cape Cod Basin, Massachusetts.....	69
31.	Wellfleet flow cell, Cape Cod Basin, Massachusetts.....	70
32,33.	Maps showing model-calculated change in the altitude of the water-table configuration for projected 2020 summer pumping rates and 180 days of zero recharge in the:	
32.	Martha's Vineyard Basin, Massachusetts .....	75
33.	Nantucket Island Basin, Massachusetts .....	76

## TABLES

1.	Estimates of hydraulic conductivity of stratified drift, as determined from analysis of aquifer tests, Cape Cod Basin, Massachusetts .....	10
2.	Hydraulic properties of stratified drift, as determined by use of the Cooper-Jacob method, Cape Cod Basin, Massachusetts .....	12
3-5.	Pumping rates of public-supply wells, Cape Cod Basin, Massachusetts, for 1975, 1989, and projected for 2020, represented in models of the:	
3.	West Cape flow cell .....	13
4.	East Cape flow cell.....	17
5.	Truro flow cell.....	19
6.	Pumping rates of public-supply wells for 1989 and projected for 2020, represented in models of Martha's Vineyard and Nantucket Island Basins, Massachusetts.....	24
7.	Vertical layering, horizontal hydraulic conductivity, and vertical conductance of calibrated models of the Cape Cod Basin, Massachusetts .....	30
8,9.	Average measured water levels for selected wells, Cape Cod Basin, Massachusetts, 1963-76, and model-calculated water levels for 1975, 1989, and projected for 2020 for the :	
8.	West Cape flow cell .....	39
9.	East Cape flow cell.....	40



# CONTENTS--Continued

10,11. Measured and model-calculated pond levels, Cape Cod Basin, Massachusetts, for selected ponds in the:	
10. West Cape flow cell .....	41
11. East Cape flow cell.....	42
12. Model-calculated streamflow for selected streams in the West Cape and East Cape flow cells, Cape Cod Basin, Massachusetts .....	43
13. Model-calculated water budgets for the West Cape and East Cape flow cells, Cape Cod Basin, Massachusetts .....	44
14. Average measured water levels for selected wells, 1963-76, and model-calculated water levels for 1975, 1989, and projected for 2020 for the Truro flow cell, Cape Cod Basin, Massachusetts .....	58
15. Model-calculated water budgets for the Truro flow cell, Cape Cod Basin, Massachusetts.....	60
16. Model-calculated water budgets for the Eastham and Wellfleet flow cells, Cape Cod Basin, Massachusetts .....	71
17. Average measured water levels for selected wells, 1963-76, measured pond levels, and model-calculated water levels and pond levels for average recharge rates and for a 5-year drought for the Eastham and Wellfleet flow cells, Cape Cod Basin, Massachusetts .....	72

## CONVERSION FACTORS AND VERTICAL DATUM

	Multiply	By	To obtain
acre		4,047	square meter
cubic foot per second (ft <sup>3</sup> /s)		0.02832	cubic meter per second
foot		0.3048	meter
foot per day (ft/d)		0.3048	meter per day
foot per day per foot [(ft/d)/ft]		0.3048	meter per day per meter
foot squared per day (ft <sup>2</sup> /d)		0.09290	meter squared per day
inch (in.)		25.4	millimeter
inch (in.)		2.54	centimeter
inch per year (in/yr)		25.4	millimeter per year
mile (mi)		1.609	kilometer
million gallons per day (Mgal/d)		0.04381	cubic meter per second
per foot (ft <sup>-1</sup> )		0.3048	per meter
square mile (mi <sup>2</sup> )		2.590	square kilometer

In this report, the unit of hydraulic conductivity is foot per day (ft/d), the mathematically reduced form of cubic foot per day per square foot [(ft<sup>3</sup>/d)/ft<sup>2</sup>]. The unit of transmissivity is foot per day (ft<sup>2</sup>/d), the mathematically reduced form of cubic foot per day per square foot times foot of aquifer thickness [(ft<sup>3</sup>/d)ft<sup>2</sup>×ft]. Chemical concentration is given in milligrams per liter. Milligrams per liter is a unit expressing the solute per unit volume (liter) of water. One milligram per liter is equivalent to 1,000 micrograms per liter. Density is given in grams per cubic centimeter (g/cm<sup>3</sup>).

**Sea Level:** In this report, "sea level" refers to the National Geodetic Vertical Datum of 1929—a geodetic datum derived from a general adjustment of the first-order level nets of the United States and Canada, formerly called Sea Level Datum of 1929.

# Effects of Simulated Ground-Water Pumping and Recharge on Ground-Water Flow in Cape Cod, Martha's Vineyard, and Nantucket Island Basins, Massachusetts

By John P. Masterson and Paul M. Barlow

## ABSTRACT

The management and protection of water resources of Cape Cod, Martha's Vineyard, and Nantucket Island water-resource planning basins are of concern to Massachusetts State and local officials because ground water is the sole source of drinking water in the basins. Significant growth in the number of summer and permanent residents has increased ground-water use during the last 30 years and placed stresses on the ground-water resources. In particular, there is concern over the extent of long-term declines in ground-water and pond levels and in the quantity of streamflow, as well as in the possibility of saltwater intrusion from the surrounding ocean. The effects of simulated ground-water pumping and recharge on the surface- and ground-water hydrology were assessed for the Cape Cod, Martha's Vineyard, and Nantucket Island Basins. Five flow cells of the Cape Cod Basin were assessed—the West Cape, East Cape, Eastham, Wellfleet, and Truro flow cells. These effects are reported as (1) changes in water-table altitudes in the three basins, (2) changes in pond altitudes and streamflow for selected ponds and streams of the Cape Cod Basin, (3) changes in the sources and sinks of water in the Cape Cod Basin, and (4) changes in the position of the freshwater-saltwater interface in the West Cape, East Cape, and Truro flow cells of the Cape Cod Basin.

Transient, three-dimensional, finite-difference models were developed to simulate freshwater and saltwater flow in the West Cape, East Cape, and Truro flow cells. Model results indicate little change in the position of the freshwater-saltwater interface in the West Cape and East Cape flow cells for ground-water pumping and recharge conditions similar to those that

occurred in the basin from predevelopment (assumed to have ended in 1950) to 1989, and for those estimated to occur from 1989 to 2020. Increases in pumping in the Truro flow cell also had a negligible effect on the position of the freshwater-saltwater interface except near the three areas of ground-water pumping in the flow cell.

Transient, three-dimensional, finite-difference models also were developed to simulate freshwater flow in the West Cape, East Cape, Wellfleet, and Eastham flow cells for the period from predevelopment to the year 2020. Total average declines in the water table at 32 observation wells in the West Cape flow cell and 19 observation wells in the East Cape flow cell are 1.8 and 2.9 feet, respectively, for the simulation period. Water-table altitudes range from 0 to nearly 75 feet in the West Cape flow cell and from 0 to nearly 45 feet in the East Cape flow cell. Declines in the average water levels of ponds during the simulation period are less than those at observation wells because of the greater storage capacity of the ponds than of the surrounding aquifer material. The average depletion in the rate of streamflow at the gaging points of eight of the largest streams in the West Cape and East Cape flow cells simulated in the models in the year 2020 was 14 percent of the model-calculated predevelopment streamflow in the rivers.

Total sources and sinks of fresh water to the West Cape and East Cape flow cells increase from predevelopment flow conditions to the year 2020 because the total amount of ground-water pumping and subsequent wastewater return flow to each system increases with time. The source of ground-water pumpage from the flow cells is fresh water removed from storage in the



aquifers and decreased rates of freshwater discharge to streams and saltwater boundaries of the flow cells. Sources and sinks of water to the Eastham and Wellfleet flow cells have not changed and are not projected to change significantly with time because there is no large-scale pumping in the flow cells for public supply.

Declines in the altitude of the water table were reported for Martha's Vineyard and Nantucket Island Basins for conditions of 180 days of no recharge for projected 2020 in-season ground-water pumping rates. Drawdowns were largest at the pumping centers. The largest decline for the Martha's Vineyard Basin was 2.5 feet near the proposed Manter site in Tisbury. The largest decline for the Nantucket Island Basin was 1.9 feet near the Wannacommet well field.

## INTRODUCTION

The peninsula of Cape Cod and the islands of Martha's Vineyard and Nantucket are in the southeastern-most part of Massachusetts (fig. 1). Cape Cod covers an area of 440 mi<sup>2</sup> that extends into the Atlantic Ocean and is separated from the mainland by a sea-level canal. Martha's Vineyard is about 5 mi south of the southwestern part of Cape Cod, and Nantucket Island is about 15 mi south of the central part of Cape Cod. Martha's Vineyard covers 95 mi<sup>2</sup> and Nantucket Island covers 46 mi<sup>2</sup>.

Ground water is the principal source of fresh water for domestic, industrial, and agricultural use on Cape Cod, Martha's Vineyard, and Nantucket Island Basins. In addition, the discharge of water from the aquifer supports freshwater ponds and streams that are important habitats for rare plants and fish spawning and maturation. Water is withdrawn from shallow sand and gravel aquifers that are susceptible to saltwater intrusion and to contamination from anthropogenic sources.

Six ground-water flow cells were delineated for Cape Cod (fig. 2), each of which is hydraulically distinct under natural hydrologic conditions (LeBlanc and others, 1986). These six flow cells are the West Cape, East Cape, Eastham, Wellfleet, Truro, and Provincetown flow cells. Martha's Vineyard and Nantucket Island each consist of a single, shallow principal flow system.

Under Massachusetts Law 313 CMR 2.00, the Massachusetts Department of Environmental Management, Office of Water Resources (MOWR), is responsible for developing management plans for the efficient and environmentally sound use of water for the State's 27 water-resource planning basins. These basins are designated by the MOWR and typically coincide with existing river basins. The Cape Cod, Martha's Vineyard, and Nantucket Island Basins are unique in that they are distinct hydrologic systems bounded by salt water rather than topographic divides. Therefore, the Cape Cod, Martha's Vineyard, and Nantucket Island Basins are of particular concern because ground water is the sole source of drinking water to residents in those basins and because significant growth in the number of summer and permanent residents has resulted in the increased use of water during the last 30 years. Federal, State, and local officials responsible for managing and protecting water resources are concerned that with increased ground-water pumping, water-table and pond altitudes will decline, ground-water discharge to streams will decrease, and saltwater intrusion will occur. In response to this concern, the U.S. Geological Survey (USGS), in cooperation with the MOWR, began an investigation in 1989 to assess the effects of changing ground-water pumping and recharge to the surface- and ground-water hydrology of Cape Cod, Martha's Vineyard, and Nantucket Island Basins.

## Purpose and Scope

The purpose of this report is to assess the effects of simulated ground-water pumping and recharge on ground-water flow of Cape Cod, Martha's Vineyard, and Nantucket Island Basins. These effects are reported as (1) changes in the water-table altitudes in the three basins; (2) changes in pond altitudes and streamflow for selected ponds and streams, respectively, of Cape Cod Basin; (3) changes in sources and sinks of water in Cape Cod Basin; and (4) changes in the position of the interface between fresh water and salt water in the West Cape, East Cape, and Truro flow cells of Cape Cod Basin.

This report describes the hydrogeology of the Cape Cod Basin and the development and application of numerical ground-water-flow models for five flow cells of Cape Cod: the West Cape, East Cape, Eastham, Wellfleet, and Truro flow cells. Because water in the Provincetown flow cell is of poor quality, it is not used

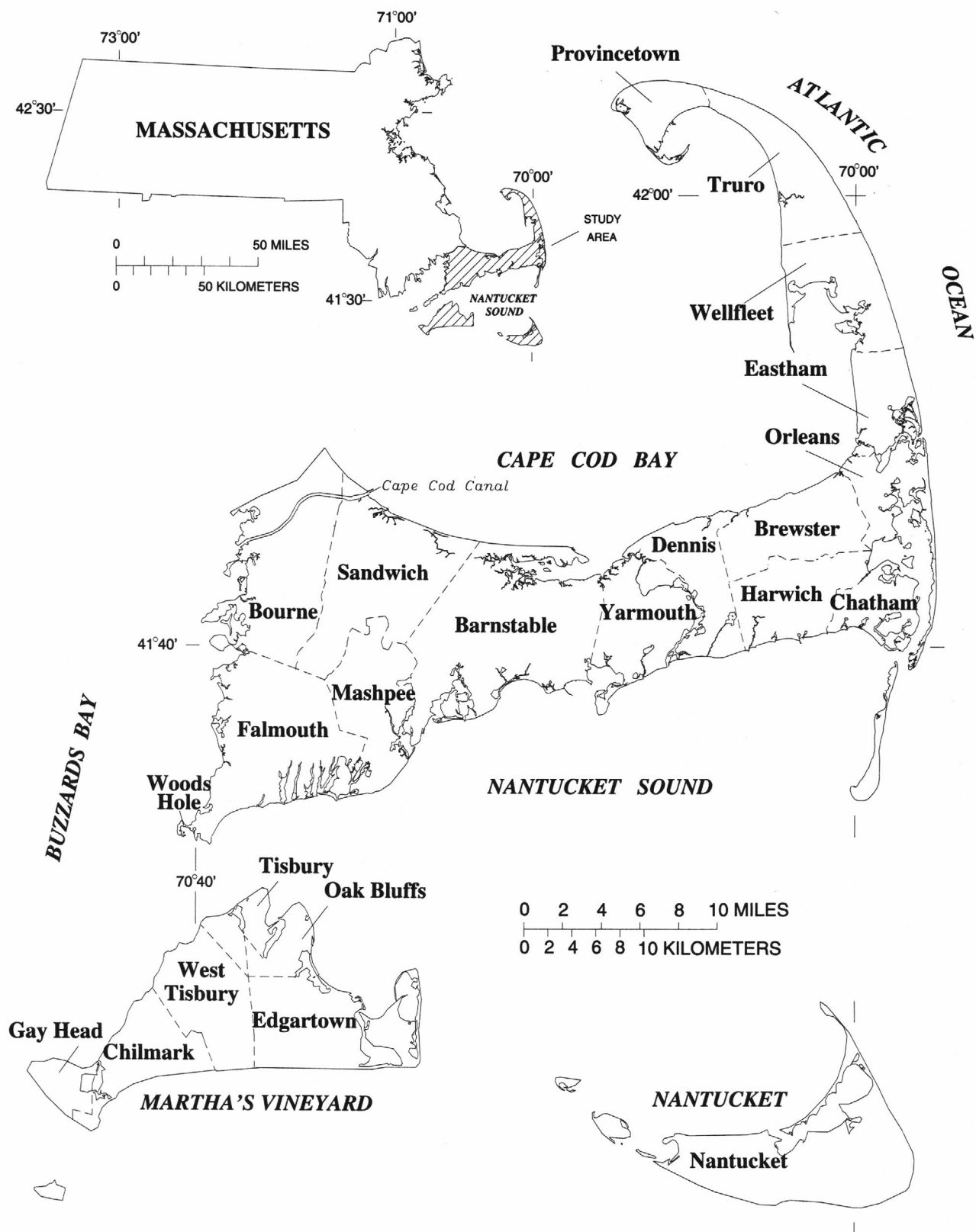


**Figure 1.** Location of Cape Cod, Martha's Vineyard, and Nantucket Island Basins, Massachusetts.





for public-water supplies, and no analysis of this flow cell is provided. Ground-water-flow models that simulate freshwater and saltwater flow were developed for the West Cape, East Cape, and Truro flow cells of Cape Cod. Flow models that simulate only freshwater flow were developed for the West Cape, East Cape, Eastham, and Wellfleet flow cells. Each of these seven models is a three-dimensional, transient, finite-difference ground-water-flow model. The models developed for the West Cape, East Cape, and Truro flow cells simulate ground-water pumping and recharge conditions similar to those that existed during the period before large-scale development up to those conditions that existed in 1989. The models also simulate conditions that are projected to occur through the year 2020. The models developed for the Eastham and Wellfleet flow cells simulate only natural hydrologic conditions because there are currently no large-capacity wells in these two flow cells.

This report also describes the hydrology of Martha's Vineyard and Nantucket Island Basins and the development of two-dimensional, finite-difference numerical flow models that simulate changes in the altitude of the water table. Application of these models was used to estimate declines in the altitude of the water table near public-supply wells on Martha's Vineyard and Nantucket Island for ground-water pumping equal to that which is projected for the year 2020.

Numerical flow models developed during this investigation provide information regarding regional-scale behavior of the ground-water-flow cells, including regional movement of the interface separating the freshwater- and saltwater-flow systems. Although detailed analyses of local hydrologic conditions were beyond the scope of the investigation, the flow models may serve as starting points for more detailed modeling investigations of smaller areas of the flow cells.

## Approach

Effects of simulated ground-water pumping and recharge to each of the three ground-water basins were determined using available hydrogeologic data and previously developed ground-water-flow models for each basin, as well as the amounts of current and projected future ground-water use in each basin. Because the annual pumping of ground water on Cape Cod is much greater than that on Martha's Vineyard and Nantucket

Island, there is a greater need for assessing the effects of changing stress conditions in the Cape Cod flow system than in the Martha's Vineyard or Nantucket Island flow systems. The effects of changing stress conditions in the Cape Cod flow cells were assessed by use of three-dimensional, transient, ground-water-flow models. The effects of changing stress conditions in the Martha's Vineyard and Nantucket Island flow systems were assessed only by use of simple, two-dimensional finite-difference models, called change models, in which declines in the altitude of the water table were determined for simulated pumping conditions that are projected to occur during summer months (June, July, and August) in the year 2020. Two-dimensional change models were used to evaluate these two flow systems because there was not enough hydrogeologic information available for the island basins to develop calibrated, three-dimensional, ground-water-flow models.

Of the five flow cells of Cape Cod, the West Cape and East Cape flow cells have had the greatest amount of domestic, industrial, and agricultural development within them, and consequently, the largest amount of ground-water use. Two flow models were developed for each of these two flow cells to assess the effects of changing stress conditions. The first flow model developed for each flow cell was a transient, three-dimensional, finite-difference model that simulates freshwater and saltwater flow separated by a sharp interface (referred to in the remainder of the report as the SHARP models) (Essaid, 1990). The SHARP models were used to assess the response of the boundary between the freshwater- and saltwater-flow systems to changing stress conditions. The SHARP models provide estimates of the location of the interface between fresh water and salt water and of the rate of discharge of fresh water to zones of the aquifer that contain salt water. Because the SHARP models indicated little movement of the interface between fresh water and salt water for the stress conditions simulated, it was assumed subsequently that a static interface exists between the freshwater and saltwater zones of the aquifer. The calculated location of the freshwater-saltwater interface and rate of discharge to zones of the aquifer that contain salt water were then used as lateral boundary conditions for freshwater-flow models of the West Cape and East Cape flow cells. The freshwater-flow models are transient, three-dimensional, finite-difference models that use the USGS modular ground-water-flow computer model



(McDonald and Harbaugh, 1988); they are referred to in the remainder of the report as the MODFLOW models. Freshwater-flow models were developed for the West Cape and East Cape flow cells because they require less computational effort than the SHARP models and may be more easily applied to the analysis of the effects of ground-water pumping on the flow systems than the computationally intensive SHARP models.

The Truro flow cell is the smallest of the five flow cells of Cape Cod that are used for water supply and is the only source of water for the communities of Truro and Provincetown. Although the sand and gravel aquifer that constitutes the Truro flow cell extends to bedrock, the freshwater-flow system is bounded at depth by the transition zone between fresh water and underlying salt water (Guswa and LeBlanc, 1985; LeBlanc and others, 1986). Contamination of public-water supplies by saltwater intrusion caused by ground-water pumping has been recorded at the Knowles Crossing well field, located 1,500 ft from Cape Cod Bay (LeBlanc and others, 1986). Evidence of saltwater intrusion precludes the assumption of a static interface between fresh water and salt water and the use of MODFLOW for the analysis of changing stress conditions in this flow cell. Consequently, changing stress conditions in the flow cell were evaluated by means of the SHARP model alone.

The Eastham and Wellfleet flow cells currently (1994) do not have any large capacity wells, and less data are available on the hydrogeology of these flow cells than for the West Cape, East Cape, or Truro flow cells. Consequently, a simpler modeling approach was used for the analysis of these two flow cells than was used for the West Cape, East Cape, or Truro flow cells. Freshwater (MODFLOW) models were developed to simulate ground-water flow in each of these flow cells. These models simulate predevelopment flow conditions in the flow cells—conditions that are assumed to exist at this time (1994). Users of these models are urged to review the section “Limitations of Numerical Modeling Analysis for the Cape Cod Basin” prior to applying the models to any assessment of the flow cells.

## Previous Investigations

The basin-wide hydrogeology of Cape Cod has been described by Strahler (1972), Ryan (1980), and LeBlanc and others (1986). A detailed summary of the geology of Cape Cod is provided by Oldale and Barlow (1986). The hydrogeology of Martha's Vineyard and Nantucket Island have been described by Delaney (1980) and Walker (1980), respectively. More recently, the hydrogeology of Nantucket Island has been described by Horsley Witten Hegemann, Inc. (1990).

In addition to these basin-wide studies, recent hydrogeologic investigations of the West Cape flow system have been reported by LeBlanc (1984a and 1984b), Barlow (1994), and Barlow and Hess (1993), of the East Cape flow cell by Johnson (1990), of the Eastham flow cell by Barlow (1994), and of the Truro flow cell by LeBlanc (1982) and Cape Cod Planning and Economic Development Commission (1989).

Numerical models of ground-water flow were developed previously by Guswa and LeBlanc (1985) for the West Cape, East Cape, Eastham, Wellfleet, and Truro flow cells and by Barlow (1994) for the Eastham and part of the West Cape flow cells. The flow models developed by Guswa and LeBlanc (1985) used a modified version of the three-dimensional flow model of Trescott (1975) that solved for the steady-state position of the interface between fresh water and salt water. The models of Guswa and LeBlanc (1985) were not used in this investigation because they cannot simulate (1) transient flow conditions, (2) ground-water flow in the saltwater zones of the aquifer, or (3) freshwater discharge to saltwater zones of the aquifer such as occurs beneath Cape Cod Bay.

## Acknowledgments

The authors thank several individuals who provided data or assisted in the acquisition of data during this investigation: William Wilcox, Martha's Vineyard Commission; Tony Maevisky, USGS (retired); Joseph Bergin, Massachusetts Division of Fisheries and Wildlife; James Cook, Provincetown Water Department; and facilities personnel at the Falmouth, Hyannis, Otis, and Chatham wastewater-treatment facilities.

## HYDROGEOLOGIC SETTING

### Cape Cod Basin

#### Geologic Setting

The Cape Cod Basin consists of glacial drift ranging in size from clay to boulders deposited during the glaciation of the Pleistocene Epoch. Ice sheets advancing south from northern New England and Canada transported eroded rock debris scoured from the underlying Paleozoic crystalline bedrock until reaching the southernmost extent at Martha's Vineyard and Nantucket Island.

During the late Wisconsinan stage of the Pleistocene glaciation, the coalescing Buzzards Bay, Cape Cod Bay, and South Channel glacial lobes deposited the glacial drift that now comprises Cape Cod (fig. 3). The glacial drift overlies an igneous and metamorphic basement complex. The altitude of the top of this complex ranges from 100 ft below sea level near Cape Cod Canal to more than 900 ft below sea level near the town of Provincetown (Oldale, 1969). A thin veneer of compact basal till was deposited on the bedrock as the ice sheets advanced south.

Hydrogeologic sections of glacial drift were made for eight north-south trending transects and one east-west trending transect across the Cape Cod Basin to characterize the vertical and spatial distribution of grain sizes (pl. 1). Although lithologic variations over short distances can be extreme, the general trend in grain distribution is an overall decrease in grain size with depth.

Overlying the basal till are thick deposits of fine sand, silt, and clay that were deposited in a pro-glacial lake located in front of the retreating ice sheets that was dammed in the south by glacial-drift deposits of Martha's Vineyard and Nantucket Island. These fine sand, silt, and clay deposits vary in thickness and are as much as 200 ft thick in the eastern part of Cape Cod (Oldale, 1984).

As the melting ice sheets receded to what is now the northern and western shores of Cape Cod, isolated blocks of buried ice left by the receding glaciers melted to form depressions in which kettle ponds and marshes are located throughout the present-day Cape Cod. Extensive deposits of stratified drift were deposited on the fine-grained lake-bottom deposits by meltwater streams flowing from the Buzzards Bay and Cape Cod Bay glacial lobes during a period of ice standstill (fig. 3C). The stratified-drift deposits show a decrease in

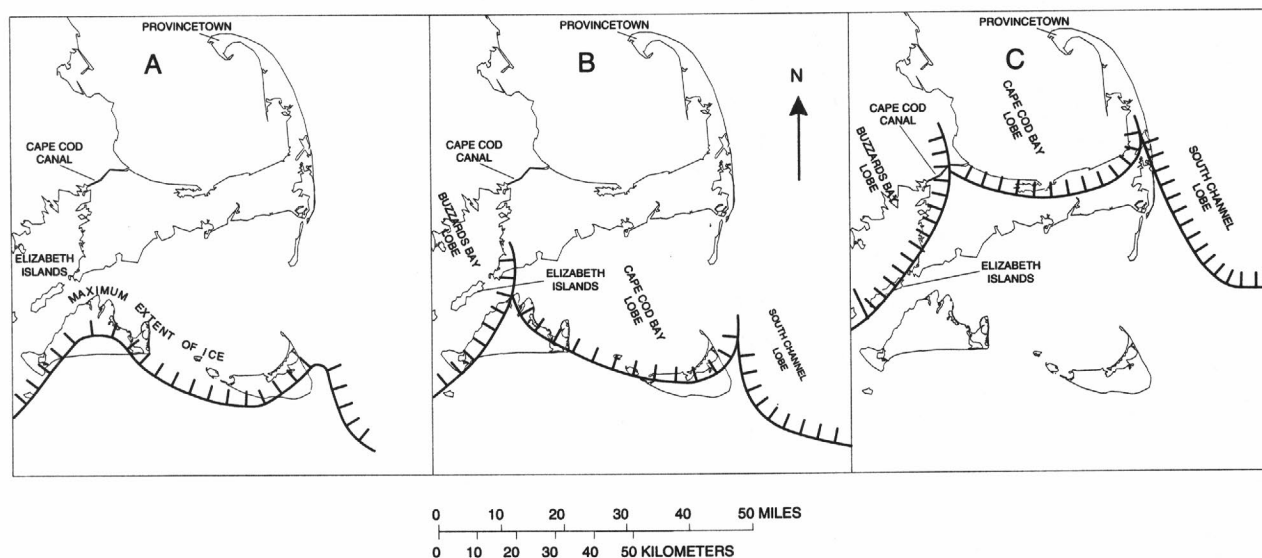


**Figure 3.** Ice recession and lobe formation in southeastern Massachusetts (modified from Oldale and Barlow, 1986). A, Approximately 21,000 to 16,000 years before present. B, Approximately 16,000 years before present. C, 15,000 years before present.



the percentage of coarse-grained material from the Buzzards Bay and Sandwich moraines south and southeastward to Nantucket Sound.

The Buzzards Bay and Sandwich glacial moraines (pl. 1), which border the western and northern shores of Cape Cod, were deposited during minor advances of the ice lobes that occurred during this period of standstill. The re-advancing lobes thrust outwash material on previously deposited outwash plain deposits, forming ridges of reworked outwash material that consist of unsorted sediment ranging from clay to boulders. The lobes then advanced over these ice-thrust ridges, depositing a veneer of pulverized rock or glacial till over the reworked outwash deposits (Oldale, 1984).

Between the retreating Cape Cod Bay glacial lobe and the Sandwich moraine, fine sand, silt, and clay were deposited in a pro-glacial lake occupying what is now the Cape Cod Bay. These fine-grained glaciolacustrine deposits rim the south shore of the Cape Cod Bay from Sandwich to Orleans. Localized topographic highs of unsorted sand, gravel, boulders, and lenses of fine silt and clay lie between the moraine and lacustrine deposits (pl. 1).

Outer Cape Cod consists of stratified drift from meltwaters flowing westward from the South Channel glacial lobe that was located east of the present day outer Cape Cod (fig. 3C). This outwash material was deposited as deltas prograded into the glacial lake occupying the area left by the retreating Cape Cod Bay lobe. These deposits consist of stratified fine-medium sand, medium-coarse sand and gravel with lenses of fine silt and clay that overlie the glaciolacustrine deposits consisting of fine sand, silt, and clay.

After the retreat of the last ice sheets, sea level rose during the Holocene Epoch, nearly 300 ft to its present-day altitude. The rise in sea level flooded the low-lying areas surrounding Cape Cod, including the pro-glacial lakes of Cape Cod Bay and Nantucket Sound. Post-glacial wave erosion and redeposition has had a pronounced effect on the shoreline of Outer Cape Cod (Oldale, 1984).

## Hydrologic System

The Cape Cod ground-water-flow system consists of six flow cells that are hydraulically distinct under present hydrologic conditions (Guswa and LeBlanc,

1985). These flow cells are bounded laterally by salt-water bodies that include Cape Cod Bay, Nantucket Sound, and the Atlantic Ocean (fig. 1). Fresh water is less dense than the surrounding salt water and forms lens-shaped bodies that are underlain by salt water. An interface separates the freshwater- and saltwater-flow systems within the unconsolidated deposits except in areas where the freshwater lens in the unconsolidated deposits is truncated by bedrock. This interface actually consists of a zone of mixing between the two flow systems that generally is thin in comparison to the total thickness of each aquifer.

Under natural hydrologic conditions, the freshwater- and saltwater-flow systems are assumed to be in hydrodynamic equilibrium—ground-water discharge from the freshwater system is balanced by aquifer recharge from precipitation, which results in a static interface between the two flow systems. Decreases in aquifer recharge and (or) increases in ground-water pumping may result in a decrease in the rate of coastal freshwater discharge and a consequent landward movement of the interface position.

The source of fresh water to the Cape Cod Basin is precipitation, which ranges from about 40 to 47 in/yr. An estimated 45 to 48 percent of this amount (or about 18 to 22 in/yr) recharges the ground-water-flow system (LeBlanc and others, 1986) and precipitation that is not recharged to the aquifer evaporates and is transpired by plants. Surface-water runoff is assumed to be negligible because of the highly permeable soils of Cape Cod.

The water-table configuration in the Cape Cod Basin is characterized by six oblong mounds, one in each flow cell (fig. 2). Water-table contours approximately follow the shape of the coast. Ground water flows radially from the centers of the mounds toward coastal discharge areas. The altitude of the water table fluctuates by as much as 7 ft because of seasonal changes in aquifer recharge and ground-water pumping (Letty, 1984). Annual water-table altitudes are highest during early spring when recharge is high and ground-water pumping is low. Water-table altitudes are lowest during late summer when ground-water recharge is low and water use is highest. Water-table fluctuations at observation wells vary in magnitude across Cape Cod and are dependent on the proximity of the observation wells to the coast and to nearby pumping wells. Annual water-table fluctuations are lowest near the coast where a nearly constant sea level keeps ground-water levels

from fluctuating substantially. Water-table fluctuations are highest near the center of each flow cell and near areas of pumping.

Most lakes and streams of Cape Cod are hydraulically connected to the ground-water-flow system, and lake levels and streamflow fluctuate in consonance with ground-water levels. In some areas, however, such as within the moraine deposits, discontinuous lenses of fine-grained material above the regional water table have caused perched ponds. Water levels in these perched ponds do not reflect the regional water table.

Many streams on Cape Cod are fed by ground-water discharge. Most of these streams are ungaged, and the total quantity of ground water that discharges from the flow cells to the streams is unknown. Continuous-measurement, USGS streamflow-gaging stations have been in operation on only two streams on Cape Cod. These have been on the Herring River in Harwich (1967-88) and Quashnet River in Falmouth (1989-94). Daily mean streamflow was  $10.0 \text{ ft}^3/\text{s}$  on the Herring River during 1967-88 and  $13.5 \text{ ft}^3/\text{s}$  on the Quashnet River during 1989-92. Streamflow is typically above average in the spring and below average during the summer and autumn. Streamflow on Cape Cod remains relatively constant during the year in comparison to streamflow of other areas of New England because of the large infiltration and storage capacity of the glacial outwash deposits that cover the basin and tend to reduce the effect of climatic variability on streamflow (Barlow and Hess, 1993).

Streamflow measurements have been made only sporadically or intermittently on a few other streams in the West Cape and East Cape flow cells. In the West Cape flow cell, measurements were made within 2,100 ft of the mouth of the Coonamessett, Backus, Bourne, and Childs Rivers on August 9, 1989, when ground-water levels and streamflow of the Quashnet River were near average conditions (Barlow and Hess, 1993). Streamflow was 8.2, 2.3, 1.5, and  $6.0 \text{ ft}^3/\text{s}$  for the Coonamessett, Backus, Bourne, and Childs Rivers, respectively, on this date (Socolow and others, 1991, p. 178-179). However, streamflow on these rivers is highly dependent on cranberry-bog activities, and the reported streamflow may be unrepresentative of average streamflow conditions. Only one streamflow measurement is recorded for the Mashpee River. This measurement was made 1,250 ft upstream from the mouth of the river on August 4, 1978, and was  $15.5 \text{ ft}^3/\text{s}$  (Socolow and others, 1991, p. 180). Streamflow on the Quashnet

River on the same date was  $19.3 \text{ ft}^3/\text{s}$ . Because the streamflow in the Quashnet River was much higher than average on the same date, it was assumed that streamflow on the Mashpee River also was much higher than average. In the East Cape flow cell, streamflow on the Stony Brook in Brewster was  $3.6 \text{ ft}^3/\text{s}$  in October 1978, at a point near the mouth of the river.

### Aquifer Hydraulic Properties

Horizontal and vertical hydraulic conductivity, specific yield, specific storage, storage coefficient, and porosity are needed for an analysis of the response of the Cape Cod ground-water-flow system to changing stress conditions. These hydraulic properties have been estimated for the flow system as part of this and previous investigations by analysis of aquifer tests, permeameter tests, and field tracer tests.

Estimates of horizontal and vertical hydraulic conductivity of stratified drift on Cape Cod, as determined during previous investigations by analysis of aquifer tests, are summarized in table 1. The estimates indicate that there is a general increase in horizontal hydraulic conductivity with increase in grain size, from about 40 ft/d for fine sand and silt to 300 ft/d for medium coarse sand and gravel. The exceptionally high value of horizontal hydraulic conductivity of 380 ft/d at well site Falmouth 214 reported by LeBlanc and others (1988) may be the result of a particularly uniform sediment of fine to medium sand with little percentage of other grain sizes. The ratio of vertical to horizontal hydraulic conductivity ranges from 1:1 to 1:30 for all sediment classes except fine sand and silt, for which the estimated ratio is 1:50 (table 1).

Little information is available on the hydraulic conductivity of the moraine and glaciolacustrine deposits of Cape Cod. Estimates of horizontal and vertical hydraulic conductivity of glaciolacustrine deposits from Eastham were reported by Barlow (1994). The horizontal and vertical hydraulic conductivity of these deposits varied depending on the percentage of clay present in the sample; however, the hydraulic conductivities for all of these glaciolacustrine deposits were 3 to 5 orders of magnitude less than those reported in table 1 for stratified drift.

Estimates of specific yield, specific storage, and storage coefficient of the aquifer have been made at only a few locations on Cape Cod. The storage coefficient is equal to the specific storage of the aquifer multiplied by

**Table 1.** Estimates of hydraulic conductivity of stratified drift, as determined from analysis of aquifer tests, Cape Cod Basin, Massachusetts

[ft/d, foot per day. --, no data. <, actual value is less than value shown]

Predominant grain size of tested interval	Aquifer test well	Latitude ° ' "	Longitude ° ' "	Horizontal hydraulic conductivity (ft/d)	Ratio of vertical to horizontal hydraulic conductivity	Source of data
Fine sand and silt.	Mashpee 108	41 36 06	70 30 29	40	1:50	Barlow and Hess (1993)
Fine sand.	Barnstable 406	41 39 13	70 22 15	160	1:30	Barlow (1994)
	Yarmouth 74	41 40 00	70 14 52	160	1:30	Do.
Fine to medium sand.	Wellfleet 41	41 54 00	69 58 42	180	1:3-1:5	Do.
	Yarmouth 176	41 39 16	70 11 48	200	--	Guswa and LeBlanc (1985)
	Falmouth 214	41 37 03	70 33 00	380	1:2-1:5	LeBlanc and others (1988)
Fine to coarse sand and gravel.	Truro 200	42 00 51	70 02 48	220	1:1-1:5	Guswa and Londquist (1976)
	Mashpee 108	41 36 06	70 30 29	240	1:3	Barlow and Hess (1993)
	Yarmouth 59	41 40 10	70 13 53	220	1:10	Barlow (1994)
	Yarmouth 129	41 40 22	70 14 19	240	1:3-1:5	Do.
Medium to coarse sand and gravel.	Orleans 37	41 45 16	69 59 39	300	<1:10	Guswa and LeBlanc (1985)

its saturated thickness. Analysis of aquifer tests in Truro by Guswa and Londquist (1976) and in Orleans by Guswa and LeBlanc (1985) indicate specific yields of 0.10 and 0.15, respectively. Palmer (1977) reports a range of specific yield of 0.13 to 0.26 based on four aquifer tests in Falmouth. Garabedian and others (1988) report a range in specific yield of 0.1 to 0.2 and a range of specific storage of  $4.4 \times 10^{-5}$  to  $8.7 \times 10^{-5}$  ft<sup>-1</sup> from the analysis of an aquifer test in Falmouth. Dufresne-Henry, Inc. (1990) reports a range of specific yield of 0.13 to 0.21 for an aquifer test at a well site in Mashpee, and Barlow and Hess (1993) report a specific yield of 0.25, a specific storage of  $1 \times 10^{-6}$  ft<sup>-1</sup>, and a storage coefficient of  $2 \times 10^{-4}$  for the aquifer at a nearby test site. These estimates of specific yield are similar to those reported for the stratified-drift sediments of Long Island, N.Y. of 0.10 to 0.26 (Perlmutter and Geraghty, 1963; Getzen, 1977; Lindner and Reilly, 1983).

Porosity was estimated for stratified drift at two sites in Falmouth using ground-water tracer experiments and laboratory tests of cored sediment samples. Estimates of porosity from the tracer tests range from 0.38 to 0.42 (Garabedian and others, 1988; LeBlanc and others, 1988; Barlow, 1989), whereas that of the cored samples

was 0.32 (Wolf, 1988). Porosity also was determined for fine to medium sand in Orleans. An average porosity of 0.34 was determined for five samples using laboratory volumetric measurements of cored samples (L.A. DeSimone, U.S. Geological Survey, written commun., 1992). These estimates are similar to those of 0.34 to 0.38 reported for the porosity of stratified drift on Long Island, N.Y. (Perlmutter and Leiber, 1970).

Horizontal hydraulic conductivity and specific yield of the stratified drift were estimated by analysis of 10 aquifer tests in the West Cape and East Cape flow cells. Data used in the analysis were from engineers' reports of aquifer tests done as part of the process required for development of a new water supply. The analysis was done to improve the existing data base of hydraulic conductivity and specific yield of the Cape Cod ground-water-flow system.

The Cooper-Jacob approximation to the Theis solution of radial flow to a well was used in the analysis. The approximation is applied subject to assumptions from Marsily (1986, p. 164-165): (1) the aquifer is infinite, homogeneous, and isotropic; (2) if the aquifer is unconfined, then drawdowns are small relative to the



saturated thickness of the aquifer; (3) hydraulic head does not vary in the vertical direction and water velocity is parallel to a horizontal, impermeable boundary; and (4) the pumped and observation wells fully penetrate the aquifer, the pumping rate of the well is constant, and the borehole radius of the pumped well is negligibly small. Although several of these assumptions were not strictly met during the tests, the Cooper-Jacob method is a widely applied analysis technique that should provide reasonable estimates of horizontal hydraulic conductivity and specific yield. A complete description of the Cooper-Jacob approximation is provided by Marsily (1986, p. 163-165).

In the analyses, measured drawdowns were corrected to account for unconfined conditions according to the method reported by Kruseman and de Ridder (1983, p. 107) and the following criterion was used to determine the time at which the Cooper-Jacob approximation was assumed valid (Marsily, 1986):

$$t \geq \frac{S_y r^2}{4Tu} \quad (1)$$

where

- $t$  is the time since start of test (days),
- $r$  is radial distance of observation well from pumped well (feet),
- $S_y$  is specific yield (dimensionless),
- $T$  is transmissivity (feet square per day), and
- $u$  is Theis' dimensionless time.

An upper limit of 0.02 was selected for the parameter  $u$  because Marsily (1986, p. 164) states that the error between the Cooper-Jacob approximation and the Theis solution is 0.5 percent at this limit. Two additional criteria were used to account for the effect of partial penetration of the pumped and observation wells to the parameter estimates. These criteria are (Neuman, 1974):

$$r \geq \frac{b}{\sqrt{\frac{K_v}{K_h}}} \quad (2)$$

and

$$t \geq \frac{10S_y r^2}{T} \quad (3)$$

where

- $b$  is saturated thickness of the aquifer near the well (feet),
- $K_v$  is vertical hydraulic conductivity of the aquifer (feet per day), and
- $K_h$  is horizontal hydraulic conductivity of the aquifer (feet per day).

The use of these two criteria is based on the results of Neuman (1974, p. 309), who found that the effect of partial penetration on drawdown in an unconfined aquifer disappears completely at distances from the pumped well greater than  $b/\sqrt{K_v/K_h}$  at times greater than  $10S_y r^2/T$ . The ratios of  $K_v/K_h$  used to assess the effects of partial penetrations ranged from 1:3 to 1:5 for fine-medium sand to 1:30 for fine sand. These values are based on the results of table 1.

Horizontal hydraulic conductivity was determined by dividing the transmissivity determined from the aquifer-test data by the saturated thickness of the aquifer at or near the site of the aquifer test. Because the pumped and observation wells did not fully penetrate the aquifer, a saturated thickness was estimated from available information. In the analysis, the saturated thickness of the aquifer was assumed to be the distance from the water table to an assumed impermeable boundary at the contact between overlying sand and gravel and underlying fine-grained sediments, such as silt and clay. The fine-grained sediments were assumed to act as confining units that do not yield water to the overlying sand and gravel during the aquifer tests.

Although 22 aquifer tests were analyzed using the above methodology, only the 10 reported in table 2 satisfied the three criteria of equations 1, 2, and 3 and had sufficient information to allow an estimate of the saturated thickness of the aquifer near the pumped well. Values of horizontal hydraulic conductivity determined from the 10 aquifer tests (table 2) are similar to those determined by previous investigators, and generally tend to increase with increasing grain size of the aquifer. Horizontal hydraulic conductivity estimated at wells Yarmouth 74 (180 ft/d) and Yarmouth 129 (220 ft/d) are within 13 percent of those determined for the aquifer at these two wells by Barlow (1994), who used a more comprehensive method of analysis than the Cooper-Jacob method, in which type curves were developed for each pumped and observation well pair (Neuman, 1974). The strong agreement between the hydraulic conductivities determined by the two

**Table 2.** Hydraulic properties of stratified drift, as determined by use of the Cooper-Jacob method, Cape Cod Basin, Massachusetts

[ft, foot; ft/d, foot per day; ft<sup>2</sup>/d, foot squared per day; gal/min, gallon per minute]

Predominant grain size of tested interval	Aquifer test well	Length of test (days)	Well discharge (gal/min)	Latitude ° ' "	Longitude ° ' "	Transmissivity (ft <sup>2</sup> /d)	Saturated thickness (ft)	Horizontal hydraulic conductivity (ft/d)	Specific yield
Fine sand.	Yarmouth 155	6	299	41 40 10	70 14 18	5,000	40	125	0.15
	Yarmouth 74	5	250	41 40 00	70 14 52	11,000	60	180	.02
Fine to coarse sand and gravel.	Dennis 200	7	204	41 42 54	70 10 03	13,000	40	325	.25
	Dennis 211	8	500	41 42 42	70 08 21	8,000	30	270	.17
	Barnstable 253	7	300	41 38 42	70 19 23	9,000	40	225	.20
	Yarmouth 129	5	246	41 40 22	70 14 19	12,000	55	220	.17
Medium to coarse sand and gravel.	Harwich 128	4	191	41 41 09	70 02 06	12,000	40	295	.08
	Dennis 225	6	271	41 42 53	70 08 25	12,000	65	185	.23
	Falmouth 177	6	350	41 35 44	70 32 04	18,000	50	360	.12
	Sandwich 282	5	505	41 42 04	70 44 28	32,000	100	320	.12

methods indicates that the Cooper-Jacob approximation and three criteria used in this investigation seem to be a valid estimation method for hydraulic conductivity of the Cape Cod ground-water-flow system.

Estimates of specific yield range from 0.02 to 0.25 and are highest for fine to medium sand and gravel to medium to coarse sand. The average value of specific yield determined for the 10 aquifer tests was 0.15.

### Ground-Water Pumping

Ground water is the principal source of fresh water for domestic, industrial, and agricultural use on Cape Cod. Public water-supply systems service communities in the West Cape, East Cape, and Provincetown flow cells. Water-supply needs for residents in the Wellfleet and Eastham flow cells, and most of the Truro flow cell are met by domestic wells. Pumping-well locations and pumping rates for 1975-76 were reported by Guswa and LeBlanc (1985) and pumping-well locations and pumping rates for 1989 were obtained directly from public-water suppliers of Cape Cod (tables 3-5; figs. 4 and 5). Projected pumping rates for the year 2020 were provided by the Massachusetts Office of Water Resources; these rates are based on 1989 estimates of future water needs. Agricultural and industrial pumpage have not been considered in this study because (1) they represent a small percentage of the total pumping, (2) daily demand information for pumping less than 0.1 Mgal/d

is not readily available, and (3) pumped water is typically returned to the aquifer within the same model node from which it is pumped.

Public-water supply systems began operation on Cape Cod as early as 1893. The total quantity of water pumped from the West Cape and East Cape flow cells increased substantially between 1975 and 1989; total pumpage is projected to continue to increase through the year 2020 as a result of the projected continuing increase in the number of permanent and summer residents throughout Cape Cod. Average daily demand increased by more than 40 percent between 1975 and 1989 in the West Cape flow cell (table 3) and by more than 70 percent between 1975 and 1989 in the East Cape flow cell (table 4). Average daily demands are projected to increase by about 100 percent between 1989 and 2020 in the West Cape and East Cape flow cells (tables 3 and 4). Most wells in the West Cape and East Cape flow cells are screened at depths less than 70 ft below sea level and are more than 1 mi inland of the coasts (figs. 4 and 5). Average daily demand for water pumped from the Truro flow cell actually decreased slightly from 1975 to 1989, but is projected to increase by more than 40 percent between 1989 and 2020 (table 5). Seasonal fluctuations in ground-water use are due to the substantial population increases during June, July, and August, resulting in average daily pumpage during the summer that is more than double that of the winter.

**Table 3.** Pumping rates of public-supply wells for 1975, 1989, and projected for 2020, represented in models of the West Cape flow cell, Cape Cod Basin, Massachusetts

[Map No.: Wells shown in bold are proposed wells; all other wells are existing. Location of wells shown in figure 4. Model node: Model grid shown in figure 8. Year and pumping rate: ADD, average daily demand; IN, inseason pumping rates from June through August; OFF, offseason pumping rates from September through May. Ab, abandoned well. No., number. --, no data]

Map No.	Well No.	Well Name	Model node			Year and pumping rate, in cubic feet per second						
			Layer	Row	Column	1975	1989	1989	1989	2020	2020	2020
						ADD	IN	OFF	ADD	IN	OFF	ADD
BARNSTABLE FIRE DISTRICT												
1	A1W228	Phinney's Lane	1	34	87	0.172	0.148	0.068	0.077	0.188	0.091	0.123
2	A1W370	Old Barns. Rd #2	2	38	90	.269	.148	.068	.077	.376	.182	.247
3	A1W416	Route 132 #3	2	36	84	--	.829	.380	.433	.502	.243	.329
4	--	Oak Street	1	34	78	--	--	--	--	.441	.213	.289
5	--	District Well #4	1	36	83	--	--	--	--	.350	.169	.229
Total .....						0.441	1.125	0.516	0.587	1.857	0.898	1.217
BARNSTABLE WATER COMPANY												
6	A1W300	Airport Well #1	2	41	92	--	0.389	0.219	0.248	1.300	0.633	0.855
7	A1W229	Hyannisport	2	48	84	0.210	.753	.425	.480	.648	.316	.515
8	A1W384	Simmons Pond	2	48	84	.966	1.580	.891	1.006	.908	.444	.515
	A1W377	Maher Well #1	2	44	92	1.165	.729	.411	.464	.648	.316	.542
	A1W385	Maher Well #2	2	44	92	.055	.839	.473	.534	.909	.444	.542
9	A1W386	Maher Well #3	2	44	92	.055	.839	.473	.534	.909	.444	.542
	A1W402	Mary Dunn #1	1	39	92	.072	.097	.055	.603	.648	.316	.427
	A1W383	Mary Dunn #2	1	39	92	.305	.948	.535	.325	.909	.444	.542
10	A1W387	Mary Dunn #3	1	39	91	.173	.022	.012	.014	.648	.316	.427
11	A1W403	Mary Dunn #4	1	39	91	.065	.510	.288	.328	.648	.316	.427
	A1W376	Straightway #1	4	47	84	.453	--	--	--	.909	.444	.600
	--	Straightway #2	2	46	84	--	--	--	--	.909	.444	.600
13	--	Mary Dunn #5	1	38	92	--	--	--	--	.648	.316	.426
14	--	Mary Dunn #6	1	38	92	--	--	--	--	.648	.316	.426
	--	Airport	2	40	91	--	--	--	--	.909	.444	.600
	--	Mary Dunn #7	1	39	92	--	--	--	--	.648	.316	.600
	--	Mary Dunn #8	1	39	92	--	--	--	--	.648	.316	.442
Total .....						3.519	6.706	3.782	4.536	13.494	6.585	9.028
BOURNE WATER DISTRICT												
15	BHW1	County Rd #1	2	19	26	0.084	0.209	0.102	0.116	0.418	0.148	0.238
	BHW2	--	2	19	26	.084	.208	.102	.116	.418	.148	.238
	BHW3	--	1	19	26	.084	.290	.102	.116	.418	.148	.238
	BHW136	--	1	19	26	.084	.208	.102	.116	.418	.148	.238
	16	BHW137	Route 28A #2	2	30	25	.288	.278	.136	.155	.558	.197
17	BHW199	Bourne Forest #3	1	19	29	.239	.361	.177	.201	.725	.256	.412
18	BHW233	Bourne Forest #4	2	18	28	.079	.389	.191	.217	.781	.276	.444
19	--	Route 28A #5	1	31	25	--	.528	.260	.294	1.060	.374	.603
20	--	Route 28A #6	2	20	27	--	--	--	--	.732	.286	.441
Total .....						0.942	2.471	1.172	1.331	5.528	1.981	3.169



**Table 3.** Pumping rates of public-supply wells for 1975, 1989, and projected for 2020, represented in models of the West Cape flow cell, Cape Cod Basin, Massachusetts--*Continued*

Map No.	Well No.	Well Name	Model node			Year and pumping rate, in cubic feet per second						
			Layer	Row	Column	1975	1989	1989	1989	2020	2020	2020
						ADD	IN	OFF	ADD	IN	OFF	ADD
CENTERVILLE/OSTERVILLE WATER DISTRICT												
21	A1W107	McShane #1	2	46	67	0.400	0.008	0.003	0.005	0.889	0.390	0.555
	--	McShane #2	2	46	67	--	.024	.009	.011	.889	.390	.555
22	A1W160	Arena #3	1	45	65	.133	--	--	--	--	--	--
	A1W158	Arena #3	1	45	67	.133	.031	.012	.015	.556	.244	.348
	A1W159	Arena #4	2	45	67	.133	.159	.061	.077	.556	.244	.348
23	A1W373	Lumbert Mill #5	2	42	72	.031	.407	.156	.201	.332	.146	.208
	A1W259	Lumbert Mill #9	1	42	72	.471	.781	.300	.387	.471	.207	.295
24	A1W368	Craigville #7	2	46	81	.119	.374	.144	.186	.386	.169	.199
	A1W227	Craigville #8	1	46	81	.071	--	--	--	--	--	--
	A1W226	Craigville #11	1	46	81	.048	.622	.239	.310	.247	.108	.196
25	A1W249	Davis #10	1	45	66	.371	.686	.263	.340	.355	.156	.295
26	A1W371	Murray #12	1	38	70	.170	.622	.239	.310	.386	.169	.242
	A1W372	Murray #13	1	38	70	.156	.526	.202	.263	.386	.169	.242
27	--	Hayden #14	1	40	61	--	1.212	.466	.603	.780	.342	.485
	--	Hayden #15	1	40	61	--	.311	.119	.155	.332	.146	.214
	--	Hayden #17	1	40	61	--	1.060	.407	.527	.780	.342	.485
28	--	Harrison #16	1	31	63	--	1.148	.441	.573	.556	.244	.348
	--	CO-16	1	31	63	--	--	--	--	.780	.342	.488
29	--	CO-19	2	30	64	--	--	--	--	1.152	.508	.725
30	--	CO-19-83	2	39	60	--	--	--	--	.780	.342	.488
31	--	CO40-8	2	40	59	--	--	--	--	.780	.342	.488
32	--	CO41-89	2	39	59	--	--	--	--	.780	.342	.488
Total .....						2.236	7.971	3.061	3.963	12.173	5.342	7.692
COTUIT FIRE DISTRICT												
33	A1W251	Electric Station	2	45	57	0.112	0.273	0.116	0.128	0.292	0.139	0.190
34	A1W369	Electric Station	1	45	56	.113	.243	.104	.139	.292	.139	.190
35	A1W224	Electric Station	1	48	57	.046	.243	.104	.128	.174	.083	.095
36	A1W59	Electric Station	1	44	57	.007	.304	.129	.155	.292	.139	.190
37	--	C-130/28	3	43	53	--	--	--	--	.609	.289	.396
Total .....						0.278	1.063	0.453	0.550	1.659	0.789	1.061
FALMOUTH DEPARTMENT OF PUBLIC WORKS, WATER, AND SEWER COMMISSION												
38	--	Long Pond	2	52	18	0.692	0.837	0.447	0.524	1.536	0.987	1.170
	--	Long Pond	2	53	18	.692	.837	.447	.524	1.536	.987	1.170
	--	Long Pond	2	54	18	.692	.837	.447	.524	1.536	.987	1.170
	--	Long Pond	2	55	18	.692	.837	.447	.524	1.536	.987	1.170
	--	Long Pond	2	53	19	.692	.837	.447	.524	1.536	.987	1.170
	--	Long Pond	2	54	19	.692	.837	.447	.524	1.536	.987	1.170
39	--	Fresh Pond	2	51	37	--	1.831	.978	1.145	.853	.548	.650
40	--	Coonamessett	1	44	28	--	1.460	0.779	0.913	0.853	0.548	0.650
41	--	F6D	2	50	23	--	--	--	--	.350	.225	.267
42	--	F-4D	1	42	25	--	--	--	--	.350	.225	.267
43	--	F-F3	1	50	38	--	--	--	--	.350	.225	.267
44	--	F-8A	2	52	38	--	--	--	--	.350	.225	.267
45	--	Beebe Woods	1	58	15	--	--	--	--	.350	.225	.267
Total .....						4.152	8.313	4.439	5.202	12.672	8.143	9.655

**Table 3.** Pumping rates of public-supply wells for 1975, 1989, and projected for 2020, represented in models of the West Cape flow cell, Cape Cod Basin, Massachusetts--*Continued*

Map No.	Well No.	Well Name	Model node			Year and pumping rate, in cubic feet per second						
			Layer	Row	Column	1975	1989	1989	1989	2020	2020	2020
						ADD	IN	OFF	ADD	IN	OFF	ADD
HIGHWOOD WATER COMPANY, MASHPEE												
46	M1W32	Wading Place	2	58	48	0.048	0.119	0.039	0.062	0.150	0.057	0.088
47	M1W35	Rock Landing #2	2	59	46	.150	.357	.117	.183	.600	.229	.362
	--	Rock Landing #3	2	59	46	--	.477	.156	.248	.600	.229	.362
48	--	High Wood #3	1	50	43	--	--	--	--	.600	.229	.362
Total .....						0.198	0.953	0.312	0.493	1.950	0.744	1.174
MASHPEE WATER DISTRICT												
49	--	T-4	1	45	51	--	--	--	--	0.735	0.294	0.441
50	--	P-1	1	51	41	--	--	--	--	.735	.294	.441
Total .....						--	--	--	--	1.47	0.588	0.882
OTIS AIR FORCE BASE WATER SYSTEM												
51	BHW23	Well G	3	33	31	0.507	Ab	Ab	Ab	Ab	Ab	Ab
52	SDW155	Well J	1	33	40	.433	0.890	0.630	0.634	0.753	0.526	0.602
53	--	Airport	2	38	43	--	--	--	--	.269	.187	.214
Total .....						0.940	0.890	0.630	0.634	1.022	0.713	0.816
SANDWICH WATER DISTRICT												
54	SDW27	BS #2	2	13	56	0.104	0.690	0.390	0.449	0.515	0.349	0.404
	SDW37	BS #3	2	13	56	.320	.660	.380	.433	.515	.349	.404
55	--	Pinkham #4	2	25	55	--	.420	.230	.279	.715	.485	.562
	--	Pinkham #6	2	25	55	--	.560	.330	.371	.715	.485	.562
56	SDW208	Pinkham #5	1	29	42	--	.380	.220	.248	.715	.485	.562
57	SDW249	Boiling Springs	2	6	50	.031	--	--	--	--	--	--
	SDW250	Boiling Springs	2	6	50	.031	--	--	--	--	--	--
58	S23	--	2	29	57	--	--	--	--	.715	.485	.562
59	S13	--	2	20	63	--	--	--	--	.715	.485	.562
	--	Boiling Springs(A)	1	13	56	--	--	--	--	.715	.485	.562
Total .....						0.486	2.710	1.550	1.780	5.320	3.608	4.180
SOUTH SAGAMORE WATER DISTRICT												
60	BHW232	Route 6A Tub Well	2	5	46	0.124	0.304	0.129	0.155	0.366	0.202	0.243
Total .....						0.124	0.304	0.129	0.155	0.366	0.202	0.243
YARMOUTH WATER DEPARTMENT												
61	YAW103	Main Station	2	35	104	0.223	0.918	0.418	0.528	0.887	0.410	0.854
62	YAW41	Higgins Crow PS #1	1	38	97	--	.243	.111	.139	.222	.103	.297
63	YAW42	Higgins Crow PS #2	1	37	98	.248	.324	.147	.186	.308	.143	.297
	YAW43	Higgins Crow PS #3	1	37	98	.266	.378	.172	.217	.370	.171	.297

**Table 3.** Pumping rates of public-supply wells for 1975, 1989, and projected for 2020, represented in models of the West Cape flow cell, Cape Cod Basin, Massachusetts--*Continued*

Map No.	Well No.	Well Name	Model node			Year and pumping rate, in cubic feet per second						
			Layer	Row	Column	1975	1989	1989	1989	2020	2020	2020
						ADD	IN	OFF	ADD	IN	OFF	ADD
YARMOUTH WATER DEPARTMENT--Continued												
64	YAW64	Long Pond #4	2	43	107	.345	.324	.147	.186	.308	.143	.217
	YAW5	Long Pond #5	2	43	107	.309	.351	.160	.201	.370	.171	.217
65	YAW53	N. Main St. #6	2	40	112	.223	.270	.123	.155	.222	.103	.192
	YAW146	N. Main St. #7	2	40	112	.238	.243	.111	.139	.222	.103	.192
	YAW144	N. Main St. #8	2	40	112	.256	.270	.123	.155	.222	.103	.192
	YAW54	N. Main St. #9	2	40	112	.467	.594	.270	.340	.530	.245	.192
66	YAW61	Forest Rd. #10	2	41	104	.279	.297	.135	.170	.265	.123	.170
67	YAW63	Forest Rd. #11	2	42	104	.208	.324	.147	.186	.265	.123	.170
68	YAW193	Chickadee Ln. #13	2	43	100	--	.459	.234	.263	.401	.185	.285
	YAW58	Chickadee Ln. #18	2	43	100	.310	.459	.209	.294	.444	.205	.285
	YAW194	Chickadee Ln. #19	2	43	100	--	.432	.197	.248	.401	.185	.340
69	YAW128	Higgins Crow #14	2	43	97	.125	.378	.172	.217	.308	.143	.198
70	YAW126	N. Dennis Rd. #15	2	37	110	.045	.459	.290	.263	.444	.205	.284
	YAW127	N. Dennis Rd. #16	2	37	110	.027	.513	.234	.294	.444	.205	.284
71	YAW195	Horse Pond #17	2	43	98	--	.621	.283	.356	.530	.245	.340
72	--	Higgins Crow #20	2	39	98	--	.351	.160	.201	.308	.143	.198
	--	Higgins Crow #23	2	39	97	--	.243	.111	.139	.487	.225	.312
73	--	Higgins Crow #24	1	41	95	--	.162	.074	.093	.487	.225	.312
	--	Higgins Crow #25	2	41	95	--	--	--	--	.444	.205	.285
74	--	Y-DP	3	35	100	--	--	--	--	.444	.205	.285
75	--	Y-GP	3	36	100	--	--	--	--	.444	.205	.285
76	--	Y-MP	3	34	101	--	--	--	--	.444	.205	.285
77	--	YBP1	3	44	100	--	--	--	--	.444	.205	.285
	--	YBP2	2	44	100	--	--	--	--	.444	.205	.285
	--	YBP4	2	44	100	--	--	--	--	.444	.205	.285
78	--	YBP3	2	44	101	--	--	--	--	.444	.205	.285
79	--	Y-Union	2	35	104	--	--	--	--	.444	.205	.285
80	--	Y-Dennis	2	37	109	--	--	--	--	.444	.205	.285
81	--	Y-F Pond	2	40	111	--	--	--	--	.444	.205	.285
Total .....						3.569	8.613	4.028	4.970	13.329	6.162	9.260

**WEST CAPE FLOW CELL TOTALS**

Map No.	Town name	Year and pumping rate, in cubic feet per second						
		1975 ADD	1989 IN	1989 OFF	1989 ADD	2020 IN	2020 OFF	2020 ADD
1	Barnstable	3.96	7.831	4.298	5.123	15.351	7.483	10.245
2	Bourne	.942	2.471	1.172	1.331	5.528	1.981	3.169
3	Centerville/Osterville	2.236	7.971	3.061	3.963	12.173	5.343	7.692
4	Cotuit	.278	1.063	.453	.550	1.659	.789	1.061
5	Falmouth	4.152	8.313	4.439	5.202	12.672	8.143	9.655
6	Mashpee	.198	.953	.312	.493	3.420	1.332	2.056
7	Otis	.940	.890	.630	.634	1.022	.713	.816
8	Sandwich	.486	2.710	1.550	1.780	5.320	3.608	4.180
9	South Sagamore	.124	.304	.129	.155	.366	.202	.243
10	Yarmouth	3.569	8.613	4.028	4.970	13.329	6.162	9.26
Totals for the West Cape flow cell.....		16.885	41.119	20.072	24.201	70.840	35.756	48.377



**Table 4.** Pumping rates of public-supply wells for 1975, 1989, and projected for 2020, represented in models of the East Cape flow cell, Cape Cod Basin, Massachusetts

[Map No.: Wells shown in bold are proposed wells; all other wells are existing. Location of wells shown in figure 5. Model node: Model grid shown in figure 9. Year and pumping rate: ADD, average daily demand; IN, inseason pumping rates from June through August; OFF, offseason pumping rates from September through May. No., number. --, no data]

Map No.	Well No.	Well Name	Model node			Year and pumping rate, in cubic feet per second						
			Layer	Row	Column	1975	1989	1989	1989	2020	2020	2020
						ADD	IN	OFF	ADD	IN	OFF	ADD
BREWSTER WATER DEPARTMENT												
1	BMW37	Well #1	2	22	47	0.287	0.830	0.390	0.495	1.300	0.528	0.785
2	BMW41	Freeman's Way #2	2	21	46	.231	.910	.420	.542	1.300	.528	.785
3	BMW55	Freeman's Way #3	2	20	49	--	.956	.440	.573	1.347	.528	.814
4	--	P-B-21-85	3	21	30	--	--	--	--	.962	.391	.581
5	--	P-B5	2	24	32	--	--	--	--	.722	.294	.437
Total.....						0.518	2.696	1.250	1.610	5.631	2.269	3.402
CHATHAM WATER DEPARTMENT												
6	CGW211	Indian Hill W-1	2	35	52	0.776	1.096	0.520	0.681	0.471	0.337	0.382
7	CGW153	South Chat- ham #1	2	37	44	.086	--	--	--	--	--	--
	CGW1-3	South Chat- ham #2	1	37	44	.171	1.021	.484	.634	.807	.578	.654
8	--	RCA	2	33	53	--	.025	.012	.016	.336	.240	.272
9	--	P-CWC-9	2	35	45	--	--	--	--	.466	.334	.387
	--	P-CWC-13	2	35	45	--	--	--	--	.466	.334	.387
10	--	P-CWC-RCA-N	2	34	52	--	--	--	--	.466	.334	.387
11	--	P-CWC-GP	2	33	49	--	--	--	--	.466	.334	.387
Total.....						1.033	2.142	1.016	1.331	3.478	2.491	2.856
DENNIS WATER DEPARTMENT												
12	DGW1-5	Main Station	1	28	18	0.246	0.927	0.369	0.495	0.887	0.336	0.520
13	DGW56	Chatham Road #1	1	25	21	.226	.261	.104	.139	.887	.336	.520
	DGW57	Chatham Road #2	1	25	21	.013	.116	.046	.062	.887	.336	.520
	DGW58	Chatham Road #3	1	25	21	.123	.116	.046	.062	.887	.336	.520
14	DGW67	Bass Road #4	1	22	18	.059	.290	.115	.155	.887	.336	.520
	DGW232	Bass Road #6	1	22	18	.015	.058	.023	.031	.193	.073	.113
15	DGW66	Route 134 #5	1	27	20	.161	.405	.161	.217	.517	.216	.334
16	DGW85	Airline Road #7	2	24	22	.232	.492	.196	.263	.571	.216	.334
17	DGW86	Airline Road #8	1	24	23	.139	.203	.081	.108	.439	.166	.257
18	DGW79	Grassy Pond #9	2	22	20	.527	.521	.207	.279	.825	.313	.484
19	DGW77	Airline Road #10	1	25	23	.273	.434	.173	.232	.877	.336	.500
20	DGW112	Bass River #11	1	23	18	.390	.290	.115	.155	.632	.239	.370
21	DGW87	Chatham #12	1	26	23	.150	.781	.311	.418	1.010	.383	.592
22	DGW205	Center Street #13	2	32	23	--	.405	.161	.217	.632	.239	.370
23	DGW244	Bakers Pond Road #14	1	22	22	--	.347	.138	.186	.571	.216	.334
24	--	Bakers Pond Road #15	1	22	21	--	0.492	0.196	0.263	0.887	0.336	0.520

**Table 4.** Pumping rates of public-supply wells for 1975, 1989, and projected for 2020, represented in models of the East Cape flow cell, Cape Cod Basin, Massachusetts--*Continued*

Map No.	Well No.	Well Name	Model node			Year and pumping rate, in cubic feet per second						
			Layer	Row	Column	1975 ADD	1989 IN	1989 OFF	1989 ADD	2020 IN	2020 OFF	2020 ADD
DENNIS WATER DEPARTMENT--Continued												
25	--	Timber Lane #16	1	23	21	--	.492	.196	.263	.755	.286	.442
26	--	Timber Lane #17	1	23	23	--	--	--	--	.887	.337	.520
27	--	Timber Lane #18	2	19	18	--	.637	.253	.340	.887	.337	.520
Total.....						2.554	7.267	2.891	3.885	14.118	5.373	8.290
HARWICH WATER DEPARTMENT												
28	HJW1-5	--	1	36	40	0.023	0.390	0.153	0.201	0.788	0.393	0.525
29	HJW49	PS #1	1	34	40	.529	.600	.236	.309	.377	.188	.257
	HJW55	PS #2	1	34	40	.148	.300	.118	.155	.377	.188	.257
30	HJW56	PS #3	1	35	40	.373	.510	.200	.263	.460	.229	.334
	HJW160	PS #4	2	35	40	.120	.270	.106	.139	.542	.270	.333
31	HJW161	PS #5	1	35	43	.032	.510	.200	.263	.375	.187	.249
	HJW162	PS #6	2	35	43	.118	.480	.189	.248	.375	.187	.249
32	HJW163	PS #7	2	36	44	.126	.540	.212	.279	.432	.216	.288
33	HJW8	PS #8	2	30	50	--	.570	.244	.294	.394	.196	.262
	HJW243	PS #9	2	30	50	--	.600	.236	.309	.394	.196	.262
34	--	P-H-10	3	25	29	--	--	--	--	.411	.205	.273
35	--	P-H-11	2	26	29	--	--	--	--	.411	.205	.273
36	--	P-H-12	2	27	29	--	--	--	--	.411	.205	.273
37	--	P-H-5R	2	26	45	--	--	--	--	.411	.205	.273
		(Spruce Road)										
38	--	P-H-PBR1	2	27	49	--	--	--	--	.411	.205	.273
		(Pleasant Bay Road)										
39	--	P-H-PBR2	2	27	50	--	--	--	--	.411	.205	.273
		(Pleasant Bay Road)										
Total.....						1.469	4.770	1.894	2.460	6.980	3.480	4.654
ORLEANS WATER DEPARTMENT												
40	OSW11	GP#1	2	16	56	0.322	0.179	0.148	0.108	0.447	0.226	0.300
41	OSW14	GP#2	2	15	56	.206	.307	.086	.186	.323	.163	.216
	--	P-O-G2	2	15	56	--	--	--	--	.323	.163	.216
	OSW15	GP#3	2	15	56	.277	.486	.148	.294	.619	.313	.415
42	OSW42	GP#4	2	18	55	.041	.614	.233	.371	.646	.326	.432
43	OSW43	GP#5	2	17	55	.088	.307	.296	.186	.619	.313	.415
	--	P-O-G5	2	17	55	--	--	--	--	.689	.348	.461
44	--	GP#6	2	16	55	--	.639	.308	.387	.688	.348	.461
Total.....						0.934	2.532	1.219	1.532	4.354	2.200	2.916
YARMOUTH WATER DEPARTMENT												
45	--	Setucket Rd	2	23	12	--	0.432	0.197	0.248	0.401	0.185	0.257
46	--	Setucket Rd	2	23	13	--	.513	.234	.294	.487	.225	.352
Total.....						--	0.945	0.431	0.542	0.888	0.410	0.609

**Table 4.** Pumping rates of public-supply wells for 1975, 1989, and projected for 2020, represented in models of the East Cape flow cell, Cape Cod Basin, Massachusetts--*Continued*

EAST CAPE FLOW CELL TOTALS								
Town No.	Town name	Year and pumping rate, in cubic feet per second						
		1975 ADD	1989 IN	1989 OFF	1989 ADD	2020 IN	2020 OFF	2020 ADD
1	Brewster	0.518	2.696	1.250	1.610	5.631	2.269	3.402
2	Chatham	1.033	2.142	1.016	1.331	3.478	2.491	2.856
3	Dennis	2.554	7.267	2.891	3.885	14.118	5.373	8.290
4	Harwich	1.469	4.770	1.894	2.460	6.980	3.480	4.654
5	Orleans	.934	2.532	1.219	1.532	4.354	2.200	2.916
6	Yarmouth	--	.945	.431	.542	.888	.410	.609
Totals for the East Cape flow cell .....		6.508	20.352	8.701	11.360	35.449	16.223	22.727

**Table 5.** Pumping rates of public-supply wells for 1975, 1989, and projected for 2020, represented in models of the Truro flow cell, Cape Cod Basin, Massachusetts

[Map No.: Only existing wells are shown. Location of wells shown in figure 22. Model node: Model grid shown in figure 21. Year and pumping rate: ADD, average daily demand; IN, inseason pumping rates from June through August; OFF, offseason pumping rates from September through May. No., number. --, no data]

Map No.	Well No.	Well Name	Model node			Year and pumping rate						
			Layer	Row	Column	1975 ADD	1989 IN	1989 OFF	1989 ADD	2020 IN	2020 OFF	2020 ADD
PROVINCETOWN WATER DEPARTMENT												
1	TSW58	Air Force	3	14	12	--	0.303	0.137	0.170	0.371	0.175	0.240
2	TSW115	Knowles Crossing	1	7	21	0.696	.331	.150	.186	.405	.190	.262
3	TSW78	South Hollow	2-3	10	14	.716	1.516	.688	.851	1.855	.873	1.200
Total.....						1.412	2.150	0.975	1.207	2.631	1.238	1.702
Total for the Truro flow cell.....						1.412	2.150	0.975	1.207	2.631	1.238	1.702



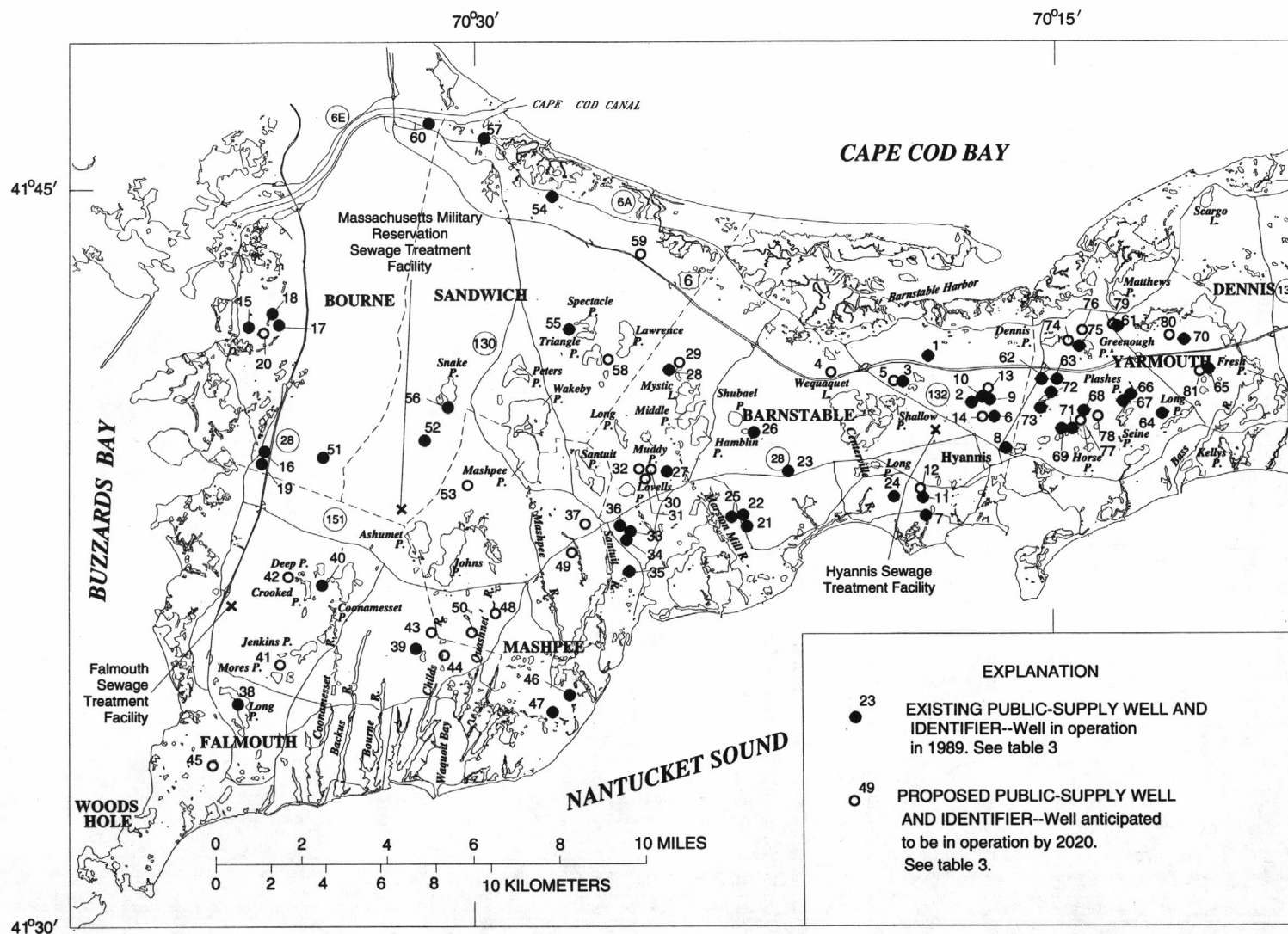
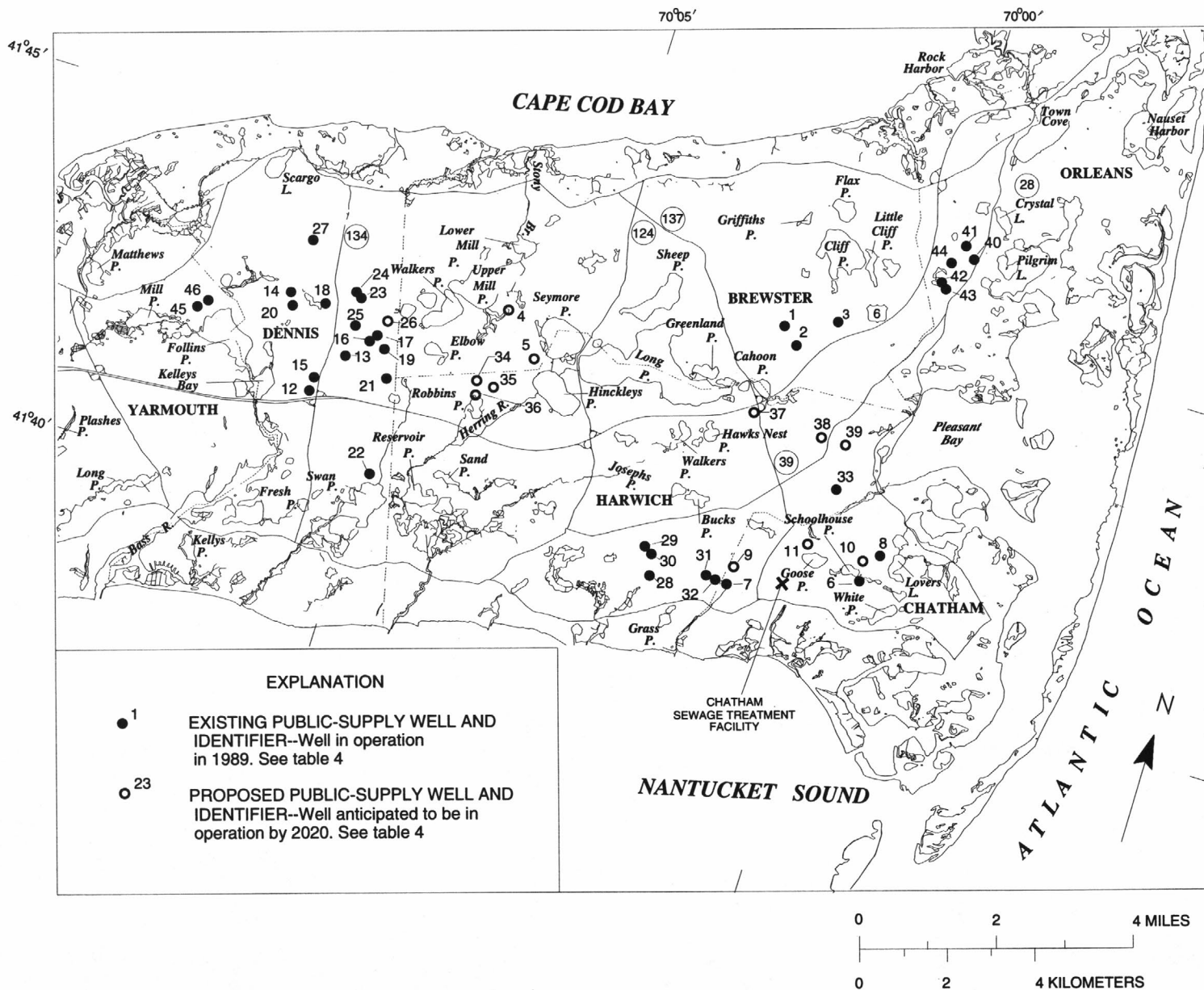


Figure 4. Existing and proposed public-supply wells in the West Cape flow cell, Cape Cod Basin, Massachusetts.



**Figure 5.** Existing and proposed public-supply wells in the East Cape flow cell, Cape Cod Basin, Massachusetts.

## Martha's Vineyard Basin

The Martha's Vineyard Basin is the second largest and second most populated of the three ground-water basins. Unlike Cape Cod Basin, only a single comprehensive investigation of the hydrogeology of the Martha's Vineyard Basin has been completed (Delaney, 1980). Most of the following information is based on that investigation.

Martha's Vineyard consists of more than 600 ft of Cretaceous- and Tertiary-aged coastal-plain deposits that overlie crystalline bedrock (Delaney, 1980). These coastal-plain deposits are mantled by Pleistocene glacial formations deposited by the Buzzards Bay and Cape Cod Bay ice lobes (fig. 3B). There are three principal physiographic regions on Martha's Vineyard (fig. 6): the western moraine, the eastern moraine, and the central outwash plain. The western moraine is a complex sequence of thrust sheets of coastal-plain deposits interbedded with till, gravel, sand, silt, and clay, with land-surface altitudes greater than 250 ft. The eastern moraine is less rugged than the western moraine, with land-surface altitudes of only one-half those of the western moraine. The eastern moraine consists of poorly sorted silt, sand, and till, which is overlain by sand and gravel outwash. The central outwash plain consists of interbedded sand and gravel outwash formed by the meltwaters of the retreating ice lobes (Delaney, 1980).

The principal ground-water-flow system of Martha's Vineyard Basin consists of a primary and a secondary aquifer, both of which consist of glacial deposits that are within the upper 160 ft of saturated material (Delaney, 1980). The silty sands of the Cretaceous- and Tertiary-aged coastal-plain deposits and deposits of the western moraine are not considered part of the principal flow system. The western moraine is not considered part of the principal flow system because Delaney (1980) reports that most ground-water levels in the western moraine are significantly higher than those of the central outwash plain and eastern moraine. Delaney (1980) determined that the primary sand and gravel aquifer extends from the water table to about 70 ft below sea level. A 20-foot thick unit of silty sand separates the primary aquifer from the underlying secondary aquifer, which consists of a 70-foot thick deposit of interbedded fine to coarse sand.

Martha's Vineyard Basin is completely surrounded by salt water that forms the outer boundary of the fresh ground-water-flow system. Because the island is

hydraulically isolated, precipitation is the only source of fresh water to the ground-water-flow system. Delaney (1980) reports that about one-half of the average annual precipitation (46 in.) is lost to evapotranspiration, and that about 22 in/yr recharges the ground-water-flow system. There is no significant streamflow or overland runoff on Martha's Vineyard.

A water-table contour map was made from water levels measured on October 28-30, 1991 (fig. 6). Ground water flows from the area that borders the western moraine to the Nantucket Sound and the Atlantic Ocean. Local highs in the water table in the town of Edgartown represent perched conditions and are due to discontinuous deposits of low hydraulic conductivity in the eastern moraine. Ground water is locally confined in parts of the towns of Oak Bluffs and Tisbury; where these confining conditions are present, ground-water seepage may occur when ground-water levels rise above the land surface.

Ponds and streams on Martha's Vineyard are surface-water expressions of the principal ground-water-flow system. However, perched water bodies are present in the western moraine and parts of the eastern moraine, where water levels overlying discontinuous deposits of low hydraulic conductivity intersect land surface.

The horizontal hydraulic conductivity of the primary and secondary aquifers has been determined by analysis of aquifer tests made at public-supply wells and estimated from lithologic information. Delaney (1980) reported horizontal hydraulic conductivities of 200 ft/d for the primary aquifer, 35 ft/d for the secondary aquifer, and less than 1 ft/d for the silt layer between the aquifers.

Ground water is the principal source of drinking water for the residents of Martha's Vineyard. Public-water supply systems provide water for the residents of Tisbury, Edgartown, Oak Bluffs, and parts of West Tisbury. Average annual pumping for 1989 and average annual and seasonal pumping from the public-supply wells of Martha's Vineyard projected by MOWR for the year 2020 are shown in table 6. Ground-water pumping during the summer months of 2020 are anticipated to be more than double those of the rest of the year; average daily demand for the year 2020 is projected to be nearly twice those of 1989.



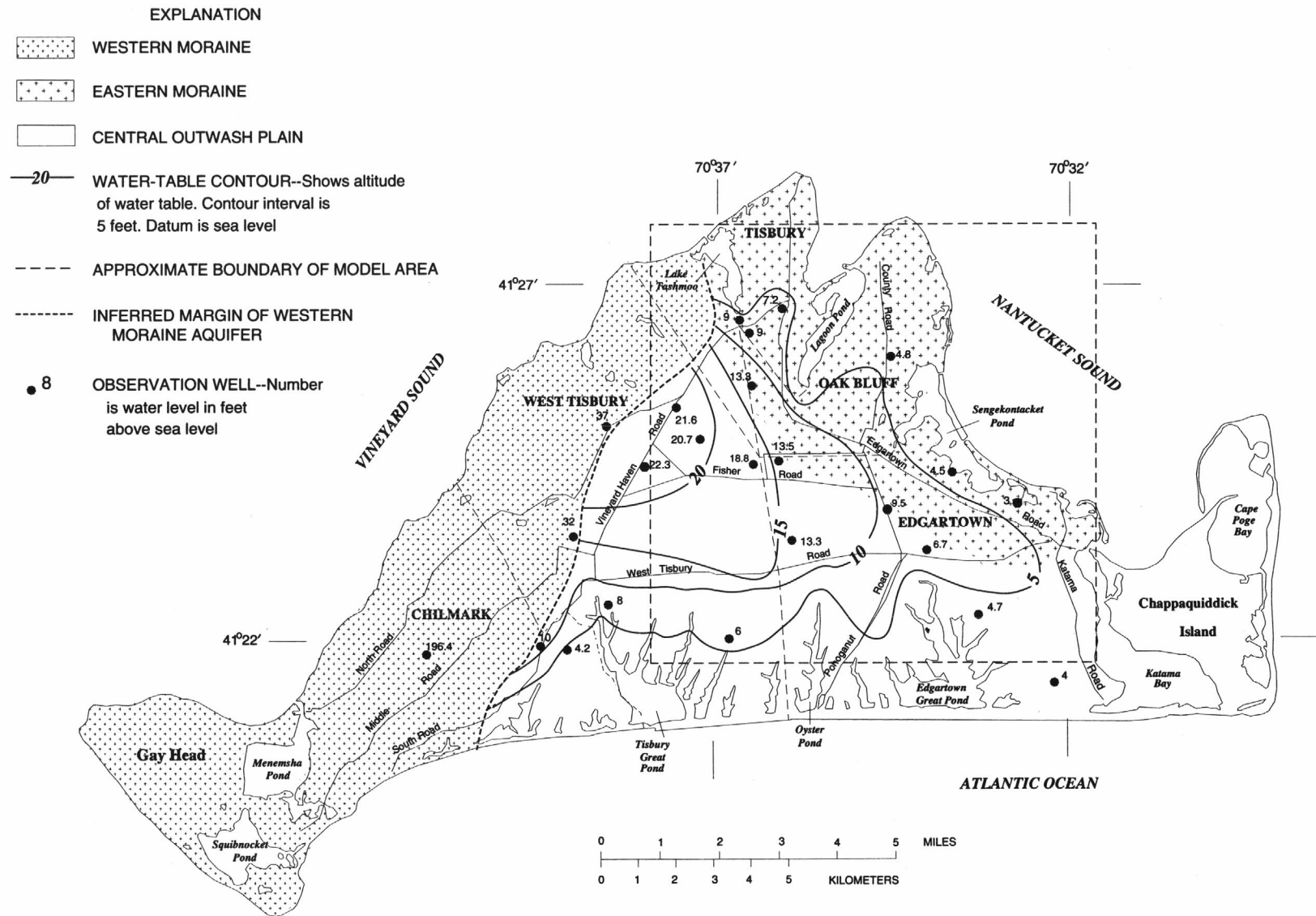


**Figure 6.** Water-table configuration on October 28-30, 1991, surficial geology, and location of modeled area, Martha's Vineyard Basin, Massachusetts.

**Table 6.** Pumping rates of public-supply wells for 1989 and projected for 2020, represented in models of Martha's Vineyard and Nantucket Island Basins, Massachusetts

[Map No.: Wells shown in bold are proposed wells; all other wells are existing. Location of wells shown in figures 32 and 33. Year and pumping rate: ADD, Average daily demand; IN, in-season pumping rates from June through August; OFF, off-season pumping rates from September through May. --, no pumping]

Map No.	Well name	Year			
		1989 ADD	2020 IN	2020 OFF	2020 ADD
MARTHA'S VINEYARD BASIN					
Edgartown Water Department					
1	Machacket Well	0.217	0.758	0.248	0.402
2	Lily Pond Well	.217	.758	.248	.402
3	Wintucket Well #1	.634	1.13	.379	.596
4	Wintucket Well #2	--	1.13	.379	.595
Oak Bluffs Water Department					
5	Lagoon Pond Well	0.124	0.371	0.155	0.217
6	Farm Neck Well	.124	.371	.155	.217
7	State Forest Well	.805	1.207	.519	.720
8	State Forest Well	--	1.207	.518	.719
Tisbury Water Works					
9	Sanborn Well	0.495	0.712	0.294	0.433
10	Tashmoo Well	.495	.712	.294	.433
11	Manter Well	--	1.470	.619	.882
Total.....		3.111	9.826	3.808	5.616
NANTUCKET ISLAND BASIN					
Siasconset Water District					
--	Gravel Pack Well <sup>1</sup>	0.186	0.464	0.046	0.186
Wannacomet Water Company					
1	Well #1	1.222	1.370	0.689	0.842
2	Well #2	--	1.370	.689	.842
Total.....		1.408	3.204	1.424	1.870

<sup>1</sup>Siasconset Water District Gravel Pack Well is not shown in figure 33 because drawdown is negligible.

## Nantucket Island Basin

The Nantucket Island Basin is the smallest and least populated of the three basins. There have been two comprehensive investigations of the hydrogeology of the basin (Walker, 1980; Horsley Witten Hegemann, Inc., 1990). Most of the following information is based on those investigations.

Nantucket Island consists of nearly 1,500 ft of Cretaceous- and Tertiary-aged coastal-plain deposits overlying crystalline bedrock (Walker, 1980). The coastal-plain deposits are mantled by 150 to 250 ft of sand and gravel deposited by the Cape Cod Bay ice lobe (fig. 3B). There are two principal physiographic regions on Nantucket Island (fig. 7)—the moraine and the outwash plain. The moraine consists of unsorted sand, gravel, silt, and clay that was deposited during the final readvancement of the Cape Cod Bay ice lobe. The subsequent standstill and downwasting of the ice sheets in the area of the moraine accounts for its hummocky terrain, with altitudes greater than 100 ft. The outwash plain consists of stratified sand and gravel deposited by the meltwaters of the retreating ice lobe.

The ground-water-flow system of Nantucket Island can be divided into a shallow and a deep aquifer. The upper 250 ft of sand and gravel outwash deposits constitutes the shallow aquifer. The thick wedge of fine sand, silt, and clay of the underlying coastal-plain deposits contain the deep aquifer, which is poorly understood. Walker (1980) reports a wide range in hydraulic conductivity for the coastal-plain deposits that generally are much lower than the glacial deposits.

Nantucket Sound and the Atlantic Ocean completely surround Nantucket Island and form the outer boundary of the fresh ground-water-flow system. Precipitation is the only source of fresh water to the shallow flow system. Walker (1980) estimated that of the 44 in./yr of precipitation, 25 in. are lost to evapotranspiration, resulting in 19 in. of aquifer recharge. Kohout and others (1977) have explored the possibility that the deep aquifer is part of a larger ground-water-flow system that underlies Nantucket Sound and provides an hydraulic connection to remote recharge areas on Martha's Vineyard or Cape Cod. The findings of the study proved to be inconclusive.

A water-table contour map was made from water levels measured in observation wells between August 10-22, 1989, and reported by Horsley Witten Hegemann, Inc. (1990) (fig. 7). Ground water flows radially outward from the center of the island toward coastal discharge areas. Local highs in the water table in the central part of the island may be caused by discontinuous lenses of low hydraulic conductivity in the moraine. Ponds, streams, and swamps are surface-water expressions of the ground-water-flow system; perched water bodies present in the moraine may go dry in summer months.

The hydraulic properties of the shallow aquifer have been determined by analysis of aquifer tests made at public-supply wells and estimated from lithologic information. Walker (1980) reported a horizontal hydraulic conductivity of 970 ft/d and a specific yield of 0.25 for the shallow aquifer.

Ground water is the principal source of drinking water for the residents of Nantucket. Two public-water supply systems service nearly one-half the population of Nantucket. Average annual pumping rates from public-supply wells for 1989 and average annual and seasonal pumping rates projected to occur in the year 2020 by MOWR are shown in table 6. Ground-water pumping increases nearly fourfold during the summer to accommodate the significant increase in seasonal population.

## EFFECTS OF SIMULATED GROUND-WATER PUMPING AND RECHARGE ON GROUND-WATER FLOW IN CAPE COD BASIN

This section describes the development and application of numerical flow models for the West Cape, East Cape, Eastham, Wellfleet, and Truro flow cells in the Cape Cod Basin. Each flow system is conceptualized as a single, unconfined system that may be confined locally by units of low hydraulic conductivity, such as the unit of silt and clay that underlies Cape Cod Bay. The entire thickness of the unconsolidated deposits of each flow cell is explicitly simulated in each model. As discussed in the "Approach" section of this report, three different modeling strategies were used to analyze the

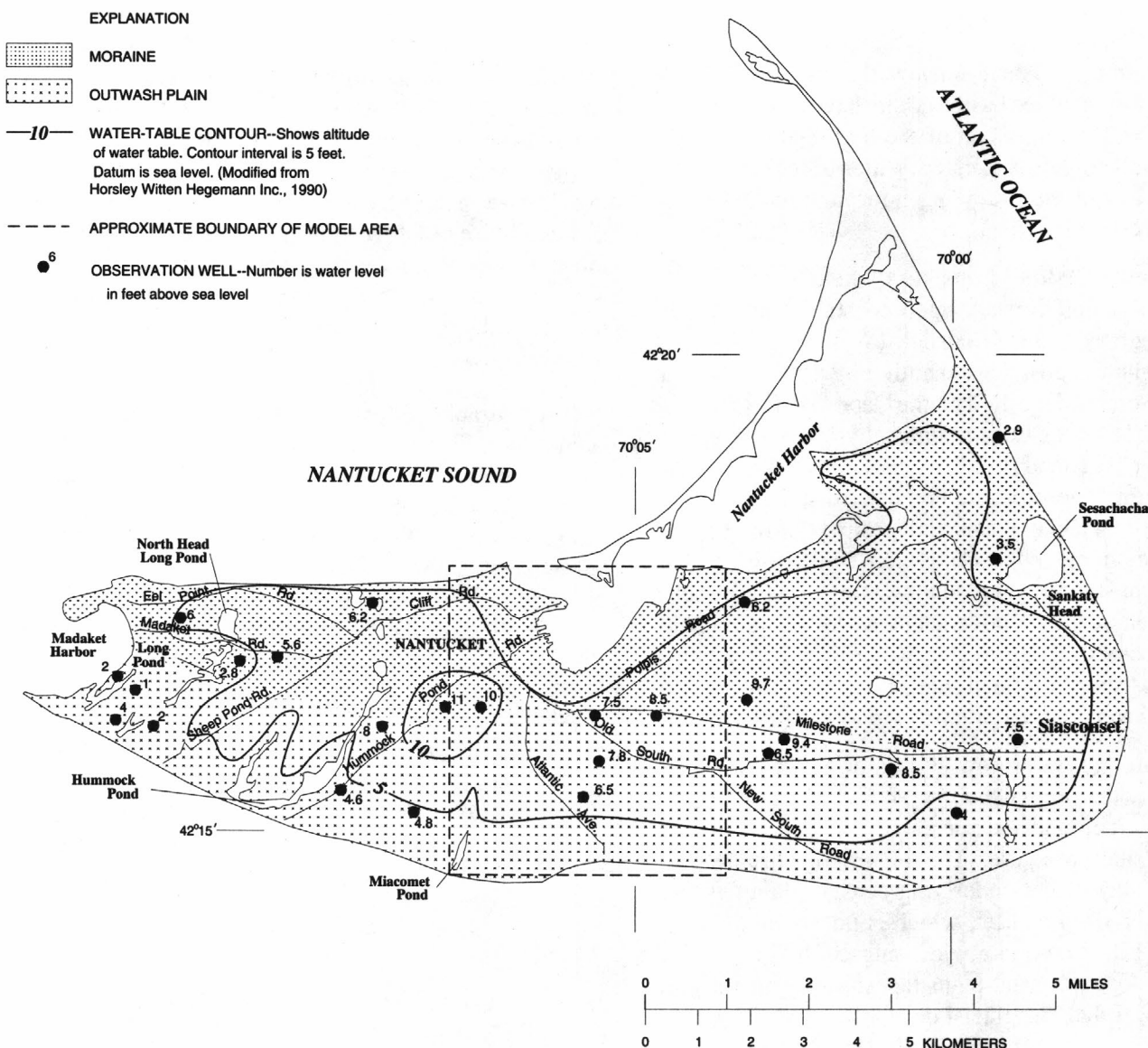


**Figure 7.** Water-table configuration on August 10-22, 1989, surficial geology, and location of modeled area, Nantucket Island Basin, Massachusetts.

effects of ground-water pumping and recharge on the ground-water-flow systems. The analysis is divided into three sections, in which flow cells are grouped by similar modeling approaches: the West Cape and East Cape flow cells are discussed first, followed by the Truro flow cell, and, finally, by the Eastham and Wellfleet flow cells.

### West Cape and East Cape Flow Cells

The West Cape and East Cape flow cells are the largest flow cells on Cape Cod. Flow models developed for the West Cape flow cell extend from the Cape Cod Canal eastward to the Bass River and from Cape Cod Bay southward to Nantucket Sound (fig. 8). Flow models for the West Cape flow cell include the towns of



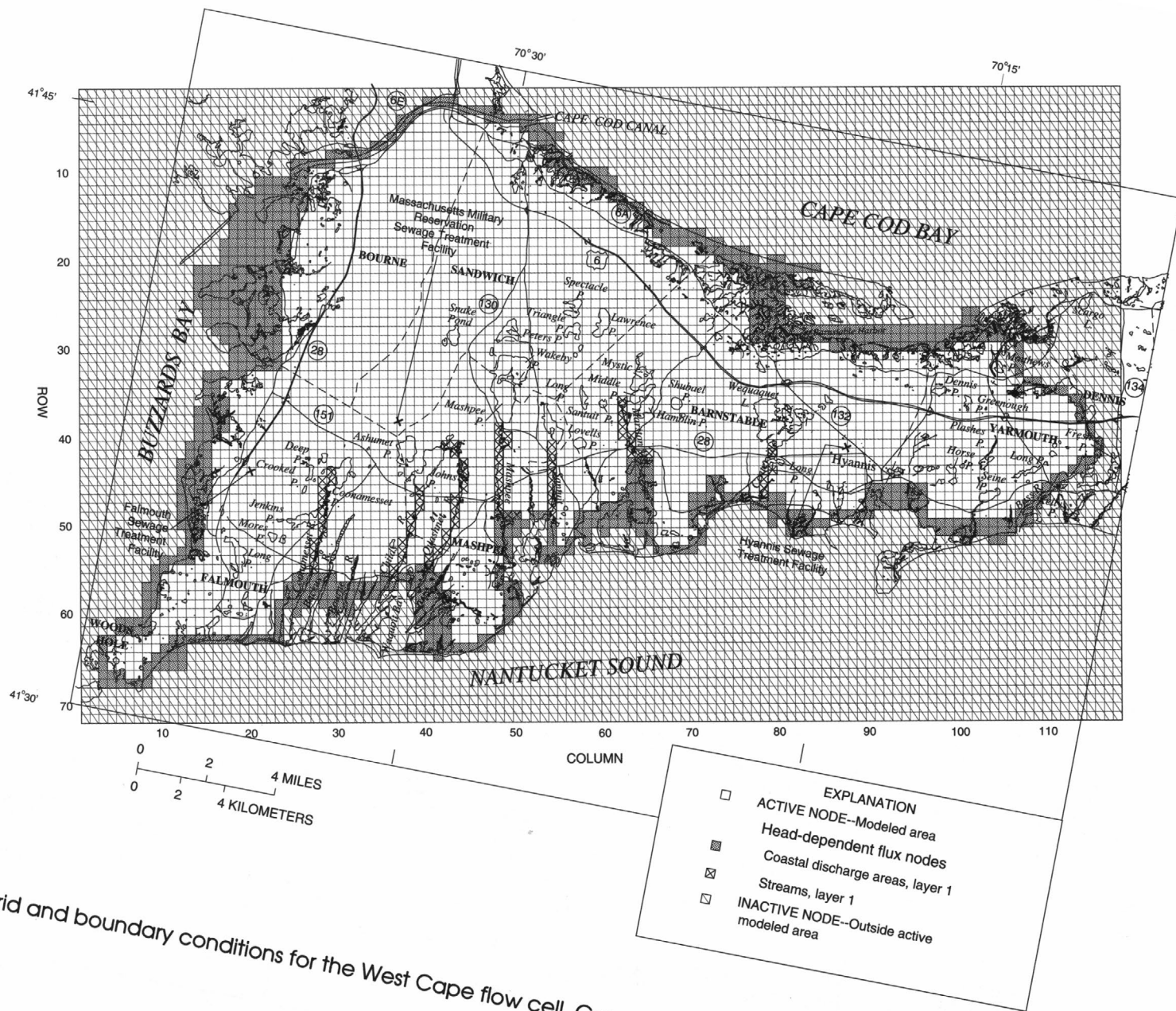


Figure 8. Grid and boundary conditions for the West Cape flow cell, Cape Cod Basin, Massachusetts.

Bourne, Sandwich, Falmouth, Mashpee, Barnstable, and most of Yarmouth. Flow models developed for the East Cape flow cell adjoin the eastern edge of the West Cape flow models and extend from the Bass River in Dennis eastward to Town Cove and Rock Harbor in Orleans, and from the Cape Cod Bay southward to Nantucket Sound (fig. 9). Flow models for the East Cape flow cell include a small part of Yarmouth and all of the towns of Dennis, Brewster, Harwich, Chatham, and Orleans.

## Modeling Approach

The analysis of changing stress conditions in the West Cape and East Cape flow cells consisted of three modeling phases. Within each phase, a freshwater-saltwater flow model (SHARP model) was developed first, followed by a freshwater-flow model (MODFLOW model). The three phases are summarized as follows:

First phase.--Model data developed by Guswa and LeBlanc (1985) were used in the SHARP models of the first phase to determine an initial estimate of the location of the freshwater-saltwater interface and the rate of freshwater discharge to overlying saltwater zones of the aquifer for simulated predevelopment flow conditions through to those projected to occur in the year 2020. Details on recharge and pumping conditions used in the simulations are discussed in the section "Stresses and Stress Periods." The boundary conditions along the freshwater-saltwater interface calculated by the SHARP models then were used as boundary conditions in the MODFLOW models of the first phase. Details on the incorporation of the freshwater-saltwater interface into the boundary conditions of the MODFLOW models are discussed in the section "Boundary Conditions." Model data related to the hydraulic properties of the aquifer that were developed by Guswa and LeBlanc (1985)—including horizontal hydraulic conductivity, vertical conductance, and the contact between unconsolidated deposits and bedrock—were then modified to reflect data made available since the work of Guswa and LeBlanc (1985). The MODFLOW models then were calibrated. In the calibration process, initial estimates of hydraulic conductivity and vertical conductance were adjusted within reason such that model-calculated ground-water levels, pond levels, and streamflow were

approximately equal to measured values. Details on the calibration process are discussed in the section "Calibration."

Second phase: The same stress conditions used in the first phase then were simulated with the SHARP models using the calibrated model hydraulic property data sets of the first phase. These simulations provided a second estimate of boundary conditions along the freshwater-saltwater interface that then was used in a second phase of MODFLOW simulations. Using these updated freshwater-saltwater interface conditions, model hydraulic property data sets were modified slightly in the MODFLOW models in a second calibration process.

Third phase: Calibrated model hydraulic property data sets of the second phase were simulated for a third time using the SHARP models. The location of the freshwater-saltwater interface changed little between the second and third phases because changes made to the hydraulic property data sets in the second phase were minor. Consequently, the SHARP and MODFLOW models developed in the second phase were considered to be calibrated models and were used in the final analysis of the flow system.

The SHARP model assumes that freshwater and saltwater zones of each aquifer are immiscible fluids separated by a sharp interface, which implies that there is no transition zone between the freshwater- and saltwater-flow systems. This sharp-interface approximation is appropriate for the analysis of regional flow systems in which the width of the transition zone is very small relative to the total saturated thickness of the aquifer. A sharp-interface approximation was assumed for the West Cape and East Cape flow cells because the thickness of the transition zone measured at 11 observation wells in the flow cells ranges from about 3 to 11 percent of the total saturated thickness of the aquifer and the mean thickness of the zone of transition at these 11 wells is 8 percent of the total saturated thickness (LeBlanc and others, 1986).

## Description of Models

### Grids

The finite-difference grids of the two flow cells consist of uniform nodes 1,320 by 1,320 ft. These nodes are one-quarter the size of those used by Guswa and

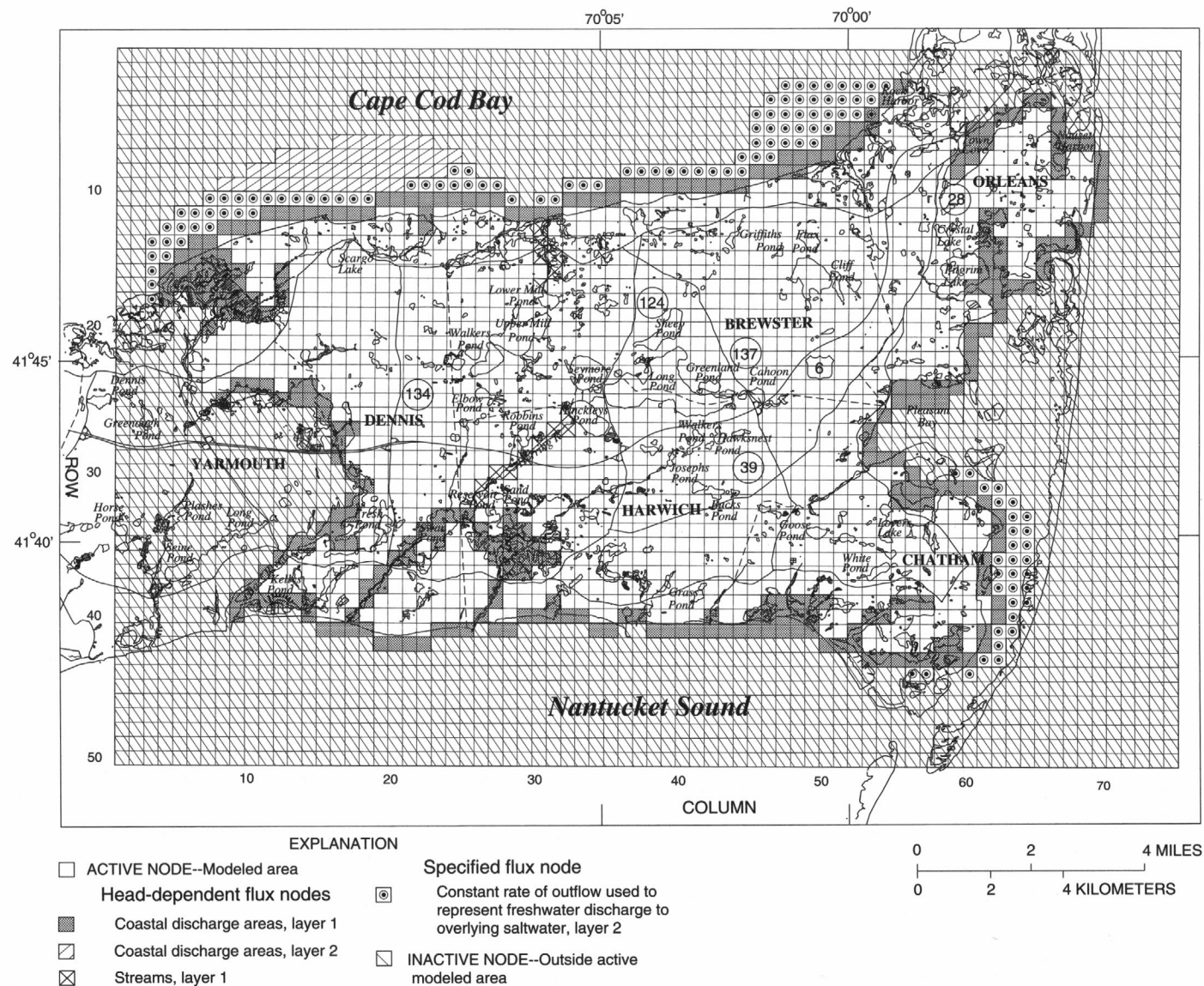


**Figure 9.** Grid and boundary conditions for the East Cape flow cell, Cape Cod Basin, Massachusetts.



LeBlanc (1985) and were necessary in order to improve the numerical stability of the freshwater-saltwater flow models (Essaid, 1990, p. 54). The West Cape grid consists of 72 rows and 118 columns (fig. 8); the East Cape grid consists of 50 rows and 74 columns (fig. 9).

Each model consists of five layers (table 7) and the definition of layers in each model is similar to that used by Guswa and LeBlanc (1985). The bottom altitude of model nodes in the top layer of each of the MODFLOW models that are coincident with ponds equal to or greater than one model node in size (about 40 acres) were set equal to measured pond-bottom altitudes where known (McCann, 1969). The bottom of each model is the contact between unconsolidated deposits and bedrock; bedrock altitudes have been mapped in the two flow cells from available lithologic and seismic-refraction data by B.D. Stone (U.S. Geological Survey, written commun., 1990).

#### Hydraulic properties

Horizontal hydraulic conductivity and vertical conductance (referred to as vertical leakance in the freshwater-saltwater models) were determined for the models by comparing hydrogeologic sections shown in plate 1 to values of hydraulic conductivity generalized for individual grain sizes from the results of the aquifer-test analyses shown in tables 1 and 2. The generalized values of horizontal hydraulic conductivity used were 40 ft/d for fine sand and silt, 150 ft/d for fine sand, 220 ft/d for fine-medium sand, and 350 ft/d for medium-coarse sand and gravel. Fine silt and clay were assigned a horizontal hydraulic conductivity of  $1 \times 10^{-3}$  ft/d, which is the average value reported by Barlow (1994) based on permeameter tests of fine silt and clay samples from the town of Eastham. The generalized values of the ratio of vertical to horizontal hydraulic conductivity were 1:30 for very fine and fine sand and 1:5 for medium sand to gravel. Vertical conductance between vertically adjacent nodes was calculated following McDonald and Harbaugh (1988, p. 5-11), which is based on layer thicknesses and vertical hydraulic conductivities.

Zones of lithologically similar deposits were defined using the hydrogeologic sections and geologic maps of the study area (plate 1 of this report; Oldale and Barlow, 1986). Uniform values of horizontal hydraulic conductivity and vertical conductance were used for each zone. Calibrated values of horizontal hydraulic conductivity

**Table 7.** Vertical layering, horizontal hydraulic conductivity, and vertical conductance of calibrated models of the Cape Cod Basin, Massachusetts

[The SHARP model used in the Truro flow cell numbering convention shows model layer 7 as the top layer. --, vertical conductance was not specified for the bottom layer]

Model layer	Maximum depth of layer, in feet below sea level	Horizontal hydraulic conductivity, in feet per day	Vertical conductance, in day <sup>-1</sup>
WEST CAPE FLOW CELL			
1	20	<sup>1</sup> 3-250	0.0005-0.080
2	70	1-200	0.001-0.068
3	140	1-150	0.001-0.280
4	240	10-125	0.0001-0.034
5	500	1-30	--
EAST CAPE FLOW CELL			
1	20	<sup>1</sup> 3-250	0.00002-0.8000
2	70	1-150	0.0013-0.044
3	140	10-75	0.002-0.060
4	240	10-75	0.00001-0.050
5	500	1-30	--
TRURO FLOW CELL			
1	900	75	--
2	280	75	0.0125
3	200	75	0.0180
4	140	75	0.015-0.021
5	80	50-150	0.03-0.08
6	40	150-200	0.08-0.48
7	10	200-350	0.36-0.50
EASTHAM FLOW CELL			
1	10	<sup>1</sup> 100-150	0.005-1.0
2	35	10-100	0.001-1.0
3	60	0.001-100	0.0001
4	90	0.001-100	0.00001
WELLFLEET FLOW CELL			
1	10	<sup>1</sup> 50-350	0.4-1.870
2	40	200-250	0.003-1.515
3	80	10-200	0.003-0.286
4	140	10-100	0.003-0.167
5	200	100	0.1430
6	280	100	--

<sup>1</sup>Grid nodes underlying ponds represented in the models were assigned a horizontal hydraulic conductivity of 50,000 feet per day.



and vertical conductance that were determined in the second phase, calibrated models, are summarized in table 7. In general, calibrated model values are less than initial estimates.

A uniform specific yield of 0.15 was specified in the models where unconfined conditions exist; it was based on the results of the aquifer-test analyses reported in table 2. A uniform value of the storage coefficient of  $2 \times 10^{-4}$  was used for both flow models where confined conditions exist, and was based on the work of Barlow and Hess (1993). Porosity, which is required for the SHARP models, was set equal to 0.30.

### **Boundary conditions**

#### **Freshwater-saltwater flow models**

The models of the West Cape and East Cape flow cells are bounded on top by the water table, which is a free-surface boundary that receives spatially and temporally variable rates of recharge. Recharge rates specified for the models are discussed in the next section "Stresses and Stress Periods." The lower boundary of each model was the contact between the unconsolidated glacial sediments and underlying bedrock, which were assumed to be impermeable. Each model layer is bounded laterally by inactive nodes that separate modeled areas from unmodeled areas (figs. 8 and 9).

Head-dependent flux boundary conditions were used to simulate saltwater discharge areas. The head values specified at saltwater discharge boundaries are equivalent freshwater heads equal to the height of the column of saltwater overlying the seabed at the discharge boundary divided by 40.0, the ratio of the specific weight of fresh water ( $1.000 \text{ g/cm}^3$ ) to the difference between the specific weight of salt water ( $1.025 \text{ g/cm}^3$ ) and fresh water (Essaid, 1990). The height of the column of saltwater in each node was determined from bathymetric maps of the area. Head-dependent flux boundaries are specified at saltwater discharge areas in the top layer in the West Cape flow cell and in the top two layers in the East Cape flow cell. A vertical leakance of  $20 \text{ day}^{-1}$  for the seabed deposits was used in the simulations, which assumes a 1-foot thick sediment deposit on the seabed with a vertical hydraulic conductivity of  $20 \text{ ft/d}$ . This value of the vertical leakance of seabed deposits also was used by Guswa and LeBlanc (1985) in their models of the area.

Streams also were modeled as head-dependent flux boundaries. Heads specified at stream boundaries were estimated from topographic maps or, where available, from survey data. Streambed conductance values were estimated from available data and modified during model calibration to match measured streamflow. Streams represented in the models are the Coonamesett, Childs, Quashnet, Mashpee, Santuit, Centerville, and Marston Mill in the West Cape flow cell, and the Herring River and Stony Brook in the East Cape flow cell (figs. 4, 5, 8, and 9).

#### **Freshwater flow models**

Several boundary conditions used for the freshwater-flow models were the same as those used for the freshwater-saltwater models. These include: (1) recharge to the water table; (2) the contact between unconsolidated deposits and bedrock; and (3) the use of head-dependent flux boundaries at saltwater discharge areas, in which the heads specified at these boundaries were equivalent freshwater heads.

Boundary conditions at the freshwater-saltwater interface calculated by the SHARP models were incorporated into the MODFLOW freshwater models. A schematic figure illustrating how these boundary conditions were incorporated into the MODFLOW models is shown in figure 10. Grid nodes determined to be completely filled with salt water by the SHARP models were made inactive in the MODFLOW models. Grid nodes determined to be partially filled with salt water by the SHARP models (called mixed nodes) were reduced in total thickness in the MODFLOW models to account for those parts of the aquifers containing salt water. Coastal discharge of fresh water to the saltwater zones of the aquifer in the top layer of the model was simulated as a head-dependent flux boundary, as described in the previous section "Freshwater- and Saltwater-Flow Models." Subsea discharge of fresh water to overlying saltwater zones of the simulated aquifer in the bottom four layers of the SHARP models was removed from the MODFLOW models by creating freshwater sinks where this discharge occurred; these sinks were simulated using pumping wells. The pumping rate of each of these wells was set equal to the model-calculated rate of fresh water discharged to the overlying zone containing salt water. The total model-calculated rate of freshwater discharge removed from the models by these wells was 4 percent of recharge for the West Cape model and 11 percent of recharge for the East Cape model.

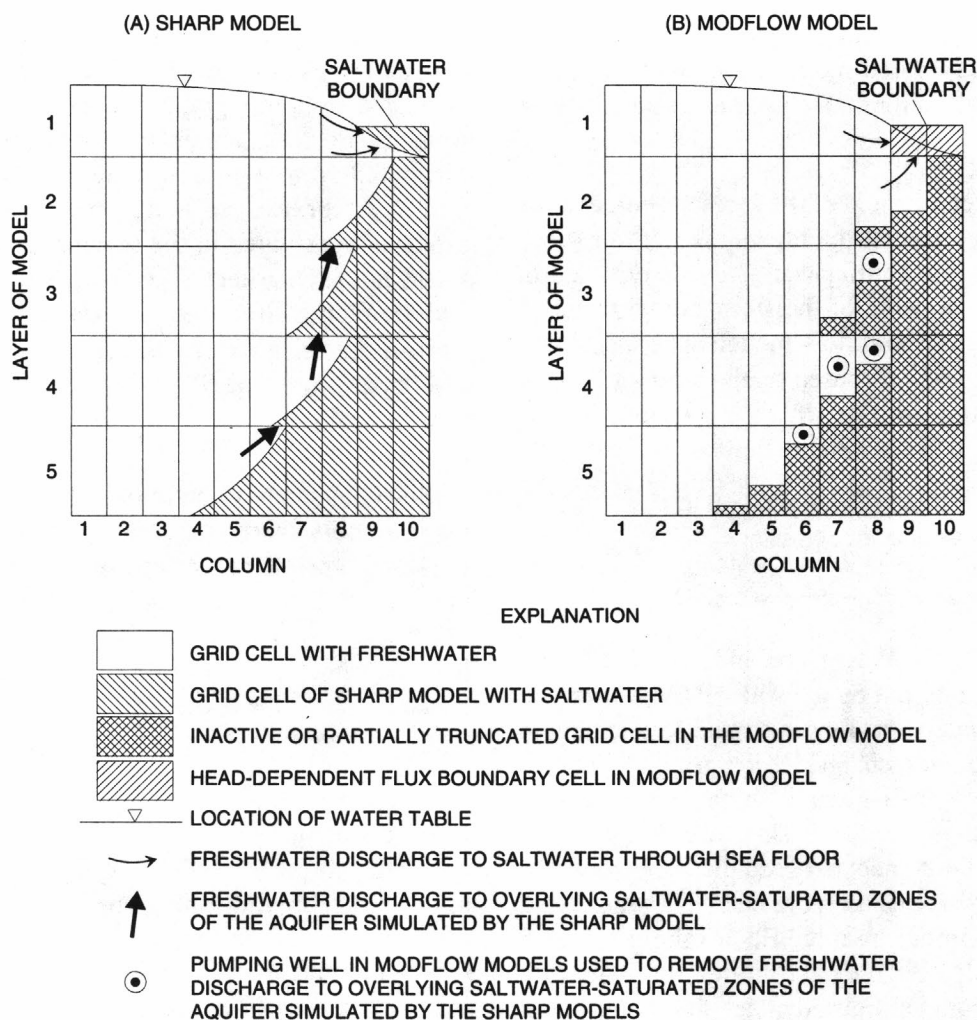


**Figure 10.** Incorporation of hydraulic dynamics along the freshwater-saltwater boundary as represented in the SHARP model (A) into the MODFLOW model (B) for the West Cape and East Cape flow cells, Cape Cod Basin, Massachusetts.

Freshwater streams were simulated using head-dependent flux boundaries. Streams were simulated such that they could only receive ground-water discharge (that is, as gaining streams); water could not flow from simulated streams to underlying aquifer. Streams represented in the models were the same as those represented in the SHARP models (the Coonamesset, Childs, Quashnet, Mashpee, Santuit, Marston Mill, and Centerville in the West Cape flow cell and the Herring River and Stony Brook in the East Cape flow cell).

Freshwater ponds greater than 40 acres (1 model node) were represented as zones of high horizontal hydraulic conductivity (50,000 ft/d) with a specific

yield equal to 1.0. The high value of horizontal hydraulic conductivity caused calculated hydraulic gradients in the ponds to be nearly zero, which is consistent with pond surfaces; the high value of specific yield caused pond levels to fluctuate less than heads in the surrounding aquifers because of the greater storage capacity of the ponds than of the surrounding aquifer.

#### Stresses and stress periods

Ground-water flow in the West Cape and East Cape flow cells was simulated using the SHARP models for predevelopment conditions and a 71-year stress condition that corresponds to 1950-2020. First, a

simulation was completed in which heads throughout the ground-water-flow system were calculated for conditions of no pumping (predevelopment flow conditions) —conditions that are assumed to have occurred until 1950. These conditions were simulated for long time periods, until there was virtually zero change in storage in each model layer. This simulation was completed to determine heads throughout the flow cells that were then used as initial conditions for the 71-year stress condition simulation. This simulation also provided heads and freshwater-saltwater interface conditions to compare with the effects of development.

Once the predevelopment heads and interface locations were calculated, a simulation for 1950-2020 was completed. The 71-year period was divided into three stress periods: 1950-81, 1982-2004, and 2005-2020. The stress period 1950-81 used pumping and recharge conditions of 1975-76; the stress period 1982-2004 used pumping and recharge conditions of 1989; and the stress period 2005-2020 used pumping and recharge conditions projected to occur in the year 2020 by MOWR. These three pumping and recharge stress conditions are approximations of the actual stress conditions that have increased, and are assumed to continue to increase, incrementally with time. These approximations were assumed to be sufficient for a regional analysis of changing stress conditions. Public-supply well locations and pumping rates for 1975, 1989, and those projected to occur in the year 2020 that were used in the models are summarized in tables 3 and 4.

Once the 71-year stress condition simulation was completed, approximate steady-state conditions were simulated using the projected 2020 pumping and recharge rates. The approximate steady-state distribution of heads and freshwater-saltwater interface position in each flow cell for the projected 2020 stress conditions was assumed to occur when calculated changes in storage within each model were negligible.

Recharge to the flow cells consists of precipitation and wastewater return flow from sources such as septic systems and wastewater-treatment facilities. Annual precipitation rates were estimated to be about 45 and 43 in. in the West Cape and East Cape flow cells, respectively (LeBlanc and others, 1986). Recharge from precipitation was estimated for each of the flow systems by Guswa and LeBlanc (1985) using the method of Thornthwaite and Mather (1957). The annual

precipitation recharge rates estimated by Guswa and LeBlanc (1985) were not changed during this investigation, with the exception that recharge was reduced beneath ponds to account for free-water-surface potential evaporation, which is estimated to be 28 in/yr on Cape Cod (Farnsworth and others, 1982, pl. 1). The free-water-surface potential evaporation was subtracted from annual precipitation rates in each flow cell to obtain net recharge rates beneath ponds of 17 and 15 in/yr, in the West Cape and East Cape flow cells, respectively. Finally, precipitation recharge rates were reduced by Guswa and LeBlanc (1985) in low-lying areas near the coast to account for evapotranspiration that occurs where the water table is near land surface. Precipitation recharge rates used in the West Cape and East Cape models ranged from 6 to 22 in/yr, and were applied to the top layer of each model.

Wastewater return flow from septic systems and wastewater-treatment facilities was estimated for each node of the top layer of each model. Wastewater return flow from septic systems for the 1975, 1989, and 2020 stress periods was determined from maps of distribution lines for public-water supply and the average daily rate of water supplied to unsewered areas by water companies, according to:

$$R_T = \left[ \frac{Q_{wd}}{A_{node}} \times \frac{L_{node}}{L_{total}} \right] \times 0.9, \quad (4)$$

where

- $R_T$  is return flow recharge (feet per day);
- $Q_{wd}$  is the average daily rate of water distributed to unsewered areas by the water supplier in 1975, 1989, or 2020, in cubic feet per day;
- $A_{node}$  is the area of the grid node, in square feet;
- $L_{node}$  is the length of roads in unsewered areas in the node that are served by the water supplier, in feet; and
- $L_{total}$  is the total length of roads in unsewered areas that are served by the water supplier, in feet.

Ten percent of the water supplied to unsewered areas was assumed to be lost by consumptive use. Recent data (M.A. Horn, U.S. Geological Survey, oral commun., 1992), however, suggests that this value of consumptive use may be low, and that a more realistic value of consumptive use would be 15 percent. The difference in the total recharge rate to each node of the two models

between using a value of 10 percent and that of 15 percent is small (a maximum error of 1.5 percent of total recharge to each node), and therefore the estimate of 10 percent is acceptable for this investigation.

Water discharged to sewers is returned to the aquifers through infiltration beds at three wastewater-treatment facilities in the West Cape flow cell (the Massachusetts Military Reservation facility in Sandwich, the Hyannis facility in Barnstable, and the Falmouth facility) and at a single facility (the Chatham facility) in the East Cape flow cell. Daily rates of wastewater infiltration at these four facilities were obtained from facilities personnel; the average daily volume of wastewater at each facility was distributed evenly to the grid nodes that contain the infiltration beds. Wastewater infiltration at these four facilities in 1989 was about 9 percent of the total rate of public-water supplies pumped from the flow cells.

Recharge from precipitation is assumed to remain constant throughout the simulation period. However, simulated wastewater return flow was specified based on a percentage of the rate of simulated ground-water pumpage. As a result, simulated recharge rates increased as simulated ground-water pumping rates increased with time.

### Calibration

The West Cape and East Cape freshwater-flow models were calibrated during the first and second phases of the modeling analysis by comparison of model-calculated water levels to measured water levels at 62 well and pond locations in the West Cape flow cell and 49 well and pond locations in the East Cape flow cell (figs. 11 and 12). Comparison also was made of model-calculated streamflow to measured streamflow for the Childs, Coonamesset, Mashpee, and Quashnet Rivers in the West Cape flow cell and the Herring River and Stony Brook in the East Cape flow cell. Average water levels for 1963-76 for 32 observation wells in the West Cape flow cell and 19 observation wells in the East Cape flow cell were compared to water levels calculated by the MODFLOW models for 1975. Average water levels for 1963-76 were compared to model-calculated water levels for 1975 because (1) measured water-level information was not available for predevelopment flow conditions; (2) this time period is consistent with that used for model calibration by Guswa and LeBlanc (1985); and (3) the water levels measured in these

observation wells in 1975 are representative of long-term average water levels reported for the observation wells for the 1963-76 period (Letty, 1984). Pond levels calculated by the MODFLOW models for 1975 were compared to those determined from topographic maps of the area. Pond levels reported on the maps were assumed to be consistent with 1975 water levels. Model-calculated streamflow for 1975 and 1989 were compared to period-of-record averages for the Quashnet and Herring Rivers; model-calculated streamflow for 1989 were compared to single discharge measurements made for the Coonamesset and Child's Rivers in August 1989 during a period of near-average hydrologic conditions (Barlow and Hess, 1993).

Data reported by LeBlanc and others (1986) on the vertical location and shape of the freshwater-saltwater interface at 16 zone-of-transition observation wells in the West Cape and East Cape flow cells also were used to compare model-calculated with measured freshwater-saltwater interface locations. The data reported by LeBlanc and others (1986) consist of chloride concentrations of water samples collected at different depths at the zone-of-transition wells. Marsily (1986) reports that the  $10^4$  mg/L isochlor generally is used as the demarcation between freshwater- and saltwater-flow systems.

As discussed earlier, the SHARP model assumes a sharp interface between fresh water and salt water. Each node simulated in the SHARP model can consist completely of fresh water or salt water, or can consist of fresh water in the top part of the node separated by the interface from salt water in the bottom part of the node.

Eight zone-of-transition wells were used for comparison in each flow cell. Interface locations calculated by the SHARP models for 1975 were compared to measured data collected between January 1976 and April 1977; results for four representative wells in each flow cell are shown in figure 13. The measured data generally indicate that chloride concentrations increase with depth, which is indicative of the transition between freshwater- and saltwater-flow systems. The calculated vertical distribution of fresh water and salt water at the 16 well sites generally agreed well with data presented by LeBlanc and others (1986) and is considered adequate for the purpose of this investigation.



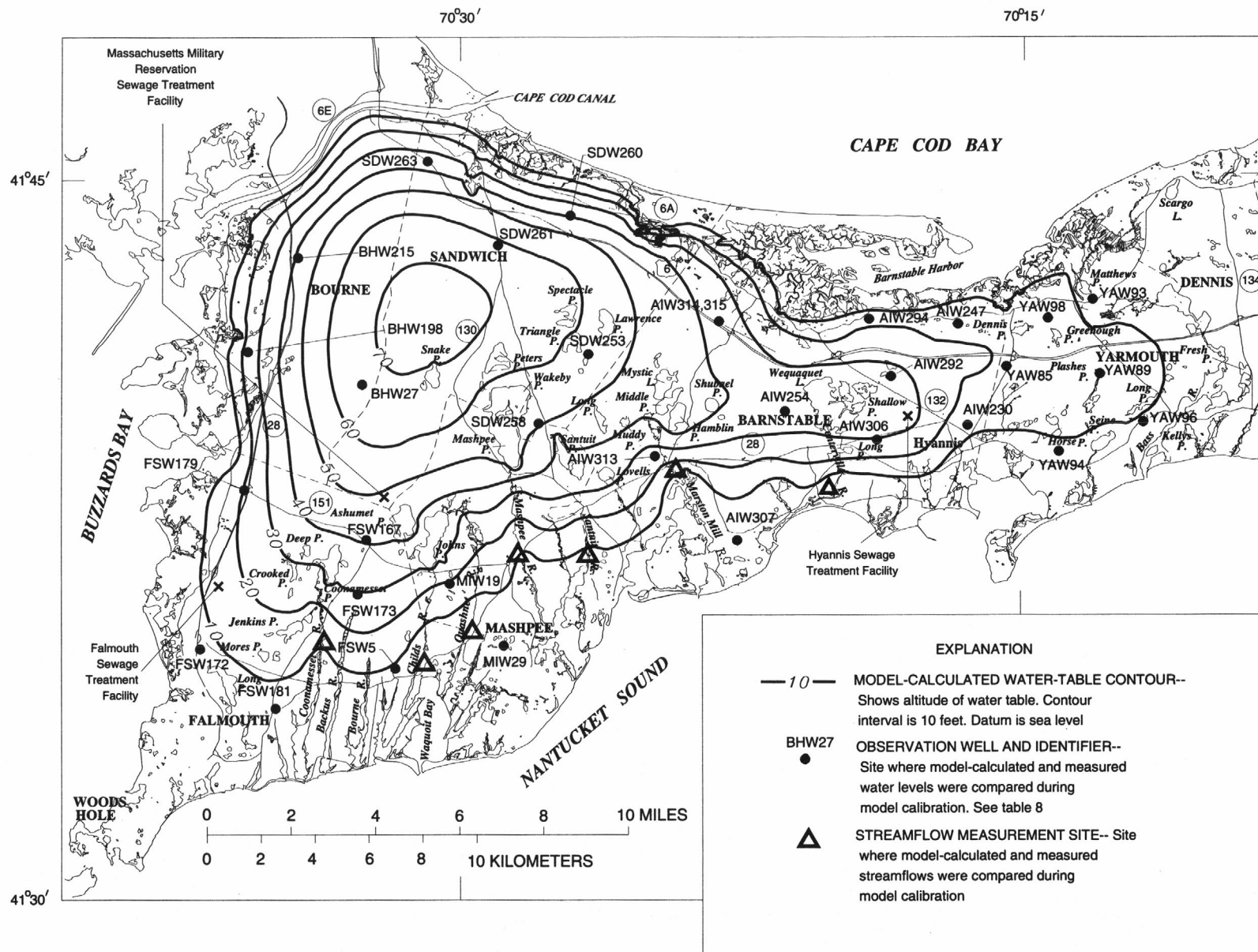


**Figure 11.** Model-calculated water-table configuration for the West Cape flow cell, Cape Cod Basin, Massachusetts, 1989.

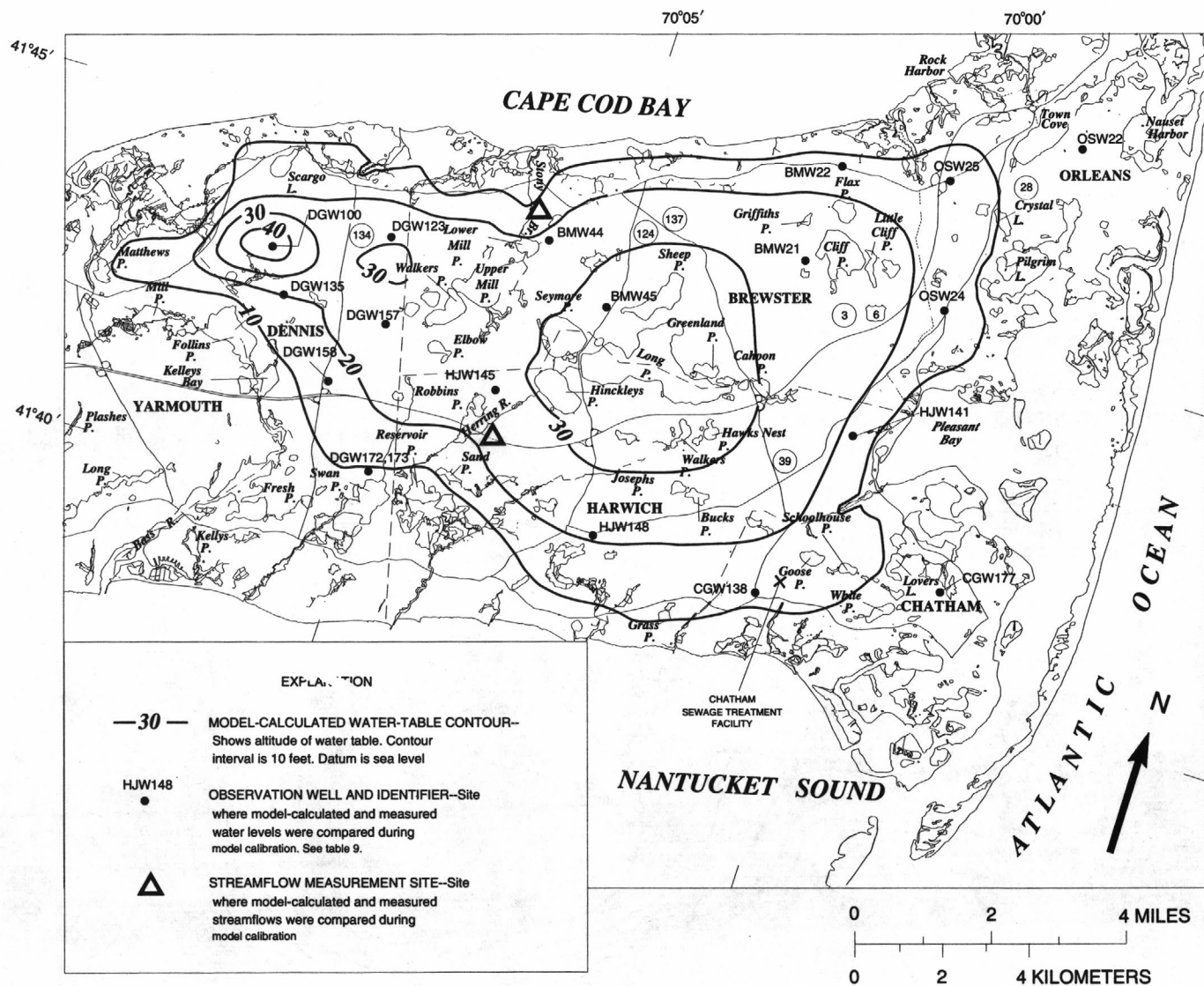


**Figure 12.** Model-calculated water-table configuration for the East Cape flow cell, Cape Cod Basin, Massachusetts, 1989.

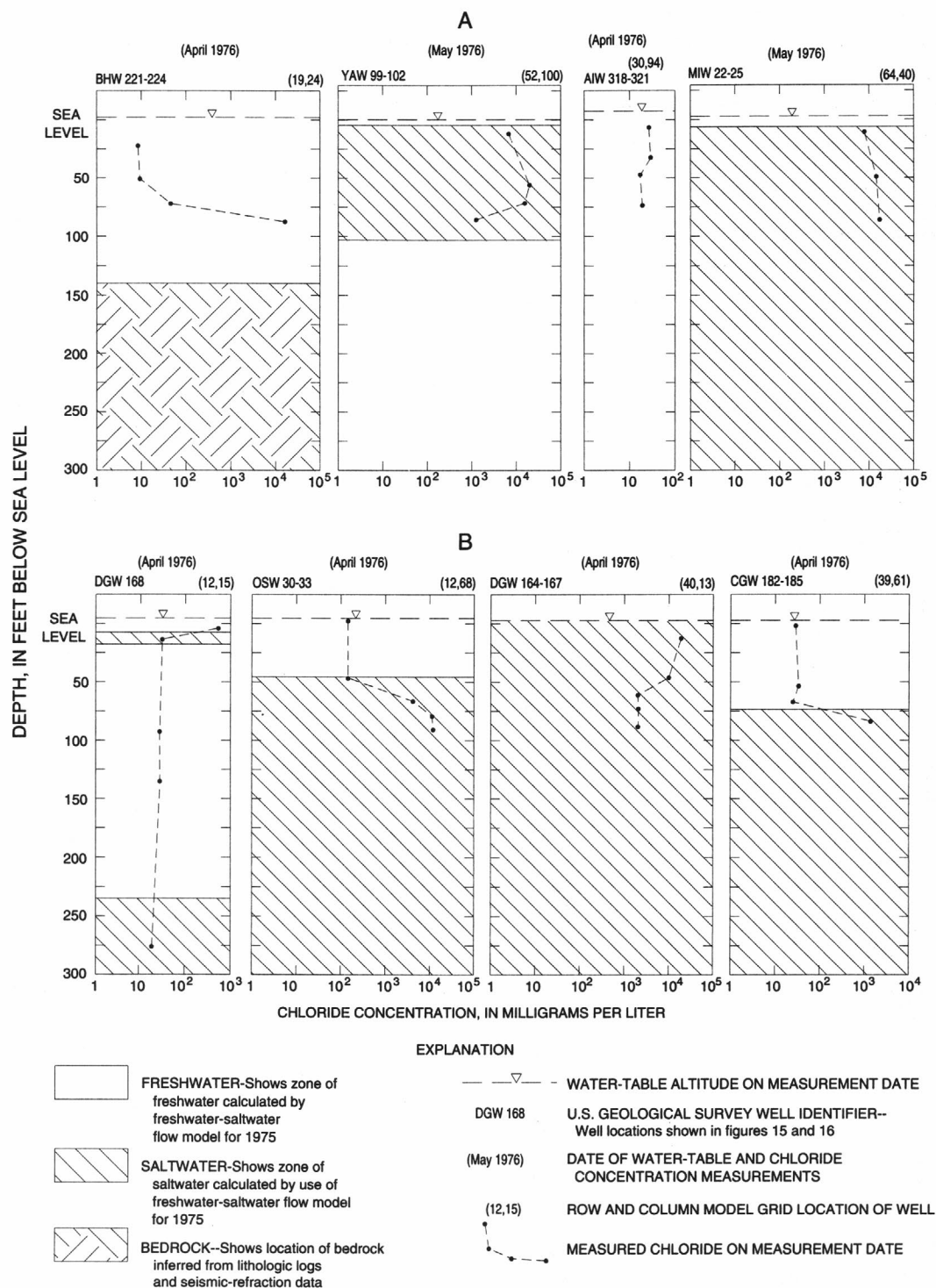


**Figure 13.** Measured chloride concentrations and model-calculated freshwater and saltwater zones at selected observation wells in the (A) West Cape and (B) East Cape flow cells, Cape Cod Basin, Massachusetts.

Initial estimates of horizontal hydraulic conductivity and vertical conductance were adjusted within reasonable limits during model calibration. Generally, agreement between model-calculated and measured water levels at observation wells and ponds is close (tables 8-11). The mean error between model-calculated water levels for 1975 and measured average water levels in observation wells (which are known more accurately than pond levels) was 2.0 ft or 3 percent of the total relief of the water table for the West Cape flow cell (table 8), and 2.2 ft or 5 percent of the total relief of the water table in the East Cape flow cell (table 9).

Streambed leakances and the heads specified for streams were modified within reasonable limits during model calibration from those used in the freshwater-saltwater models to match measured streamflow. Model-calculated streamflow for the Quashnet River at the site of the streamflow-gaging station was 13.6 ft<sup>3</sup>/s for 1975 and 13.5 ft<sup>3</sup>/s for 1989 (table 12), which compares favorably with the 1989-91 period-of-record daily mean streamflow of 13.8 ft<sup>3</sup>/s (Barlow and Hess, 1993). Model-calculated streamflow for the Herring River was 4.3 ft<sup>3</sup>/s for 1975 and 4.0 ft<sup>3</sup>/s for 1989, and were less than one-half of the period-of-record daily mean streamflow of 10.0 ft<sup>3</sup>/s; the cause of the discrepancy likely is due to the fact that a significant part of the streamflow in the Herring River results from the overflow of water to the river from Hinckely's Pond, which was not simulated in the model. Joseph Bergin (oral commun., 1992) of the Massachusetts Division of Fisheries and Wildlife estimated that nearly one-half of the discharge measured at the Herring River gaging station is due to overflow at the Hinckely's Pond spillway, which is consistent with that calculated by the model. The model-calculated values of 4.3 and 4.0 ft<sup>3</sup>/s represent ground-water discharge to the river that occurs between the outlet of the pond and the site of the streamflow-gaging station. Model-calculated 1989 streamflow for the Coonamesset and Child's Rivers at their points of measurement are 9.2 and 5.2 ft<sup>3</sup>/s, respectively, which compare reasonably well with the measured values in August 1989 of 8.2 and 6.0 ft<sup>3</sup>/s, respectively. August 1989 measurements for these rivers were assumed to be at near average conditions because the nearby Quashnet River was at near average conditions at the continuous-streamflow gaging station on the same date.

The 1975 recharge rates to the West Cape and East Cape flow cells specified in the MODFLOW models are 247.7 and 88.1 ft<sup>3</sup>/s (table 13), respectively, which are 93 and 97 percent, respectively, of the recharge rates specified for the two flow cells by Guswa and LeBlanc (1985). The small differences between recharge rates specified in these models and the Guswa and LeBlanc (1988) models likely are due to the finer discretization used in these models. Most freshwater discharge from the flow cells occurs to coastal discharge areas: for 1975, calculated freshwater discharge to coastal areas is 68 and 67 percent of the total freshwater discharge from the West Cape and East Cape flow cells, respectively. Total 1975 ground-water discharge to streams in the freshwater-flow models is 51.5 ft<sup>3</sup>/s in the West Cape flow cell (or 21 percent of total freshwater discharge from the flow cell) and 12.1 ft<sup>3</sup>/s in the East Cape flow cell (or 14 percent of total freshwater discharge from the flow cell). There was a close correlation in the water budgets calculated by the SHARP and MODFLOW models for each flow cell. For example, the steady-state volumetric flow rates of water moving between the five layers of the West Cape MODFLOW model for the 2020 pumping and recharge conditions ranged from 94 to 100 percent of those calculated for the same stress conditions by the SHARP model; for the East Cape flow models, the percentages ranged from 87 to 100. Differences between water budgets calculated by the SHARP and MODFLOW models result in part from differences in the method used to simulate the freshwater-saltwater interface in each model.

As part of the calibration process, a sensitivity analysis was done to determine the response of the freshwater models to changes in recharge, horizontal hydraulic conductivity, vertical conductance, vertical leakance of seabed deposits, specific yield, and storage coefficient specified in the models. The sensitivity analysis identifies those parameters to which the model results are most sensitive. Each parameter was uniformly increased and decreased individually, while other model parameters were held constant. The model-calculated water-table altitude, streamflow, and coastal discharge were most sensitive to increases and decreases in simulated recharge to the models and to decreases in the horizontal hydraulic conductivity and vertical conductance of the top layer of each model. However, changes in simulated vertical leakance of seabed deposits by an order of magnitude did not have a substantial effect on model-calculated results.



**Table 8.** Average measured water levels for selected wells, 1963-76, and model-calculated water levels for 1975, 1989, and projected for 2020 for the West Cape flow cell, Cape Cod Basin, Massachusetts

[Location of wells shown in figure 11. Change in model-calculated water level between stress periods: +, increase in the water level resulting from changing stress conditions; otherwise, a change is a decrease in water level]

Well No.	Model node			Average measured water level, in feet above sea level	Model-calculated water levels, in feet above sea level				Change in model-calculated water level between stress periods, in feet		
	Layer	Row	Column		Predevelopment	Year			Predevelopment-1975	1975-1989	1989-2020
						1975	1989	2020			
A1W230	1	42	91	18.4	19.1	17.9	17.0	12.5	1.2	0.9	4.5
A1W247	1	33	92	20.3	18.9	18.4	17.8	15.3	.5	.6	2.5
A1W254	1	39	74	34.9	34.9	35.1	35.4	35.3	+2	+3	.1
A1W292	1	37	85	34.1	32.9	33.4	33.2	31.9	+5	.2	1.3
A1W294	2	31	84	18.1	13.2	13.2	12.8	12.1	0	.4	.7
A1W306	1	43	83	27.2	26.3	26.7	27.4	26.8	+4	+7	.6
A1W307	1	49	68	5.0	5.0	4.4	4.8	3.7	.6	+4	1.1
A1W313	1	40	62	27.5	24.2	24.2	24.0	23.7	0	.2	.3
A1W314	3	29	70	32.5	37.2	37.2	36.9	35.5	0	.3	1.4
A1W315	1	29	70	32.5	37.2	37.3	36.9	35.6	+1	.4	1.3
BHW27	2	28	36	66.0	66.5	66.1	66.0	65.5	.4	.1	.5
BHW198	1	23	26	22.0	23.7	23.2	23.2	22.4	.5	0	.8
BHW215	1	15	33	46.0	44.5	44.2	44.1	43.4	.3	.1	.7
FSW5	2	55	34	6.2	8.5	8.5	7.9	7.9	0	.6	0
FSW167	1	42	34	41.3	41.7	42.0	41.9	41.9	+3	.1	0
FSW172	2	50	17	7.9	9.2	6.7	7.5	6.4	2.5	+8	1.1
FSW173	2	47	32	29.8	29.4	29.5	29.0	29.0	+1	.5	0
FSW179	1	35	24	25.3	21.7	21.7	22.0	21.9	0	+3	.1
FSW181	1	56	22	5.7	7.9	6.1	6.6	5.7	1.8	+5	.9
MIW19	1	48	41	26.9	18.7	18.7	18.7	18.5	0	0	.2
MIW29	2	55	45	6.4	4.4	4.4	4.3	4.1	0	.1	.2
SDW253	1	29	58	61.4	57.3	57.4	56.5	53.6	+1	.9	2.9
SDW258	1	35	52	53.7	50.0	50.2	49.9	48.9	+2	.3	1.0
SDW260	1	16	58	41.0	41.4	41.0	40.2	38.8	.4	.8	1.4
SDW261	2	18	51	63.8	63.9	63.8	63.2	62.1	.1	.6	1.1
SDW263	1	8	46	36.7	33.9	33.7	33.6	33.4	.2	.1	.2
YAW85	1	38	96	22.7	21.5	20.4	19.2	15.2	1.1	1.2	4.0
YAW89	1	40	104	18.0	17.4	16.5	16.5	15.5	.9	0	1.0
YAW93	2	34	105	9.1	14.6	14.5	14.1	12.9	.1	.4	1.2
YAW94	1	47	99	7.7	7.5	7.6	7.3	6.7	+1	.3	.6
YAW96	1	46	108	5.2	8.6	8.1	8.5	8.6	.5	+4	+1
YAW98	1	34	101	15.5	18.1	18.1	17.6	15.1	0	.5	2.5

**Table 9.** Average measured water levels for selected observation wells, 1963-76, and model-calculated water levels for 1975, 1989, and projected for 2020 for the East Cape flow cell, Cape Cod Basin, Massachusetts

[Location of wells shown in figure 12. Change in model-calculated water levels between stress periods: +, increase in the water level resulting from changing stress conditions; otherwise, a change is a decrease in water level]

Well No.	Model node			Average measured water level, in feet above sea level	Model-calculated water levels, in feet above sea level				Change in model-calculated water level between stress periods, in feet		
	Layer	Row	Column		Predevelopment	Year			Predevelopment-1975	1975-1989	1989-2020
						1975	1989	2020			
BMW21	1	16	47	27.2	26.8	26.2	25.1	24.0	0.6	1.1	1.1
BMW22	1	11	49	19.8	14.9	14.6	14.2	13.8	.3	.4	.4
BMW44	4	17	32	26.4	24.2	23.8	23.4	22.0	.4	.4	1.4
BMW45	1	21	35	31.4	31.9	31.4	31.0	29.5	.5	.4	1.5
CGW138	1	37	46	11.3	13.8	12.8	11.9	10.7	1.0	.9	1.2
CGW177	1	35	57	11.9	8.4	8.4	8.3	8.3	0	.1	0
DGW100	1	19	15	44.7	44.5	43.9	43.4	42.5	.6	.5	.9
DGW123	1	18	23	32.8	30.7	30.3	29.9	28.8	.4	.4	1.1
DGW135	1	22	17	16.7	20.9	18.9	18.0	14.4	2.0	.9	3.6
DGW157	1	24	23	25.9	28.2	25.1	24.0	18.0	3.1	1.1	6.0
DGW158	2	27	20	19.2	20.1	17.3	16.3	12.2	2.8	1.0	4.1
DGW172	5	32	23	6.2	12.2	11.9	11.4	10.6	.3	.5	.8
DGW173	4	32	23	8.2	11.7	11.4	10.8	10.1	.3	.6	.7
HJW141	2	27	51	19.2	18.0	17.7	16.7	14.8	.3	1.0	1.9
HJW145	1	27	30	31.7	26.7	26.5	26.3	25.3	.2	.2	1.0
HJW148	1	34	36	20.8	22.2	21.4	21.5	21.1	.8	+1	.4
OSW22	1	9	61	4.2	3.0	3.2	3.3	3.5	+2	+1	+2
OSW24	1	19	55	18.5	17.9	17.2	16.3	15.0	.7	.9	1.3
OSW25	1	11	54	15.1	13.9	13.7	13.5	13.2	.2	.2	.3

**Table 10.** Measured and model-calculated pond levels for selected ponds in the West Cape flow cell, Cape Cod Basin, Massachusetts

[Change in model-calculated pond level between stress periods: +, indicates an increase in the pond level resulting from changing stress conditions; otherwise, change is a decrease in the pond level]

Pond name	Model node			Average measured pond level, in feet above sea level	Model-calculated pond levels, in feet above sea level				Change in model-calculated pond level between stress periods, in feet		
	Layer	Row	Column		Predevelopment	Year			Predevelopment-1975	1975-1989	1989-2020
						1975	1989	2020			
TOWN OF BARNSTABLE											
Long	1	35	57	51.0	45.6	45.6	45.0	43.1	0	0.6	1.9
Lovells	1	41	57	38.0	34.1	34.1	33.4	32.0	0	.7	1.4
Muddy	1	36	60	45.0	42.5	42.5	41.7	39.8	0	.8	1.9
Mystic Lake	1	33	64	44.0	44.3	44.3	43.6	41.7	0	.7	1.9
Middle	1	35	64	42.0	44.3	44.3	43.6	41.7	0	.7	1.9
Hamblin	1	36	65	42.0	44.3	44.3	43.6	41.7	0	.7	1.9
Shubael	1	36	68	43.0	42.6	42.2	41.6	40.4	.4	.6	1.2
Wequaquet	1	39	79	34.0	33.1	33.8	34.0	33.3	+7	+2	.7
Long	1	43	79	26.0	23.1	23.2	23.4	23.2	+1	+2	.2
Shallow	1	38	83	34.0	33.2	33.8	34.0	33.4	+6	+2	.6
TOWN OF FALMOUTH											
Long	1	53	18	11.0	9.9	4.7	6.1	3.8	5.2	+1.4	2.3
Mares	1	51	22	13.0	15.0	13.1	13.7	12.2	1.9	+6	1.5
Jenkins	1	49	25	19.0	17.9	17.1	17.5	16.4	.8	+4	1.1
Deep	1	42	28	35.0	34.1	34.4	34.1	34.0	+3	.3	.1
Coonamesset	1	44	30	33.0	32.9	33.1	32.9	32.9	+2	.2	0
TOWN OF MASHPEE											
Ashumet	1	41	37	44.0	41.8	42.1	42.0	41.9	+0.3	0.1	0.1
Johns	1	43	40	38.0	34.9	35.1	35.0	34.9	+2	.1	.1
Wakeby	1	31	50	55.0	53.4	53.5	53.3	52.5	+1	.2	.8
Mashpee	1	35	48	55.0	52.8	52.9	52.7	51.9	+1	.2	.8
Santuit	1	39	54	43.0	38.7	38.8	38.5	37.5	+1	.3	1.0
TOWN OF SANDWICH											
Snake	1	8	43	68.0	69.9	69.7	68.9	67.7	0.2	0.8	1.2
Peters	1	27	49	67.0	65.3	65.4	64.9	63.7	+1	.5	1.2
Spectacle	1	25	57	63.0	62.5	62.6	61.1	58.4	+1	1.5	2.7
Triangle	1	8	57	62.0	60.3	60.4	59.3	56.4	+1	1.1	2.9
Lawrence	1	27	60	61.0	56.4	56.4	55.5	53.0	0	0.9	2.5
TOWN OF YARMOUTH											
Dennis	1	35	98	25.0	20.0	19.7	19.1	16.3	0.3	0.6	2.8
Horse	1	44	99	16.0	13.7	13.3	12.1	10.0	.4	1.2	2.1
Plashes	1	43	103	0	15.1	14.3	14.1	12.9	.8	.2	1.2
Seine	1	47	103	10.0	8.7	8.6	8.6	8.3	.1	0	.3
Long	1	44	108	7.0	11.1	10.1	10.8	10.8	1.0	+7	0

**Table 11.** Measured and model-calculated pond levels for selected ponds in the East Cape flow cell, Cape Cod Basin, Massachusetts

[Change in model-calculated pond level between stress periods: +, indicates an increase in the pond level resulting from changing stress conditions; otherwise, change is a decrease in the pond level]

Pond name	Model node			Average measured pond level, in feet above sea level	Model-calculated pond levels, in feet above sea level				Change in model-calculated pond level between stress periods, in feet		
	Layer	Row	Column		Predevelopment	Year			Predevelopment-1975	1975-1989	1989-2020
						1975	1989	2020			
TOWN OF BREWSTER											
Cliff	1	16	49	26.0	25.6	25.0	23.8	22.6	0.6	1.2	1.2
Elbow	1	24	26	30.0	28.5	27.6	26.9	24.4	.9	.7	2.5
Cahoon	1	24	45	31.0	31.7	30.9	29.9	27.9	.8	1.0	2.0
Flax	1	14	49	24.0	25.6	25.0	23.8	22.6	.6	1.2	1.2
Greenland	1	24	42	31.0	33.1	32.6	32.1	30.6	.5	.5	2.5
Griffith	1	18	35	33.0	30.9	30.4	30.0	28.5	.5	.4	1.5
Little Cliff	1	17	51	25.0	25.6	25.0	23.8	22.6	.6	1.2	1.2
Upper Mill	1	20	29	26.0	28.3	27.6	26.8	24.6	.7	.8	2.2
Lower Mill	1	18	31	26.0	28.0	27.3	26.5	24.4	.7	.8	2.1
Seymour	1	23	33	29.0	31.2	30.7	30.3	28.8	.5	.4	1.5
Sheep	1	20	39	31.0	32.9	32.4	32.0	30.6	.5	.4	1.4
Walkers	1	22	27	26.0	28.5	27.6	26.8	24.5	.9	.8	2.3
TOWN OF CHATHAM											
Goose	1	34	49	15.0	17.4	16.6	15.9	14.1	0.8	0.7	1.8
Lover's Lake	1	34	54	13.0	10.6	9.9	9.6	8.8	.7	.3	.8
School House	1	34	52	13.0	13.5	12.2	11.7	9.9	1.3	.5	1.8
White	1	37	53	14.0	9.0	8.2	8.0	7.6	.8	.2	.4
TOWN OF DENNIS											
Fresh	1	33	19	7.0	6.2	6.2	5.9	6.3	0	0.3	+0.4
Scargo Lake	1	15	16	12.0	15.3	15.4	15.1	15.4	+1	.3	+3
TOWN OF HARWICH											
Long (Brewster)	1	24	38	31.0	32.9	32.5	32.0	30.6	0.4	0.5	1.4
Bucks	1	31	42	30.0	29.4	28.3	27.9	26.3	1.1	.4	1.6
Grass	1	36	35	9.0	15.5	15.0	15.0	14.9	.5	0	.1
Hawk's Nest	1	27	43	32.0	32.9	32.3	31.7	30.1	.6	.6	1.6
Hinckley	1	26	33	28.0	30.9	30.5	30.1	28.8	.4	.4	1.3
Josephs	1	31	41	30.0	29.7	28.5	28.2	26.8	1.2	.3	1.4
Reservoir	1	33	27	7.0	7.8	7.8	7.1	7.8	0	.7	+7
Robbins	1	27	29	28.0	27.1	26.7	26.4	23.8	.4	.3	2.6
Sand	1	32	28	13.0	12.8	12.8	12.8	12.7	0	0	.1
Walkers	1	27	41	32.0	33.4	32.8	32.4	30.9	.4	.4	1.5
TOWN OF ORLEANS											
Crystal Lake	1	13	58	15.0	9.5	9.2	8.7	8.4	0.3	0.5	0.3
Pilgrim Lake	1	16	58	8.0	8.7	8.1	7.7	7.0	.6	.4	.7



**Table 12.** Model-calculated streamflow for selected streams in the West Cape and East Cape flow cells, Cape Cod Basin, Massachusetts

[All streamflow values are in cubic feet per second; locations of streamflow measurement sites are shown in figures 11 and 12]

Stream (Town)	Model-calculated streamflow		Year			Decrease in model-calculated streamflow between stress periods		
	Calibrated model	Predevel- opment	1975	1989	2020	Predevelopment- 1975	1975- 1989	1989- 2020
WEST CAPE FLOW CELL								
Coonamesset (Falmouth)	9.8	9.9	9.8	9.2	8.9	0.1	0.6	0.3
Childs (Falmouth)	5.8	5.8	5.8	5.2	4.5	0	.6	.7
Quashnet (Mashpee)	13.6	13.6	13.6	13.5	12.6	0	.1	.9
Mashpee (Mashpee)	10.2	10.2	10.2	10.1	9.5	0	.1	.6
Santuit (Barnstable)	4.1	4.1	4.1	3.9	3.3	0	.2	.6
Mill (Barnstable)	4.0	4.1	4.0	3.2	2.4	.1	.8	.8
Centerville (Barnstable)	1.4	1.4	1.4	1.4	1.4	0	0	0
EAST CAPE FLOW CELL								
Herring (Harwich)	4.3	4.7	4.3	4.0	2.6	0.4	0.3	1.4
Stony Brook (Brewster)	1.8	1.9	1.8	1.8	1.6	.1	0	.2

**Table 13.** Model-calculated water budgets for the West Cape and East Cape flow cells, Cape Cod Basin, Massachusetts

[All values are in cubic feet per second]

Budget item	Predevel- opment	Year		
		1975	1989	2020
WEST CAPE FLOW CELL (Area = $5.3 \times 10^9$ ft <sup>2</sup> )				
Inflow				
Recharge				
Natural .....	238.9	238.9	238.9	238.9
Wastewater return flow .....	0	8.9	13.0	22.2
Release from storage .....	0	0	0	0
Total inflow.....	238.9	247.8	251.9	261.1
Outflow				
Pumpage .....	0	16.9	24.2	48.3
Streams .....	51.3	51.5	49.2	46.2
Coastal discharge.....	178.1	170.0	169.7	158.0
Subsea discharge .....	10.3	10.3	10.3	10.3
Storage.....	0	0	0	0
Total outflow.....	239.7	248.7	253.4	262.8
Model error .....	-0.8	-0.9	-1.5	-1.7
(inflow minus outflow)				
Budget item	Predevel- opment	Year		
		1975	1989	2020
EAST CAPE FLOW CELL (Area = $2.4 \times 10^9$ ft <sup>2</sup> )				
Inflow				
Recharge				
Natural .....	83.2	83.2	83.2	83.2
Wastewater return flow .....	0	4.9	7.2	15.9
Release from storage .....	0	0	0.3	0
Total inflow.....	83.2	88.1	90.7	99.1
Outflow				
Pumpage .....	0	6.5	11.4	22.7
Streams .....	12.7	12.1	11.5	9.5
Coastal discharge.....	61.4	60.6	58.9	58.1
Subsea discharge .....	9.1	9.1	9.1	9.1
Storage.....	0	0	0	0
Total outflow.....	83.2	88.3	90.9	99.4
Model error .....	0	-0.2	-0.2	-0.3
(inflow minus outflow)				

## Response of the Freshwater-Saltwater Interface to Simulated Ground-Water Pumping and Recharge

Model-calculated changes in the position of the freshwater-saltwater interface were minimal between the two steady-state simulations, in which pumping and recharge rates were increased from predevelopment flow conditions to those projected to occur in the year 2020. For example, hydrogeologic sections in the north-south direction that show the interface location along one column of each model in which pumping is substantial indicate minimal change in the position of the interface for increased pumping and recharge rates (fig. 14). Also, the rate of freshwater discharge to overlying saltwater zones of the aquifer did not change substantially with increased pumping and recharge rates. The minimal change in the position of the freshwater-saltwater interface likely results from several factors. First, much of the existing and proposed pumping occurs more than 1 mi landward of the coasts and from the top two layers of the models, at depths less than 70 ft below sea level; the three-dimensional location of these withdrawals seems to place little landward stress on the interface. Second, the net stress on the interface due to pumping is decreased because a large percentage of the water pumped from the aquifer is returned to the aquifer through wastewater return flow. Finally, much of the wastewater return flow from septic systems occurs near the coasts where residences are concentrated. Hypothetically, this recharge of wastewater near the coasts helps to maintain a constant position of the interface with time.

Areas of fresh water overlying salt water and areas of fresh water that extend to bedrock, as determined by the SHARP models, are shown in figures 15 and 16. Salt water occurs between fresh water and underlying bedrock generally in areas that are within 1 to 2 mi landward of the coastline. Exceptions to this generalization are in the East Cape flow cell (fig. 16), where (1) water levels are low and salt water underlies a substantial part of the northeast and southeast areas of the flow cell and (2) where freshwater discharge is through clay and silt deposits that underlie Cape Cod Bay, which forces the freshwater-saltwater interface seaward of the coastline. Salt water generally is prevented from moving more than 1 to 2 mi landward of the coasts because of the high ground-water levels that occur in each flow cell, which is a reflection of the high recharge rates to the flow systems and thinness of the unconsolidated deposits.

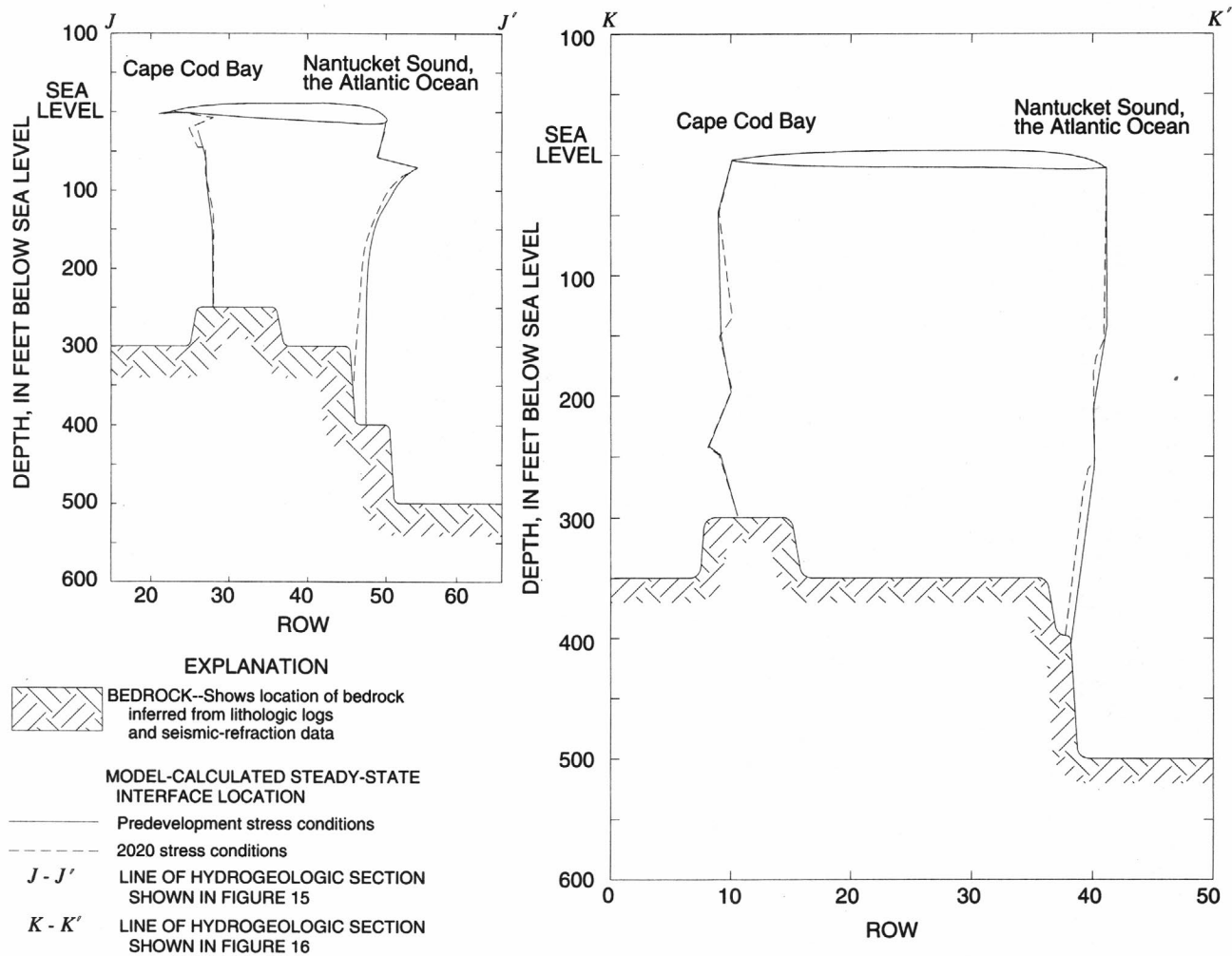


**Figure 14.** Steady-state location of the model-calculated freshwater-saltwater interface for predevelopment and projected 2020 stress conditions for (A) column 84 of the West Cape flow model and (B) column 40 of the East Cape flow model, Cape Cod Basin, Massachusetts.





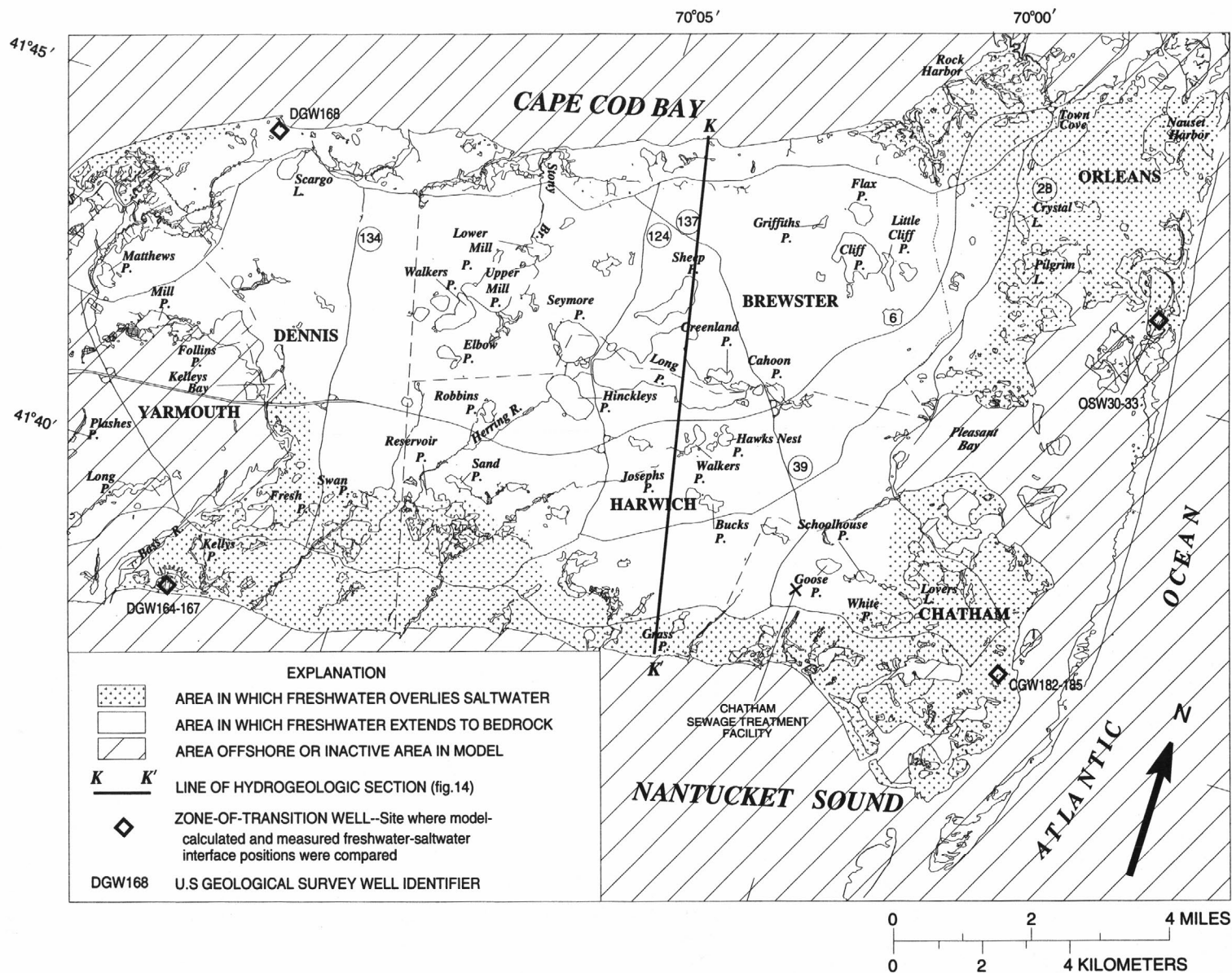


**Figure 16.** Model-calculated location of fresh water overlying salt water and fresh water extending to bedrock for the East Cape flow cell, Cape Cod Basin, Massachusetts.

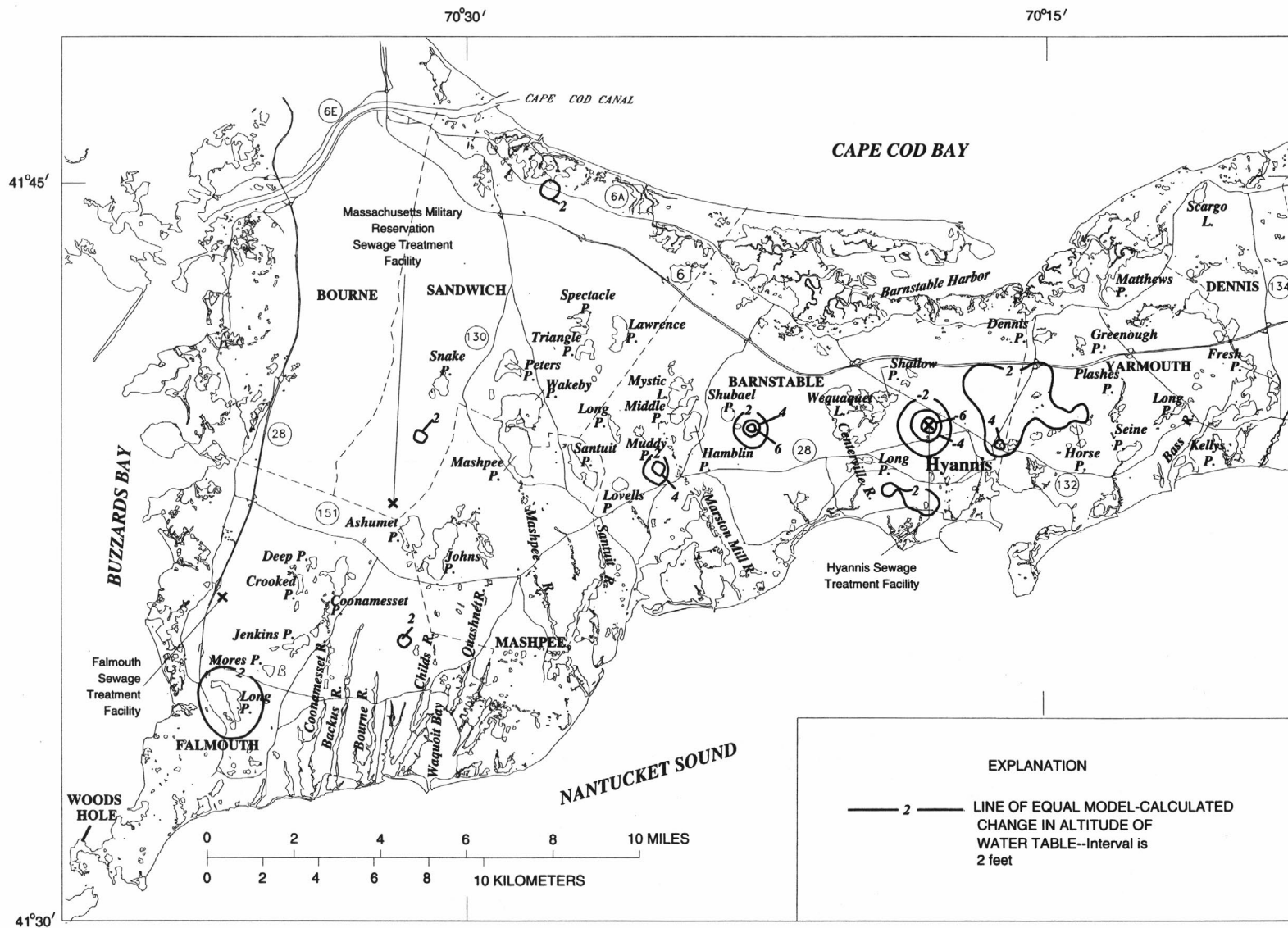
## Response of the Freshwater Flow Systems to Simulated Ground-Water Pumping and Recharge

Because the SHARP models indicated little movement of the freshwater-saltwater interface for the stress conditions simulated, boundary conditions along the freshwater-saltwater interface were assumed to remain constant with time. This assumption simplified the incorporation of the freshwater-saltwater boundary conditions calculated by the SHARP models within the MODFLOW models. This was done to complete a detailed analysis of the freshwater-flow systems with the MODFLOW models, which are less computationally intensive than the SHARP models. Boundary conditions along the freshwater-saltwater interface calculated for steady-state flow conditions using the projected 2020 pumping and recharge rates were used in the MODFLOW models. The methodology for incorporating these boundary conditions was discussed in the section "Boundary Conditions" and shown schematically in figure 10.

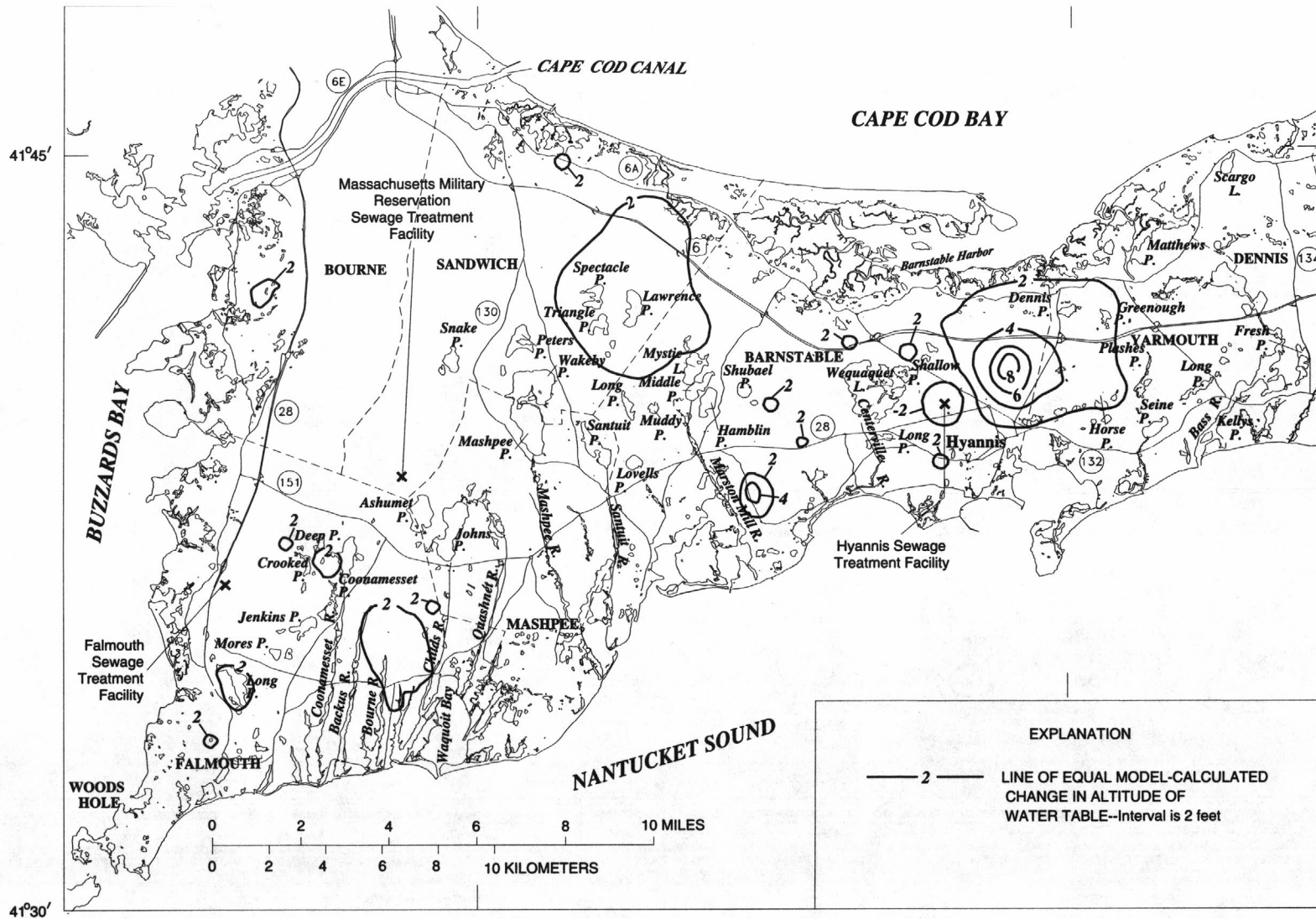
Despite the substantial increases in pumping with time, the average model-calculated decline in heads in the flow cells generally was a small percentage of the saturated thickness of the aquifer in each flow cell. The model-calculated average decline in water-table altitude at the observation wells was 0.4 and 0.8 ft for the West Cape and East Cape flow cells, respectively, from predevelopment flow conditions to 1975 (tables 8 and 9). From 1975 to 1989, the average model-calculated decline in water-table altitudes at the observation wells was 0.3 and 0.6 ft for the West Cape and East Cape flow cells. Model-calculated declines in water levels for the projected 2020 stress conditions are estimated to increase by an average of 1.1 ft in the West Cape and 1.5 ft in the East Cape flow cells between 1989 and 2020. Model-calculated total average declines in the water table at the observation wells are, then, 1.8 and 2.9 ft in the West Cape and East Cape flow cells, respectively, for the simulation period.

Model-calculated pond levels declined an average of 0.4 and 0.5 ft in the West Cape and East Cape flow cells, respectively, from predevelopment flow conditions to 1975 and 0.4 and 0.5 ft, respectively, from 1975 to 1989 (tables 10 and 11). Model-calculated pond level declines are estimated to increase by an average of 1.3 ft in the West Cape and East Cape flow cells between 1989 and 2020.

Maps showing model-calculated changes in the altitude of the water table (drawdowns) in the flow cells show areas of local stresses in response to changing pumping and recharge rates (figs. 17-20). Model-calculated declines due to ground-water pumping were largest at the sites of major pumping centers—in the towns of Falmouth and Barnstable in the West Cape flow cell and in the towns of Dennis and Harwich in the East Cape flow cell. In the West Cape flow cell, simulated pumping from Long Pond in Falmouth resulted in a 5.2-foot decline in pond-level altitude from predevelopment flow conditions to 1975 (table 10), however, the water table increased 6 ft beneath the wastewater-treatment facility in Hyannis during the same period due to simulated increased discharge rates at the facility. Model-calculated declines in water levels from 1975 to 1989 in both flow cells were, on average, less than those that occurred from predevelopment flow conditions to 1975. For example, the level of Long Pond Reservoir in Falmouth actually increased by 1.4 ft from 1975 to 1989 as a result of the decrease in the average daily pumping rate from the reservoir from 2.7 to 2.0 Mgal/d. The simulated increase from 1989 to projected 2020 pumping rates resulted in the largest drawdowns in both flow cells. Model-calculated water levels in the eastern part of Barnstable showed declines as much as 8 ft near Mary Dunn Pond. Model-calculated water-level declines in the East Cape flow cell are estimated to be the largest in Dennis, where pumping is projected to increase from 2.5 to 5.3 Mgal/d from 1989 to 2020.



**Figure 17.** Model-calculated change in the altitude of the water-table configuration in the West Cape flow cell from predevelopment to 1989, Cape Cod Basin, Massachusetts.





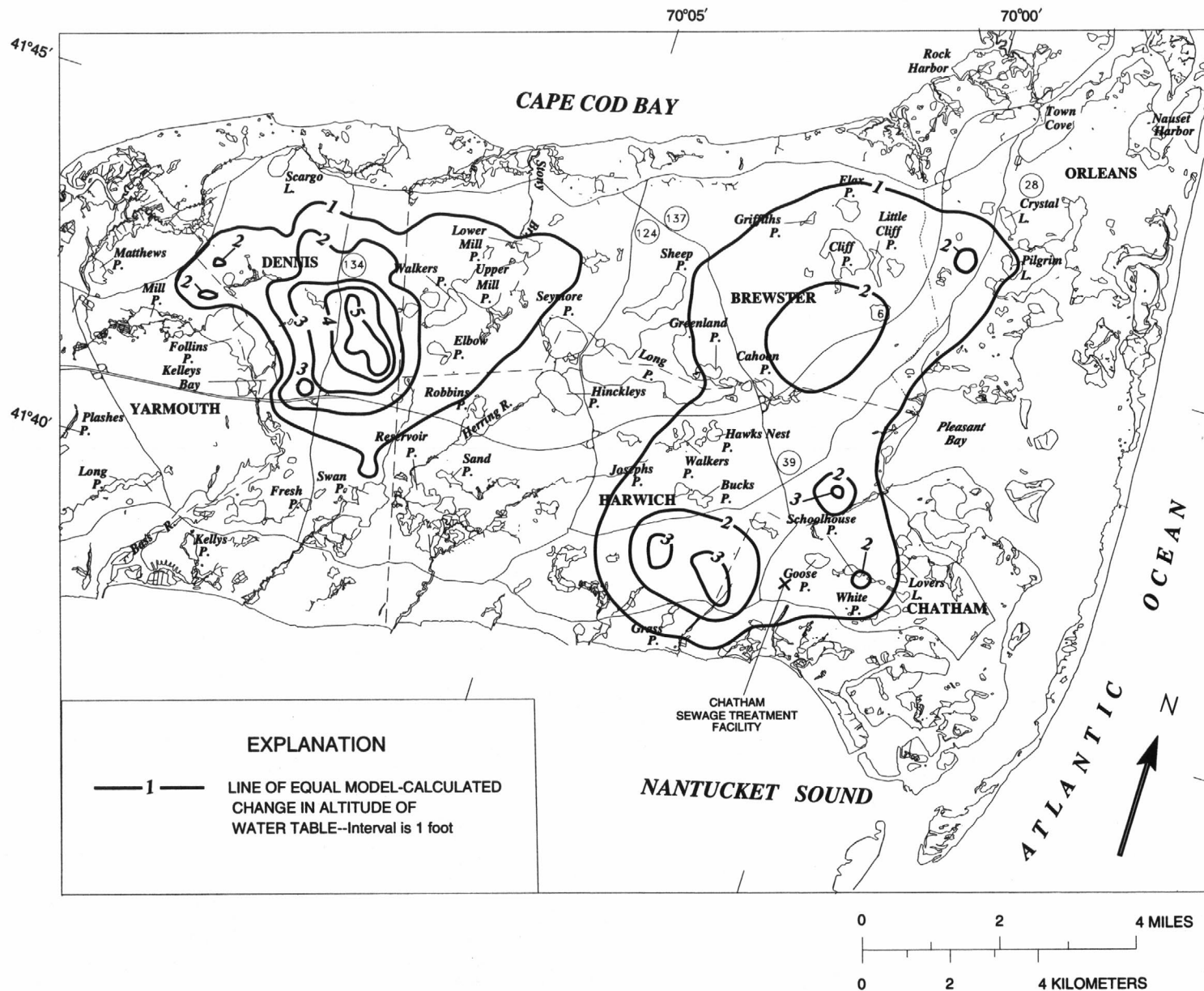


**Figure 19.** Model-calculated change in the altitude of the water-table configuration in the East Cape flow cell from predevelopment to 1989, Cape Cod Basin, Massachusetts.

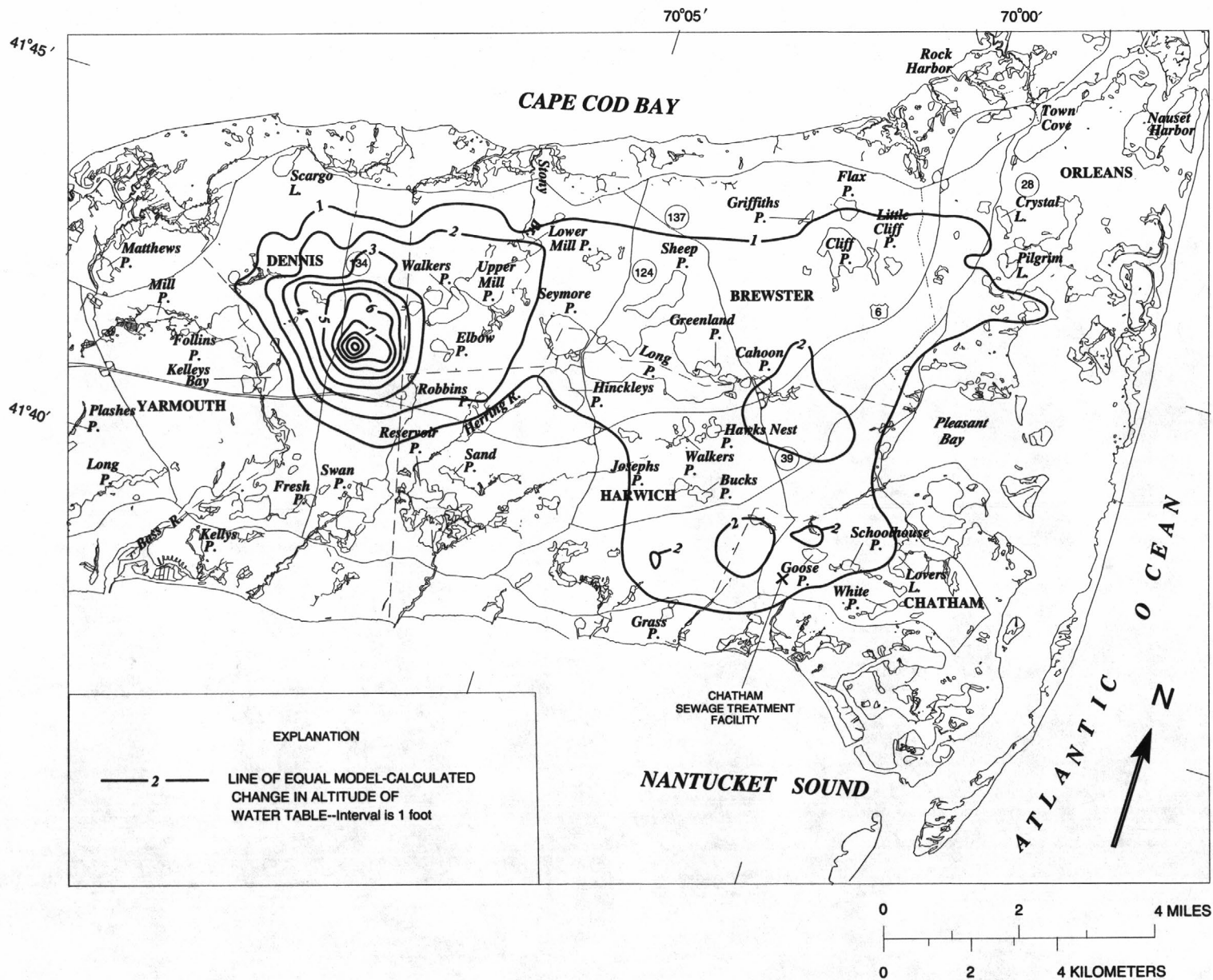


**Figure 20.** Model-calculated change in the altitude of the water-table configuration in the East Cape flow cell from 1989 to 2020, Cape Cod Basin, Massachusetts.

Model-calculated streamflow depletions from predevelopment flow conditions to 2020, as a percentage of model-calculated predevelopment flow conditions, are greatest for the Marston Mill, Santuit, and Childs Rivers in the West Cape flow cell. Model-calculated streamflow depletions from predevelopment flow conditions to 2020 are least for the Quashnet, Mashpee, and Centerville Rivers in the West Cape flow cell. The average streamflow for the nine streams simulated decreased between each of the three stress periods (predevelopment flow conditions to 1975, 1975-89, and 1989-2020) (table 12). The average depletion in the model-calculated rate of streamflow at the gaging points for eight of the nine rivers during the simulation period is 14 percent of the model-calculated predevelopment streamflow in the rivers. The Herring River in the East Cape flow cell was not included due to the significant contribution of surface-water outflow from Hinckley's Pond that could not be simulated.

The total inflow and outflow of fresh water to each of the flow cells increases from predevelopment flow conditions to 2020 because the total pumping rate and wastewater return flow to each system increases with time (table 13). The wastewater return flow recharge rates specified in the West Cape and East Cape flow models were less than 90 percent of the total public-supply pumping rates. Wastewater return flow at coastal roads is lost to the flow cells due to the approximation of the coastline used for boundary conditions for the current model grid discretization. The increased rate of ground-water pumping from the flow cells resulted in a decrease in water-table and pond altitudes in the flow cells and decreased rates of freshwater discharge to streams and saltwater boundaries. For example, total ground-water discharge to streams in the West Cape flow cell decreases from 51.3 to 46.2 ft<sup>3</sup>/s from predevelopment flow conditions to 2020 (table 13), a decrease of nearly 10 percent of the total predevelopment ground-water discharge to streams. The total model-calculated decrease in coastal discharge from predevelopment flow conditions to 2020 is 11 percent and 5 percent of total predevelopment coastal discharge in the West Cape and East Cape flow cells, respectively. The changes in the altitude of the water table and pond levels was due to the removal of freshwater from storage (tables 8-11, figs. 17-20).

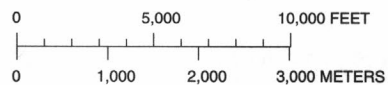
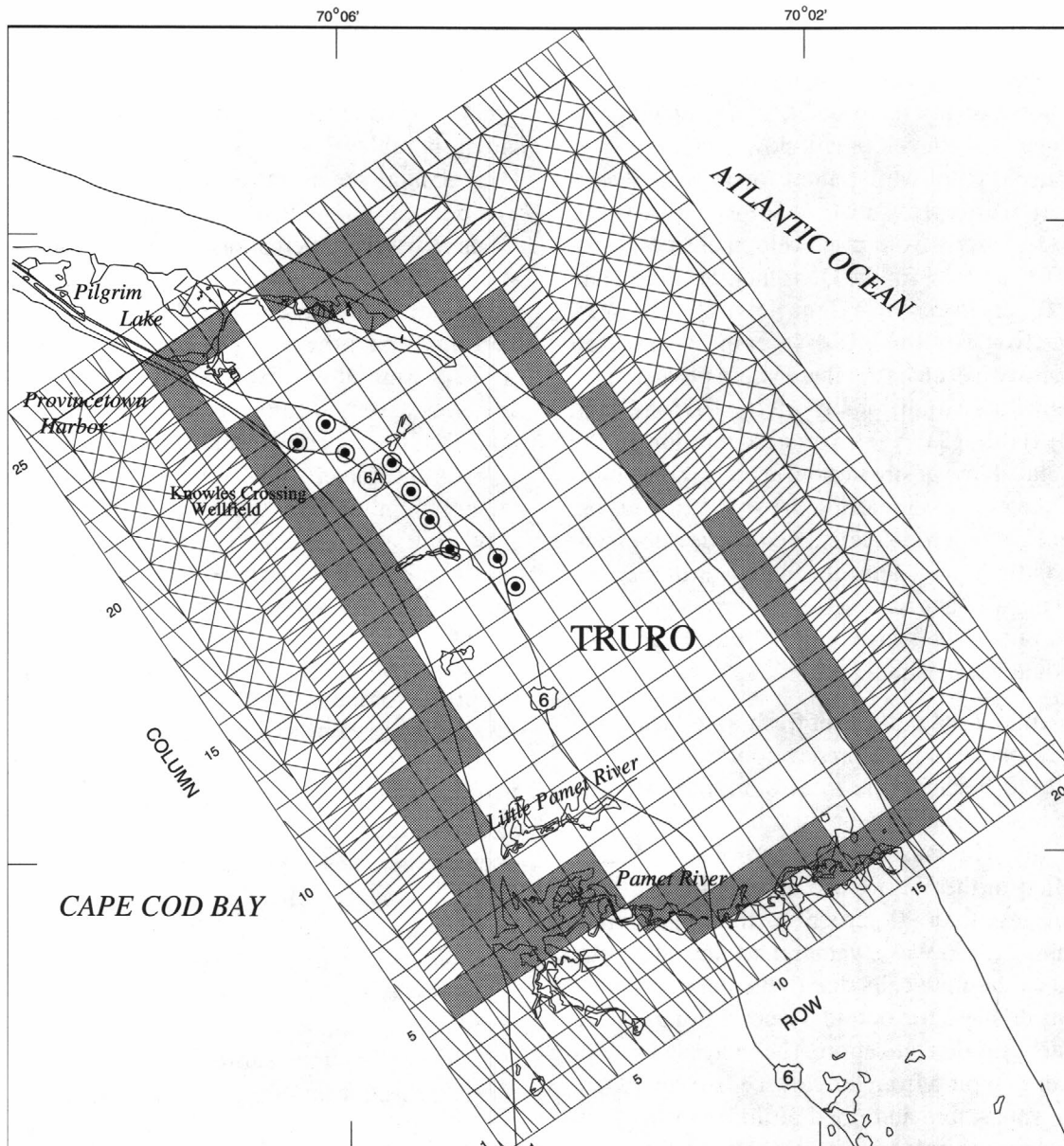
Summer and winter pumping and recharge rates for 1989 were used to investigate the effects of a 30-percent decrease in recharge to the flow cells over a hypothetical

5-year period of drought. Summer (in-season pumping rates) and winter (off-season pumping rates) for 1989 shown in tables 3 and 4 were used in the simulations. Total annual precipitation recharge to the flow cells was decreased by 30 percent, and all precipitation recharge was assumed to occur between September and May, which is consistent with the timing of precipitation recharge to the flow cells determined by LeBlanc and others (1986) and Barlow and Hess (1993). Simulated recharge from wastewater return flow was assumed to occur uniformly throughout the year. Two stress periods were simulated for each year—a 3-month summer stress period (June through August) and a 9-month winter stress period (September through May). Initial conditions used in the simulation were model-calculated water levels for 1989.

The average model-calculated range of fluctuation in water-table altitudes between summer and winter stress conditions for the 32 observation wells in the West Cape flow cell and 19 observation wells in the East Cape flow cell were 2.0 and 1.7 ft, respectively. Model-calculated fluctuations were greatest near the top of the ground-water mounds and least near the coast where water levels are held nearly constant because of the ocean discharge boundary. Changes in pumping and recharge rates resulted in a model-calculated average streamflow decrease of 36 percent between summer and winter stress conditions for the nine streams simulated. Model-calculated coastal discharge decreased 14 percent in each flow cell and the subsea discharge was negligible. Water released from storage accounts for 90 and 84 percent of the total inflow to the ground-water systems for West Cape and East Cape flow cells, respectively, for the summer stress period, which resulted from the large decrease in recharge to the systems and doubling of ground-water pumping that occurred during the summer stress period.

## Truro Flow Cell

The Truro flow cell is the smallest of the five flow cells of Cape Cod that are used for water supply. The flow cell includes the town of Truro and extends from the Pamet River northward to Pilgrim Lake (fig. 21). Although the sand and gravel aquifer that constitutes the flow cell extends to bedrock, the freshwater-flow system is bounded at depth (within the unconsolidated deposits) by the transition zone between fresh water and



EXPLANATION	
	ACTIVE NODE--Modeled area
Head-dependent flux nodes	
	Coastal discharge areas, layer 1
	Coastal discharge areas, layer 2
	Coastal discharge areas, layer 3
	Areas of wastewater-return flow layer 1
	INACTIVE NODE--Outside active modeled area

re 21. Grid and boundary conditions for the Truro flow cell, Cape Cod Basin, Massachusetts.



underlying salt water (Guswa and LeBlanc, 1985; LeBlanc and others, 1986). Upconing of the freshwater-saltwater interface and contamination of public-water supplies by saltwater intrusion caused by pumping have been recorded at the Knowles Crossing well field, located 1,500 ft from Cape Cod Bay (LeBlanc and others, 1986). Evidence of saltwater intrusion precluded an assumption of a static interface between fresh water and salt water; consequently, the ground-water-flow system was assessed using a freshwater-saltwater flow model.

## Description of Model

### Grid

The finite-difference grid of the ground-water-flow system consists of uniform nodes 1,320 by 1,320 ft. The grid contains 26 columns and 20 rows and has approximately the same orientation and extent as that used by Guswa and LeBlanc (1985). The aquifer was subdivided into seven layers to provide an adequate vertical representation of the aquifer's lithology. The model extends from the water table to the contact between unconsolidated sediments and bedrock. The bottom altitude of these layers range from 10 to 900 ft below sea level (table 7).

### Hydraulic properties

The hydraulic properties used in the model of the Truro flow cell were assigned on the basis of available aquifer test, lithologic, and geologic information. There are few deep wells in this ground-water-flow system; therefore, lithologic information necessary to determine hydraulic properties of the lower layers is limited. Hydraulic properties of the aquifer material in areas with little or no lithologic information were estimated from an interpretation of the geologic processes that formed the sand and gravel deposits in the flow cell.

Horizontal hydraulic conductivity assigned in the model ranged from 350 ft/d for medium sand to gravel to 50 ft/d for fine sand. The ratio of vertical to horizontal hydraulic conductivity ranged from 1:3 for medium sand to gravel to 1:30 for fine sand. The porosity of the aquifer was assumed to be constant throughout the aquifer and equal 0.30. A specific yield of 0.10 was used in the model, which was based on the results of aquifer

tests done in the flow cell (Guswa and LeBlanc, 1985); a storage coefficient of  $2 \times 10^{-4}$  was used in the model and was based on the results of Barlow and Hess (1993).

### Boundary conditions

The Truro model is bounded on top by the water table, which is a free-surface boundary that receives spatially and temporally variable rates of recharge. Recharge rates specified for the flow model are discussed in the next section "Stresses and Stress Periods." The lower boundary of the model was the contact between the unconsolidated glacial sediments and the underlying bedrock, which was assumed to be impermeable. Each model layer is bounded laterally by inactive nodes that separate modeled areas from unmodeled areas.

Head-dependent flux boundary conditions were used to simulate saltwater discharge areas. The head values specified at saltwater discharge boundaries are equivalent freshwater heads equal to the height of the column of salt water overlying the seabed at the discharge boundary divided by 40.0, the ratio of the specific weight of fresh water ( $1.000 \text{ g/cm}^3$ ) to the difference between the specific weight of salt water ( $1.025 \text{ g/cm}^3$ ) and fresh water (Essaid, 1990). The height of the column of salt water in each node was determined from bathymetric maps of the area. Head-dependent flux boundaries at saltwater discharge areas are in the top three model layers from 0 to 80 ft below sea level. A vertical leakance of  $20 \text{ day}^{-1}$  for the seabed deposits was used in the simulations, which corresponds to a 1-foot thick sediment deposit on the seabed with a vertical hydraulic conductivity of 20 ft/d. This value of vertical leakance of seabed deposits also was used by Guswa and LeBlanc (1985) in their model of the area.

Ground-water discharge areas at Pilgrim Lake and Pamet River were simulated as head-dependent flux boundaries in the model. Freshwater heads specified at these boundaries were determined from surface-water altitudes shown on topographic maps. A small section along the northern boundary of the model where the Truro flow cell and the adjoining Provincetown flow cell meet was designated as an inactive node because there are no surface-water discharge bodies present here.

## Stresses and stress periods

The effects of changing stress conditions in the Truro flow cell were determined for predevelopment, 1975, 1989, and projected 2020 average daily demand stresses. The response of the flow cell to fluctuations in pumping and recharge rates between in-season and off-season conditions was determined for current conditions based on 1989 in-season and off-season pumping and recharge rates.

Recharge at the water table was estimated to be 19.8 in/yr by the method of Thornwaite and Mather (1957), using 80 years of precipitation and air temperature data measured at the Provincetown weather station and an assumed soil-moisture capacity of the root zone of 4 in. This precipitation recharge estimate is consistent with others previously made for the Cape Cod flow system (LeBlanc, 1984b; LeBlanc and others, 1986; Barlow and Hess, 1993).

Predevelopment conditions assumed that there was no pumping from the public-supply well, that there was no recharge to the water table other than that from precipitation, and that change in aquifer storage was negligible. The resulting head distribution and freshwater-saltwater interface position from the predevelopment simulation was used as the initial condition for subsequent transient simulations.

The 1975 stress condition assumed an average annual pumping rate for 1950 and 1981. Aquifer recharge during the 1975 stress condition equaled the average annual recharge rate of 19.8 in/yr added to wastewater return flow from septic systems. Wastewater return flow from septic systems was estimated for the area between Route 6 and Route 6A that receives water supplies from the Provincetown Water Department. The model nodes that received wastewater return flow within the Truro flow cell are shown in figure 21.

The rate of water supplied to the area between Route 6 and Route 6A is about 12 percent of the Provincetown Water Department's total pumpage during the winter (off-season) and about 25 percent of the total pumpage during the summer (in-season) (J.M. Cook, Provincetown Water Department, oral commun., 1992). The average annual rate of water supplied to this area then is assumed equal to 15 percent of the Water Department's annual ground-water pumpage. A recharge rate from wastewater return flow was calculated by dividing the total daily rate of water supplied to the area by the area

of the grid nodes where the water supply is distributed. In order to account for consumptive losses, 90 percent of the total rate supplied to the area was returned to the simulated aquifer, as was done for the West and East Cape models. Return flow from domestic and commercial septic systems in the areas not receiving water from the Provincetown Water Department was assumed to be equal to the amount of water withdrawn at each site; therefore, net ground-water recharge from wastewater return flow was assumed to be zero. The average annual 1975 pumping rate is 0.91 Mgal/d. The simulated return-flow rate for the septic systems between Route 6 and Route 6A equaled 90 percent of the 15 percent of the total pumping, which equaled 0.12 Mgal/d.

The 1989 stress condition was simulated by use of off-season and in-season pumping periods. The off-season period was assumed to be from September through May. All annual natural recharge was assumed to occur during this 9-month period. The simulated return-flow recharge was 90 percent of the 12 percent of the ground-water pumpage distributed between Route 6 and Route 6A. The inseason pumping period simulated 3 months of summer pumping rates with no natural recharge. The only simulated recharge to the system during the in-season pumping period was that distributed between Route 6 and Route 6A (fig. 21), which equaled 90 percent of the 25 percent of the total ground-water pumpage. A hypothetical 5-year drought with a 30-percent decrease in natural recharge was simulated from 1989 to 1994 to determine the effects of a decrease in recharge on the water-table altitude and the position of the freshwater-saltwater interface. The projected stress condition for 2020 was simulated based on the projected average daily pumping rates supplied by MOWR.

## Calibration

The Truro flow model was calibrated by comparing model-calculated water levels to measured water levels at 11 observation well locations (fig. 22). Average water levels for 1963-76 were compared to water levels calculated by the model for 1975. Average water levels for 1963-76 were compared to calculated water levels for 1975 because (1) measured water-level information was not available for predevelopment flow conditions; (2) this time period is consistent with that used for model calibration by Guswa and LeBlanc (1985); and (3) water levels measured in these observation wells in

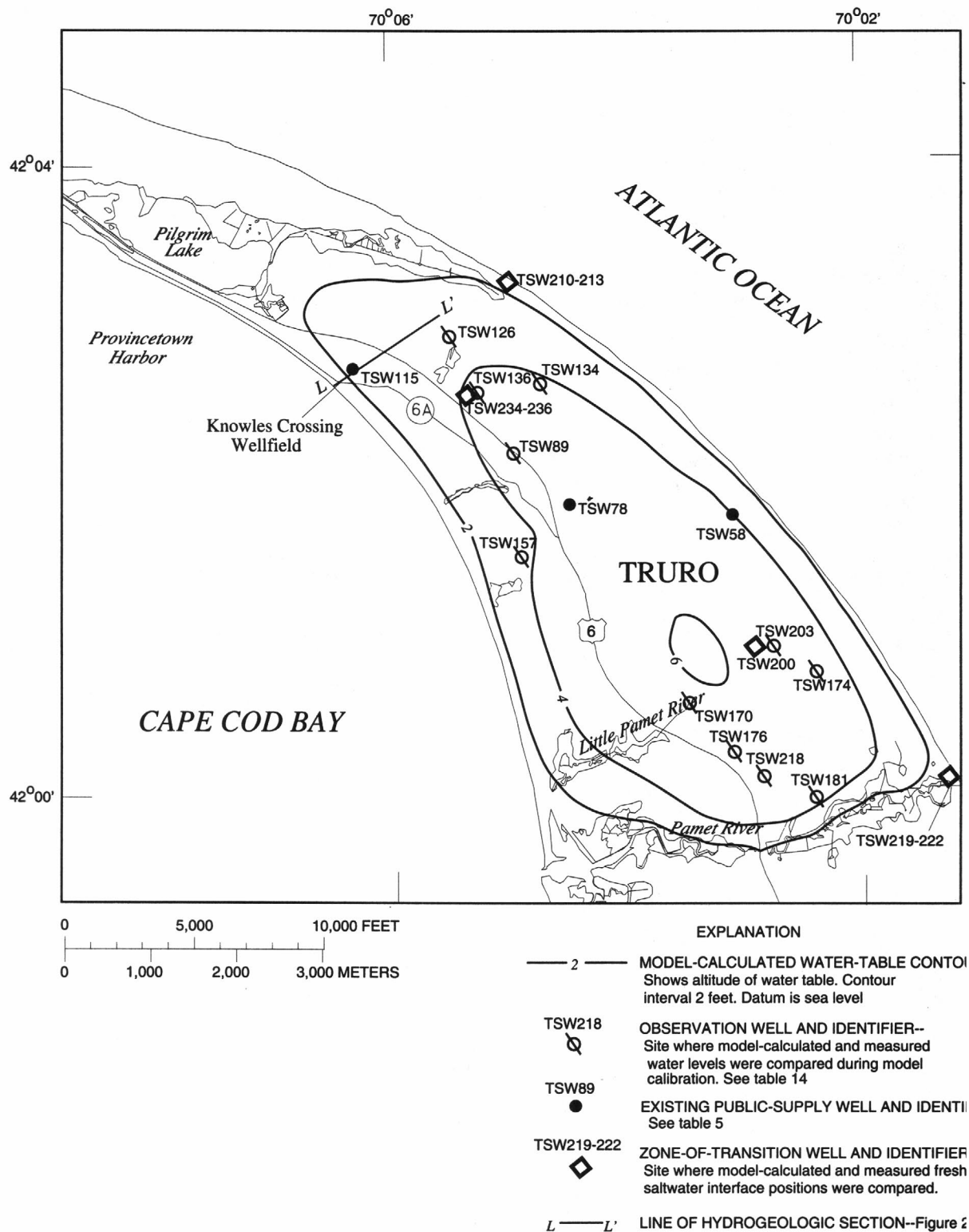


**Figure 22.** Model-calculated water-table configuration for the Truro flow cell, Cape Cod Basin, Massachusetts, 1989.

1975 are representative of long-term average water levels reported for the observation wells for the 1963-76 period (Letty, 1984).

Initial estimates of horizontal hydraulic conductivity and vertical conductance were adjusted within reasonable limits during model calibration. Generally, agreement between model-calculated and measured water levels at observation wells is close (table 14). The mean error between model-calculated water levels for 1975 and measured average water levels in observation wells was 0.3 ft, or 4 percent of the total relief of the water table in the Truro flow cell.

Chloride data from four zone-of-transition wells (LeBlanc and others, 1986) were used for comparison to freshwater-saltwater interface locations calculated by the SHARP model in the Truro flow cell. Model-calculated interface locations for 1975 were compared

to measured chloride data collected between August 1973 and April 1976; results for the four wells are shown in figure 23. The measured data generally indicate that chloride concentrations increase with depth, which is indicative of the transition between freshwater- and saltwater-flow systems. The model-calculated vertical distribution of fresh water and salt water at the four well sites generally agrees well with the chloride data and is considered adequate for the purpose of this investigation.

Total inflow to the Truro flow cell ranges from 14.9 to 15.2 ft<sup>3</sup>/s from predevelopment flow conditions to 2020 (table 15). Most ground-water discharge is to coastal discharge areas; pumping comprises a maximum of 11 percent of the freshwater discharge from the flow cell.

**Table 14.** Average measured water levels for selected wells, 1963-76, and model-calculated water levels for 1975, 1989, and projected for 2020 for the Truro flow cell, Cape Cod Basin, Massachusetts

[Location of wells shown in figure 22. Change in model-calculated water level between stress periods: +, increase in the water level resulting from changing stress conditions; otherwise, a change is a decrease in water level. --, no value reported]

Well No.	Model node			Average measured water level, in feet above sea level	Model-calculated water levels, in feet above sea level				Change in model-calculated water level between stress periods, in feet		
	Layer	Row	Column		Prede- velop- ment	Year			Predevel- opment- 1975	1975- 1989	1989- 2020
						1975	1989	2020			
OBSERVATION WELLS											
TSW157	7	8	<sup>1</sup> 13-14	4.4	4.2	3.9	3.8	3.5	0.3	0.1	0.3
TSW176	7	10	5	5.6	5.2	5.2	5.2	5.1	0	0	.1
TSW170	7	10	7	5.9	5.8	5.7	5.7	5.6	.1	0	.1
TSW 89	7	10	16	4.4	4.9	4.6	4.5	4.3	.3	.1	.2
TSW136	7	10	<sup>1</sup> 18-19	4.3	4.4	4.4	4.2	4.2	0	.2	0
TSW126	7	10	20	4.2	4.0	3.9	3.9	3.9	.1	0	0
TSW218	7	11	4	5.2	5.1	5.0	5.0	5.0	.1	0	0
TSW181	7	12	<sup>1</sup> 3-4	4.7	4.8	4.8	4.8	4.8	0	0	0
TSW134	7	12	<sup>1</sup> 17-18	4.9	4.4	4.3	4.2	4.1	.1	.1	.1
TSW203	7	13	8	5.7	5.8	5.7	5.7	5.6	.1	0	.1
TSW174	7	14	6	5.6	4.8	4.8	4.7	4.7	0	.1	0
PUBLIC-SUPPLY WELLS											
TSW115	7	7	21	--	2.8	0.9	2.2	2.2	1.9	+1.3	0
TSW 78	7	10	14	--	5.4	4.0	3.7	2.8	1.4	.3	.9
TSW 58	7	14	12	--	4.9	4.7	4.4	4.1	.2	.3	.3

<sup>1</sup>Where an observation well lies near the boundary of adjacent model cells, an average decline in levels is reported.



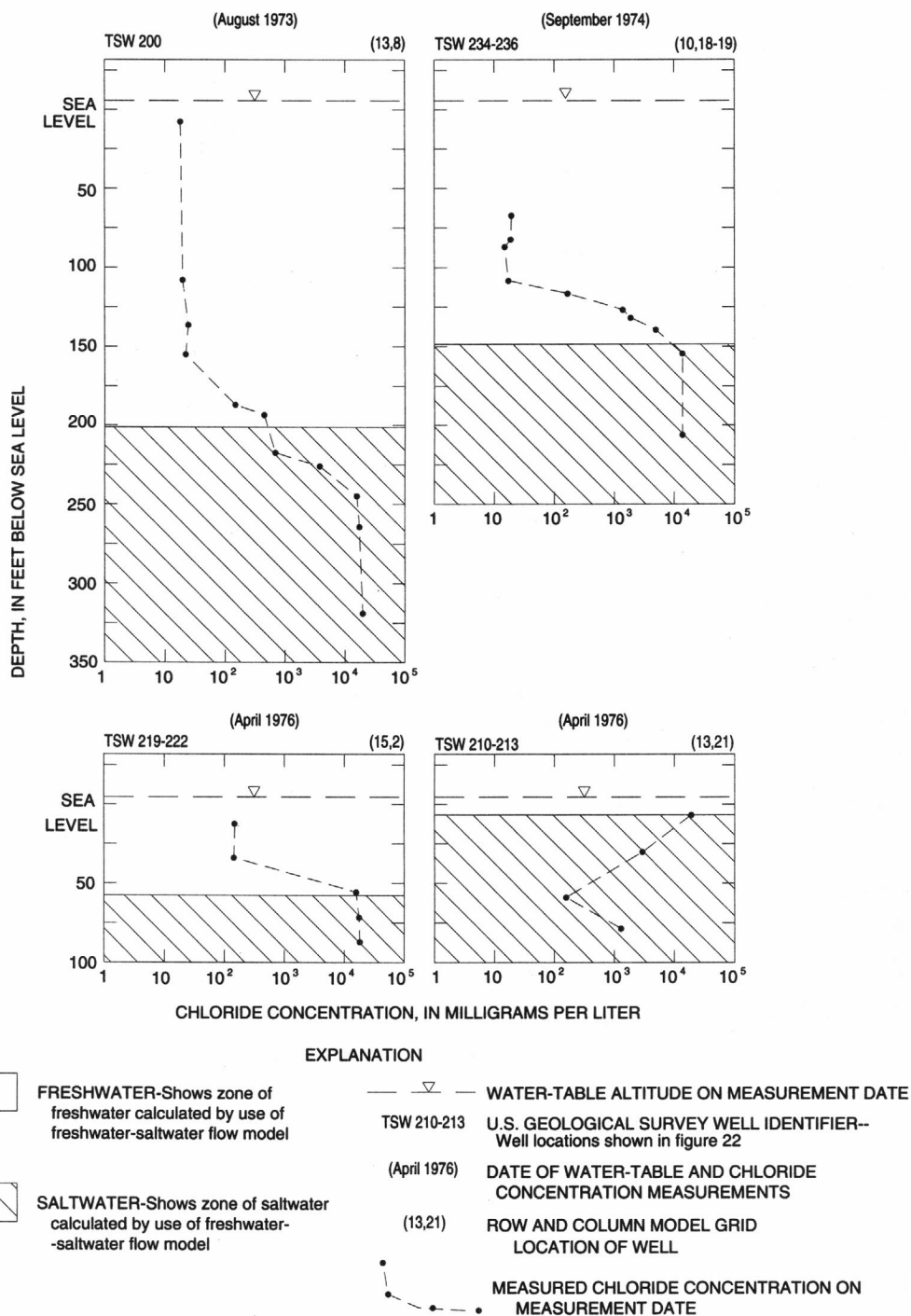


**Figure 23.** Measured chloride concentrations and model-calculated freshwater and saltwater zones at selected observation wells in the Truro flow cell, Cape Cod Basin, Massachusetts.

**Table 15.** Model-calculated water budgets for the Truro flow cell, Cape Cod Basin, Massachusetts

[All values are in cubic feet per second]

Budget item	Predevelopment	Year		
		1975	1989	2020
TRURO FLOW CELL (Area = $2.7 \times 10^8$ ft <sup>2</sup> )				
Inflow				
Recharge				
Natural .....	14.9	14.9	14.9	14.9
Wastewater return				
flow .....	0	.2	.2	.3
Release from storage .....	0	0	0	0
Total inflow .....	14.9	15.1	15.1	15.2
Outflow				
Pumpage .....	0	1.4	1.2	1.7
Coastal discharge .....	12.3	11.6	11.9	11.3
Subsea discharge .....	2.1	2.0	1.9	1.9
Storage .....	0	0	0	0
Total outflow .....	14.4	15.0	15.0	14.9
Model error .....	0.5	0.1	0.1	0.3
(inflow minus outflow)				

### Response of the Freshwater-Saltwater Flow System to Simulated Ground-Water Pumping and Recharge

The effects of changing stress conditions on the ground-water-flow system of the Truro flow cell show that increases in ground-water pumping and (or) decreases in the aquifer recharge result in (1) a decrease of discharge to coastal and subsea discharge boundaries (table 15); (2) a decline in water-table altitude (figs. 24 and 25; table 14); and (3) a decrease in the depth to the freshwater-saltwater interface. Pumping rates from the Truro flow cell generally increase from 1975 to 2020 due to projected increases in population and development. However, increases in pumping had a negligible effect on the water-table altitude, position of the freshwater-saltwater interface, and coastal and subsea discharge despite the fact that about 86 percent of the total pumpage is lost from the ground-water-flow system. The effect of changing stresses on the ground-water-flow system is most pronounced at the grid nodes where public-supply wells are located.

The Knowles Crossing well field (TSW 115) located 1,500 ft from the coast with a screen interval from 20 to 36 ft below sea level shows a model-calculated decline in water level of nearly 2 ft from the predevelopment flow conditions to 1975. The model-calculated depth to the freshwater-saltwater interface decreased from 90 to 35 ft below sea level causing saltwater contamination at the well screen (fig. 26). Simulated pumping rates were decreased for the 1975-89 stress condition; the model-calculated water-table altitude rose 1.3 ft and the position of the interface increased from 35 to 65 ft below sea level during that period. Although simulated pumping rates increased from 1989 to 2020, the model-calculated depth to the freshwater-saltwater interface had still increased, implying that the interface is still recovering from the 1975 stress condition.

Seasonal fluctuations in the water budget show that during the off-season, aquifer recharge replenishes the ground water removed from storage during the increased stress of the in-season. Although the seasonal change in aquifer recharge is significant, the effects on coastal and subsea discharge are minimal due to the changes in the storage component of the water budget. Changes in the water-table altitude at the observation well nodes show an average seasonal fluctuation of 0.2 ft.

The total simulated ground-water pumpage from the Truro flow cell from 1975 to the 1989 stress conditions were nearly equal. However, simulated pumping rates at Knowles Crossing were decreased from 0.45 Mgal/d average daily demand in 1975 to 0.12 Mgal/d average daily demand in 1989 to reverse the effects of saltwater intrusion. The simulated decrease in pumping at Knowles Crossing well field was offset by additional pumping of the public-supply well at the North Truro Air Force Base and increased pumping from the South Hollow well.

The simulated redistribution of pumping from 1975 to 1989 resulted in an increase in the depth of the freshwater-saltwater interface at Knowles Crossing well field such that the well can continue to be used for public supply. Water-quality data collected from water pumped from the well field showed a subsequent decrease in chloride concentration with a decrease in pumping rate at the well field (J.M. Cook, Provincetown Water District; written commun., 1992). The 1989 simulation shows that increased pumping at South Hollow well resulted in a model-calculated decrease in

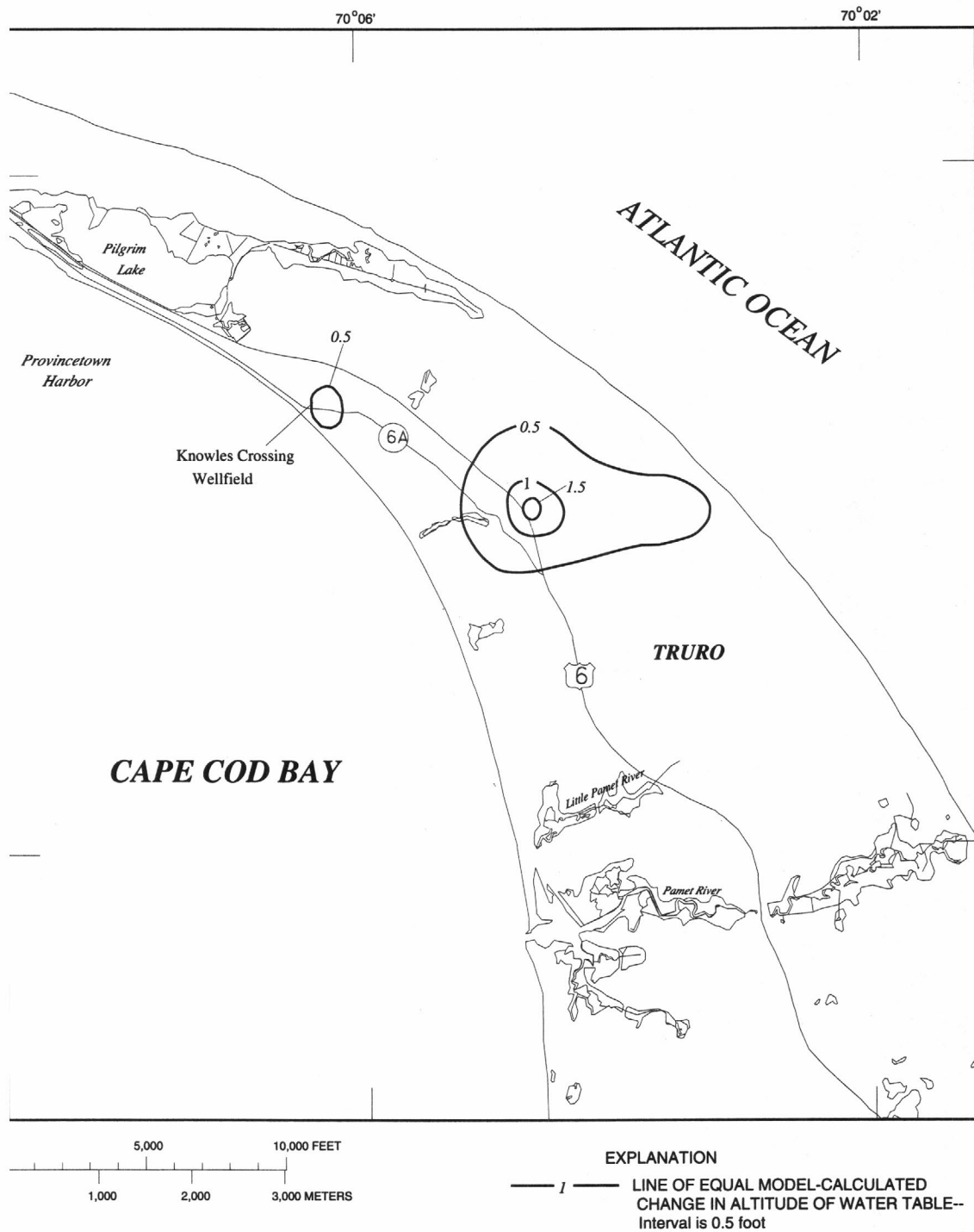


**Figure 24.** Model-calculated change in the altitude of the water-table configuration in the Truro flow cell from predevelopment to 1989, Cape Cod Basin, Massachusetts.

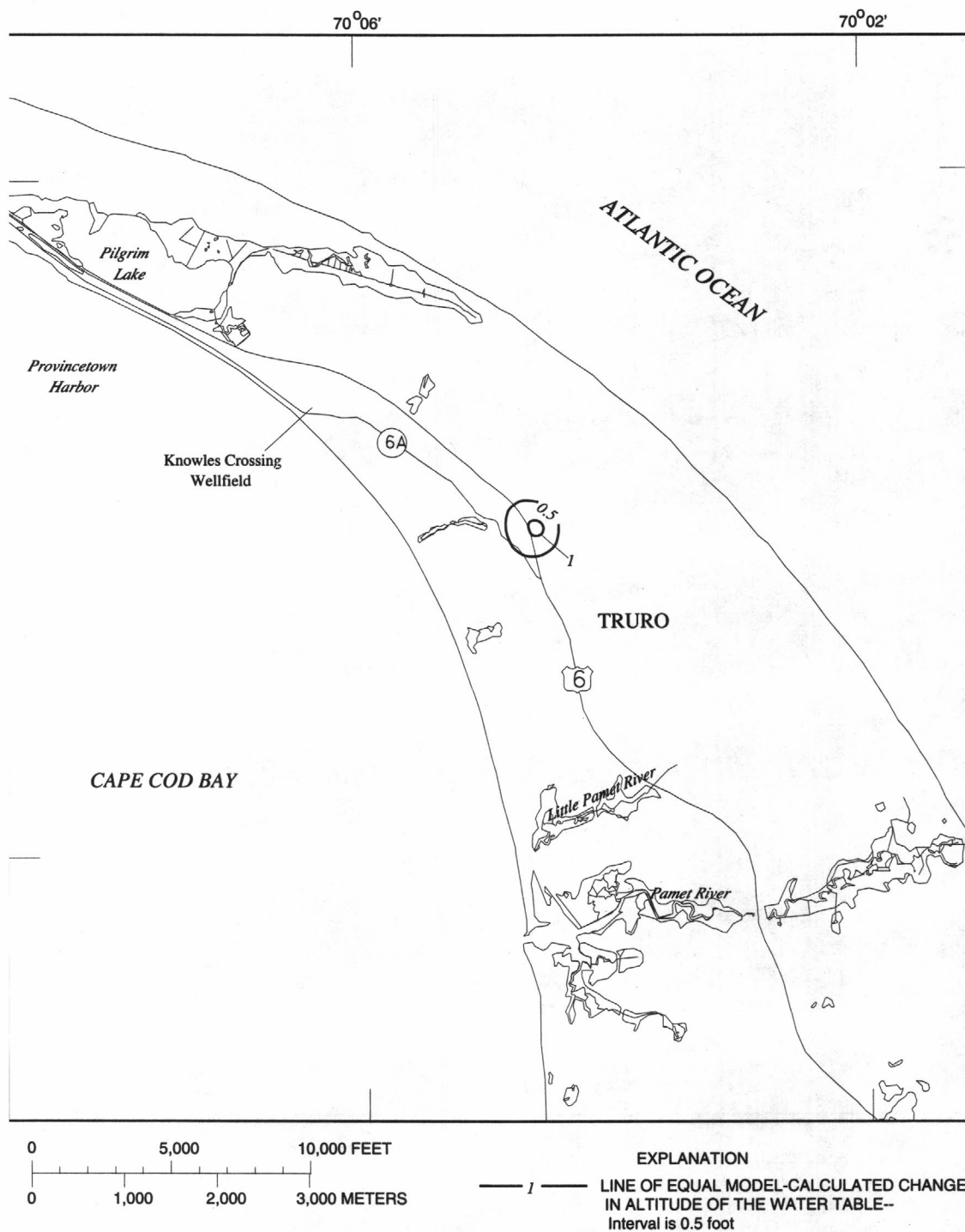


**Figure 25.** Model-calculated change in the altitude of the water-table configuration in the 10 flow cell from 1989 to 2020, Cape Cod Basin, Massachusetts.



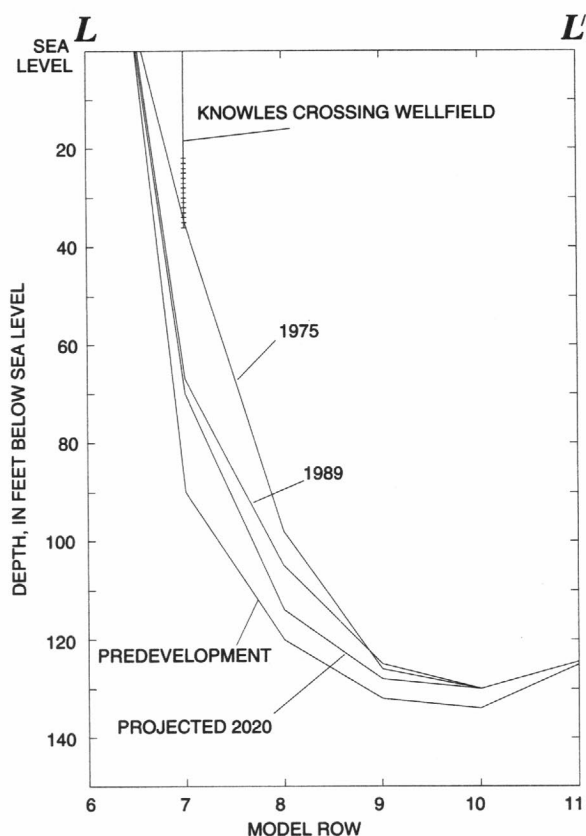


**Figure 26.** Model-calculated position of the freshwater-saltwater interface along section L-L' (see fig. 22) in the Truro flow cell for predevelopment, 1975, 1989, and projected 2020 pumping and recharge rates, Cape Cod Basin, Massachusetts.

the depth to the freshwater-saltwater interface from 159 to 149 ft below sea level. The change in simulated pumping at the North Truro Air Force Base resulted in a model-calculated decrease in the depth to the freshwater-saltwater interface from 175 to 167 ft below sea level. There was no detectable response of the freshwater-saltwater interface to simulated fluctuations between in-season and off-season pumping and aquifer recharge rates because the lag time in the response to changing stress conditions is longer than the simulated seasonal fluctuations.

An hypothetical drought was simulated for a 5-year period for 1989-94 to determine the effects of a 30-percent decrease in natural recharge on the water budget, head distribution, and the depth to the freshwater-saltwater interface. The model-calculated

effects of the simulated extended drought are most evident during the off-season pumping period. During the off-season pumping periods for the nondrought simulation, aquifer recharge replenishes the water lost during the in-season pumping period. However, during the off-season drought simulation, there was a decrease in the rate of ground water replenished to storage, resulting in a net loss of water to the system. Coastal and subsea discharge decreased by 10 percent. The comparison of the in-season nondrought to the in-season drought conditions shows that although the return-flow recharge is the same, the rate of ground water released from storage is decreased by nearly 11 percent during drought conditions. As a result of the decreased recharge to the system, the coastal and subsea discharges were decreased by 7 to 20 percent.

The average model-calculated decline in water level after 5 years of simulated drought conditions was about 0.5 ft and the position of the freshwater-saltwater interface moved vertically upward by about 3 ft. Model-calculated change in the position of the freshwater-saltwater interface was then compared at TSW-89 for 15 years from 1984 to 1999 for simulated nondrought and drought conditions (drought conditions were 1989-94). The model-calculated water-table altitude at the well responded quickly to the decrease in recharge and rose quickly at the end of the drought period as shown in figure 27. The model-calculated response of the interface to the decrease in aquifer recharge was much slower than that of the water table and the interface position consequently took longer to recover after the simulated average (nondrought) recharge rate was resumed. In addition, under simulated average in-season and off-season recharge conditions for this time period, there was a slight long-term decline in model-calculated ground-water altitude and decrease in depth to the freshwater-saltwater interface (fig. 27). This may be attributed to the fact that on average, only 14 percent of the total simulated pumpage from the flow cell is returned to the aquifer.

Seasonal fluctuations in simulated pumping and recharge show that the cyclic depletion and replenishment of ground water in storage affected model-calculated water-table altitude and coastal and subsea discharge, yet has a minimal effect on the model-calculated position of the freshwater-saltwater interface. The model-calculated freshwater-saltwater

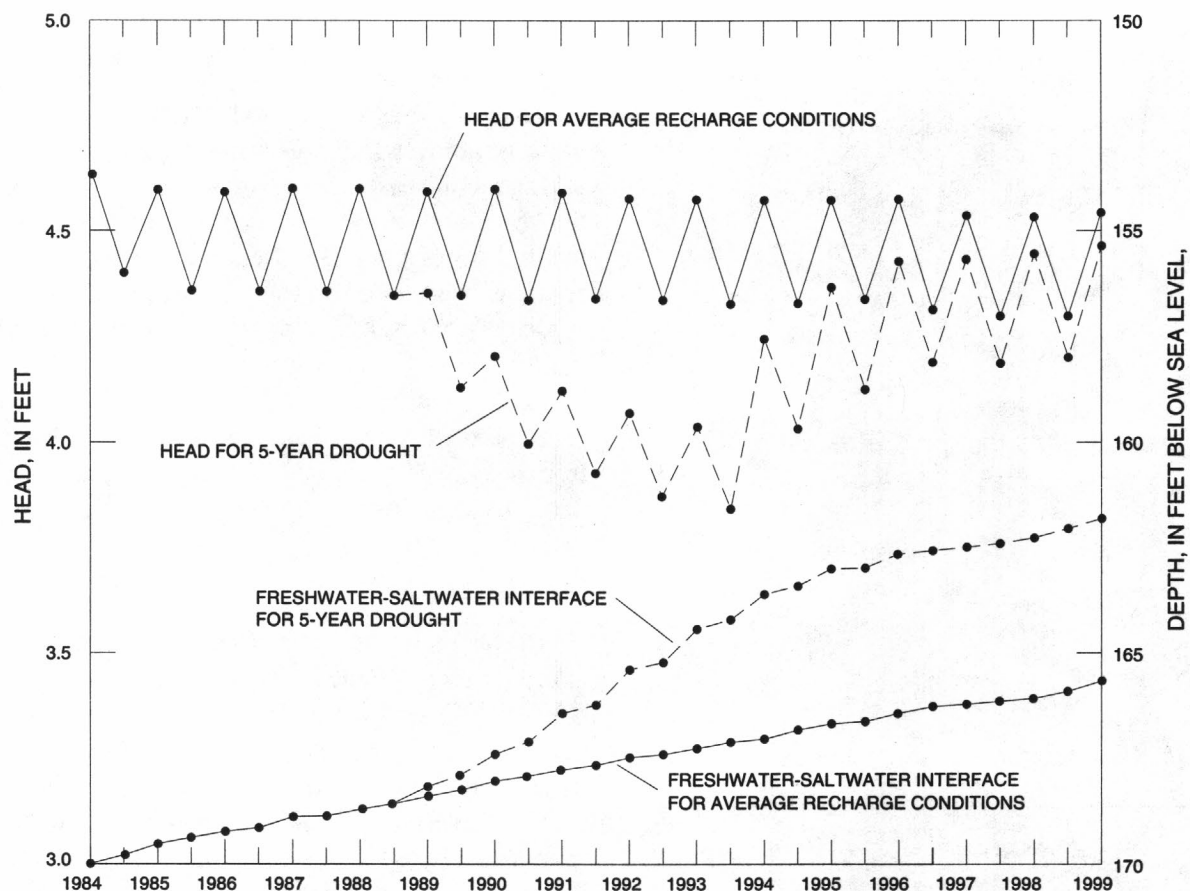


**Figure 27.** Model-calculated water-table altitude and position of the freshwater-saltwater interface at observation well TSW-89 for average recharge conditions and for simulation of a 5-year drought and 1989 pumping rates, Cape Cod Basin, Massachusetts.

interface position was most sensitive to increases in simulated pumping rates as shown at the Knowles Crossing well.

### Eastham and Wellfleet Flow Cells

The Eastham flow cell is south of the Wellfleet flow cell and north of the East Cape flow cell (fig. 2). Blackfish Creek forms the ground-water divide separating the Eastham and Wellfleet flow cells.

Town Cove and Boat Meadow River represent the ground-water divide between Eastham and East Cape. Eastham is bounded on the west by Cape Cod Bay and to the east by the Atlantic Ocean and Nauset Harbor. The unconsolidated sands, silts and clays extend to the bedrock surface, which forms the lowest extent of the Eastham ground-water-flow system. The general

direction of ground-water flow is from the potentiometric high in the center of the flow cell toward the coastal discharge boundaries. The ground-water divides at the northern and southern borders of the flow cell prevent ground-water flow between adjoining flow cells.

The Wellfleet flow cell is south of the Truro flow cell and north of the Eastham flow cell as shown in figure 2. The Pamet River represents the ground-water divide separating the Wellfleet and Truro flow cells. Wellfleet is bounded on the west by the Cape Cod Bay and Wellfleet Harbor, and to the east by the Atlantic Ocean. The water-table altitude ranges from 7 ft above sea level at the center of the flow cell to near 0 ft at the shore. Under natural conditions, fresh water enters the ground-water-flow system at the water table as recharge from precipitation. A series of small streams discharges to the Wellfleet Harbor. The unconsolidated sand and gravel aquifer of the flow cell extends to the assumed

impermeable bedrock surface. However, results from Guswa and LeBlanc (1985) show that the freshwater lens is bounded below by the freshwater-saltwater interface at about 280 ft below sea level.

The analyses for the Eastham and Wellfleet flow cells were not as detailed as those of East Cape, West Cape, and Truro flow cells because (1) there are no existing or projected large-capacity wells planned for these areas; and (2) little hydrologic information has been collected for the Eastham flow cell since the work of Barlow (1994) and for the Wellfleet flow cell since the work of Guswa and LeBlanc (1985). Barlow (1994) recently updated the modeling work of Guswa and LeBlanc (1985) for the Eastham flow cell using hydrologic data collected since Guswa and LeBlanc (1985). A freshwater-flow model was constructed for the Wellfleet flow cell by updating the model data sets used by Guswa and LeBlanc (1985) and incorporating the freshwater-saltwater interface positions calculated by Guswa and LeBlanc (1985) into the updated model.

## **Description of Models**

### **Grids**

The freshwater-flow model developed by Barlow (1994) for the Eastham flow cell consisted of 96 rows, 78 columns, and 5 layers (table 7; fig. 28). The vertical discretization was based on available information on the lithology of the glacial deposits. The horizontal discretization was finest in the areas of simulated hypothetical well sites to accurately simulate the movement of water near these wells.

The Wellfleet freshwater-flow model consists of 26 rows, 32 columns, and 6 layers. The Wellfleet flow model developed by Guswa and LeBlanc (1985) had seven layers (table 7; fig. 29). The lowest layer was not part of the freshwater-flow system and was therefore not included in the freshwater model. A uniform grid spacing of 1,320 by 1,320 ft was used.

### **Hydraulic properties**

The horizontal hydraulic conductivity and vertical conductance were estimated for the Eastham flow model by comparing lithologic logs of test holes at 31 sites to generalized values of hydraulic conductivity for glacial sediments developed by Barlow (1994). The

transmissivity of layer 5 ( $0.4 \text{ ft}^2/\text{d}$ ) was determined by multiplying the average hydraulic conductivity of silt and clay sediment cores collected in Eastham by the total thickness of the layer. The model of Barlow (1994) did not simulate transient flow conditions, therefore specific yield and storage coefficient for the flow system needed to be estimated for this analysis. Assumed values of 0.15 for specific yield and of  $2 \times 10^{-4}$  for storage coefficient were used which are consistent with those used in the West Cape and East Cape models. The range in horizontal hydraulic conductivity and vertical conductance used in the Eastham flow model for each layer is presented in table 7.

The aquifer properties used for the Wellfleet flow model were derived from estimating values of hydraulic conductivity from available lithologic logs as discussed earlier in the section "Aquifer Hydraulic Properties." Specific yield and storage coefficient values were estimated from the average values used in the West Cape and East Cape flow models. Specific yield was set at 0.15 and  $2 \times 10^{-4}$  was used for the storage coefficient. The range in horizontal hydraulic conductivity and vertical conductance used in the Wellfleet flow model for each layer is presented in table 7.

### **Boundary conditions**

The model boundaries for the Eastham flow model were determined by Barlow (1994) and are shown in figure 28. Specified head nodes were used to simulate saltwater bodies that surround much of the modeled area. Equivalent freshwater heads were used at coastal saltwater boundaries to account for the higher density salt water that overlies the freshwater system at the seabed discharge boundaries. These specified head nodes were only used in the top layer of the model. The cells in layers 2 through 5 underlying these nodes remained active and a no-flow boundary was used to simulate the freshwater-saltwater interface in the adjacent seaward nodes. No-flow boundaries were specified at the northern and southern extents of the flow model to coincide with the natural divides separating Eastham from Wellfleet and East Cape. The model is bounded above by the water table, which receives recharge at a rate equal to 18.3 in/yr, and below by a no-flow boundary that simulates the contact between glacial deposits and bedrock. Ponds simulated in the top layer were assigned a recharge rate of only 12.4 in/yr to account for evaporation losses from the pond surfaces.

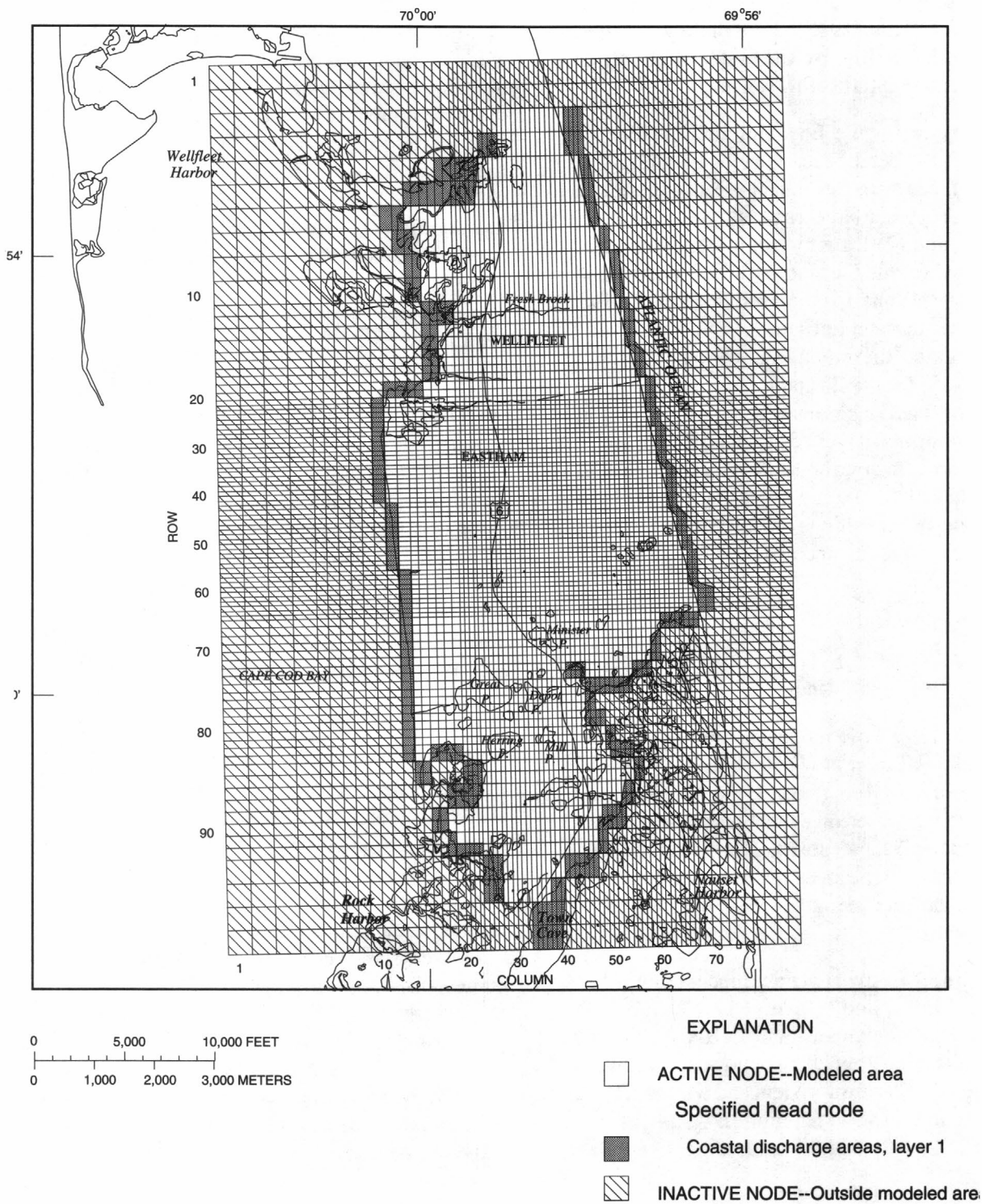


**Figure 28.** Grid and boundary conditions for the Eastham flow cell, Cape Cod Basin, Massachusetts. (Modified from Barlow, 1994.)



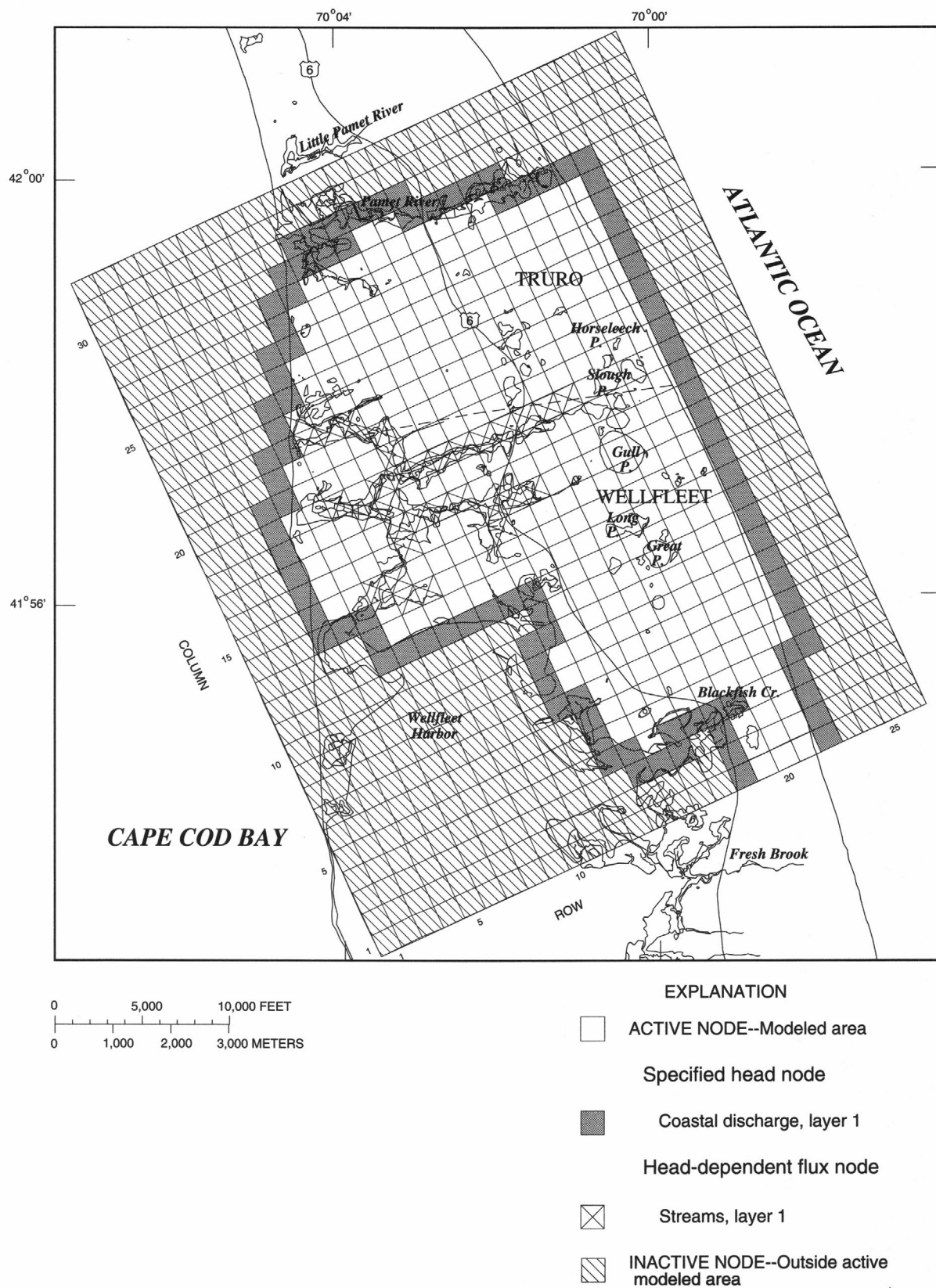


**Figure 29.** Grid and boundary conditions for the Wellfleet flow cell, Cape Cod Basin, Massachusetts.

The boundaries for the Wellfleet flow model were determined by Guswa and LeBlanc (1985). A no-flow (inactive) boundary was set at the ground-water divide that separates the Wellfleet flow cell from the Eastham flow cell. The Pamet River, which forms the northern boundary of the flow cell, was simulated as a head-dependent flux boundary.

Specified head nodes were used in the top layer to simulate the saltwater bodies of Cape Cod Bay, Wellfleet Harbor, and the Atlantic Ocean. Although the movement of the freshwater-saltwater interface was not calculated, equivalent freshwater heads were used at the coastal saltwater boundaries to account for the higher density salt water that overlies the freshwater system at the seabed discharge boundaries (fig. 29). The equivalent heads used in the Wellfleet model were obtained from Guswa and LeBlanc (1985).

The freshwater-saltwater interface position calculated by Guswa and LeBlanc (1985) was used to determine the extent of the freshwater-flow system. The freshwater-saltwater interface altitude represents the lowest extent of the freshwater-flow system and was specified as a no-flow boundary based on the results of Guswa and LeBlanc (1985). Nodes that were calculated to consist of fresh water were kept active, whereas those calculated to consist of salt water were made inactive. All subsequent nodes below a saltwater node were considered inactive.

The Wellfleet model is bounded on top by the water table, which is a free-surface boundary that receives recharge at an estimated rate of 19.8 in/yr. This recharge rate is equal to that determined for the adjoining Truro flow cell. Nodes containing ponds were assigned a reduced recharge rate of 13.9 in/yr to account for evaporation at the pond surface. A series of small streams and wetlands intersect the water table, drain the top layer, and discharge to the Wellfleet Harbor. These surface-water bodies are ground-water fed and act as local sinks to the freshwater system. Discharge in these nodes was determined by the difference between specified head in the stream and calculated head in the aquifer and by the calculated conductance between the streambed and the aquifer.

## Stresses and stress periods

Steady-state simulations for the Wellfleet and Eastham flow cells were made to determine the water budget and head distribution for long-term average recharge conditions. The water-supply needs of the residents of the towns of Eastham and Wellfleet are met by private wells. Wastewater is returned to the ground-water-flow system by on-site septic systems; the net loss to the system was assumed to be negligible. The results from the steady-state simulations then were used as the initial conditions for a transient analysis, in which a 30-percent decrease in recharge was simulated for 5 years, as discussed for the West and East Cape freshwater-flow models.

## Calibration

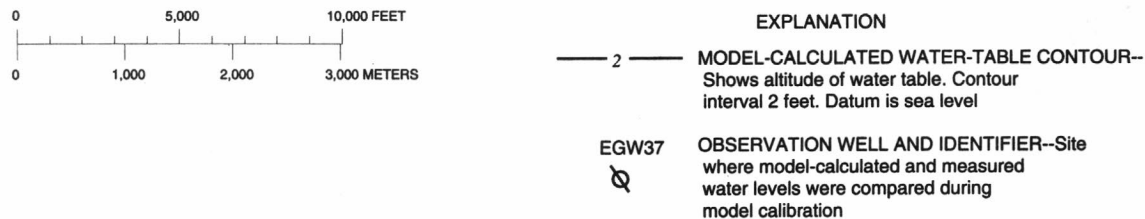
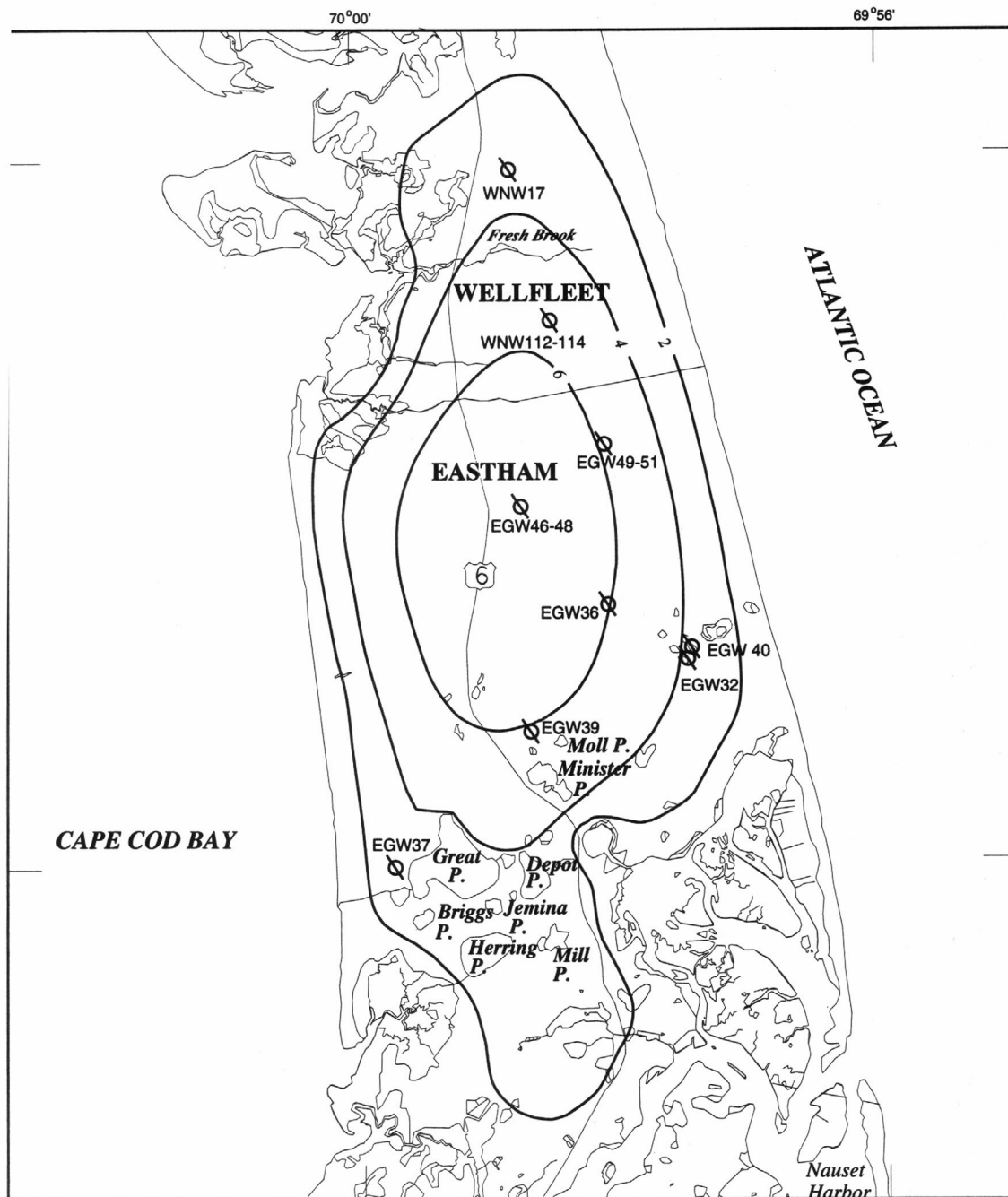
The freshwater model for the Eastham flow cell was calibrated by comparing model-calculated water levels to measured water levels and pond altitudes at 21 locations in the flow cell measured in 1988 (fig. 30). Barlow (1994) provides a more detailed discussion on the calibration of the Eastham flow model.

The aquifer properties used in the Wellfleet flow model were calibrated by comparing the model-calculated water-table altitude at the five observation wells and five pond levels shown in figure 31 with measured water levels. The water-table altitudes reported for the observation wells used in calibration represent the average water levels measured from 1963 to 1976 and are consistent with the water levels used for calibration for the West Cape, East Cape, and Truro flow models.

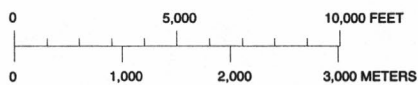
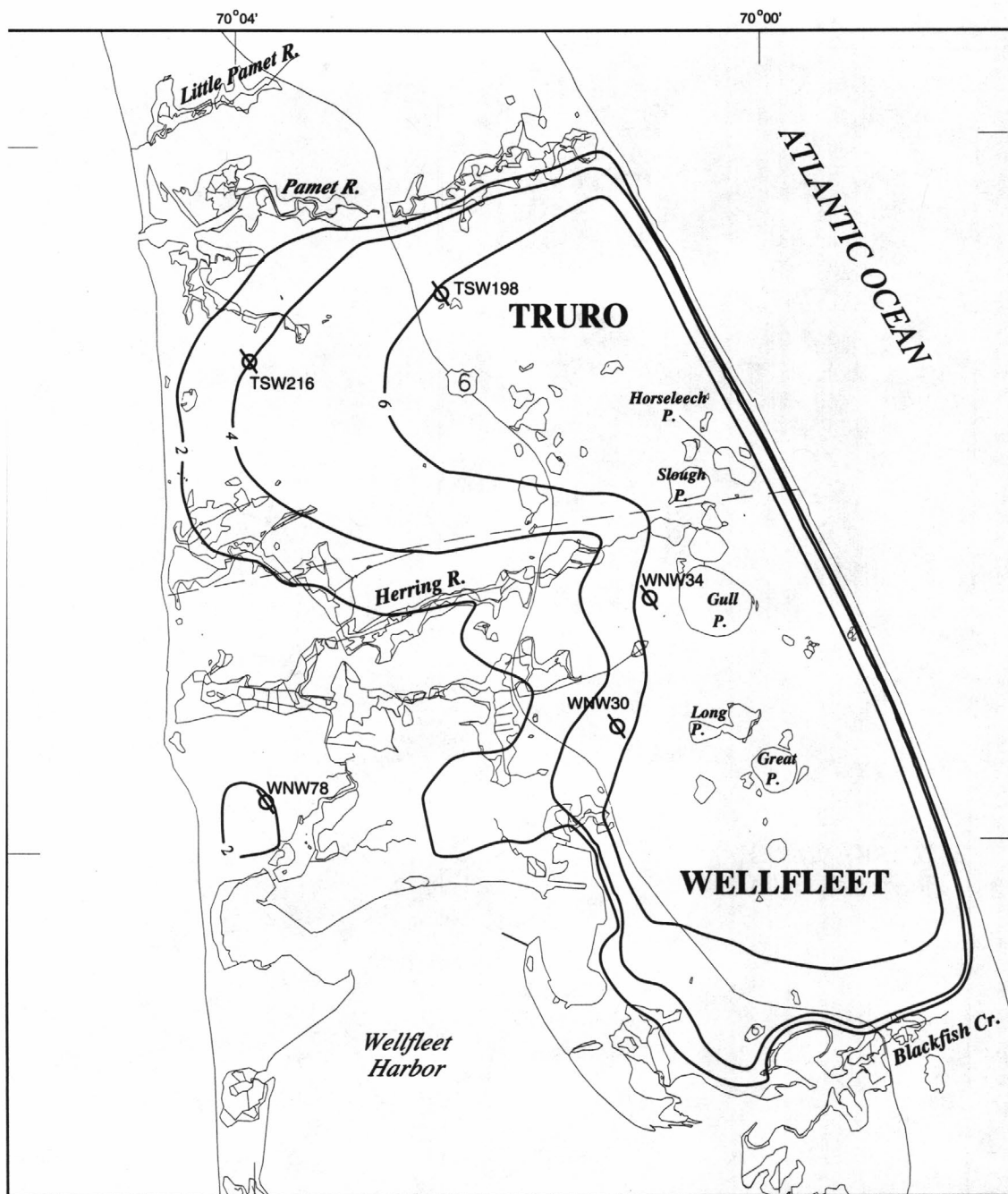
Total inflow to the Eastham and Wellfleet flow cells calculated by the freshwater models for steady-state flow conditions are 22.1 and 27.5 ft<sup>3</sup>/s, respectively (table 16). Nearly one-half of the freshwater discharge from the Wellfleet flow cell is to the several streams in the flow cell.

## Simulation of the Freshwater Flow Systems

The response of the Eastham and Wellfleet flow cells to simulated stress conditions was determined by comparing the model-calculated water-table altitude at the observation wells and ponds and the model-calculated water budgets for long-term average recharge



re 30. Model-calculated steady-state water-table configuration for the Eastham flow Cape Cod Basin, Massachusetts.



#### EXPLANATION

— 2 — MODEL-CALCULATED WATER-TABLE CONTOUR--  
Shows altitude of water table. Contour  
interval 2 feet. Datum is sea level

WNW78  
Q

OBSERVATION WELL AND IDENTIFIER--  
Site where model-calculated and measured  
water levels were compared during  
model calibration

31. Model-calculated steady-state water-table configuration for the Wellfleet flow Cape Cod Basin, Massachusetts.



**Table 16.** Model-calculated water budgets for the Eastham and Wellfleet flow cells, Cape Cod Basin, Massachusetts

[All values are in cubic feet per second]

Budget Item	Average recharge conditions	30-percent decrease in recharge after 5 years
<b>EASTHAM FLOW CELL</b> (Area = $4.6 \times 10^8$ ft <sup>2</sup> )		
<b>Inflow</b>		
Recharge.....	22.1	15.4
Release from storage.....	0	1.1
Total inflow.....	22.1	16.5
<b>Outflow</b>		
Coastal discharge .....	22.1	16.6
Storage .....	0	0
Total outflow.....	22.1	16.6
Model error .....	0	-.1
(inflow minus outflow)		
<b>WELLFLEET FLOW CELL</b> (Area = $5.4 \times 10^8$ ft <sup>2</sup> )		
<b>Inflow</b>		
Recharge.....	27.5	19.3
Release from storage.....	0	.1
Total inflow.....	27.5	19.4
<b>Outflow</b>		
Streams.....	13.0	9.0
Coastal discharge .....	14.6	10.5
Storage .....	0	0
Total outflow.....	27.6	19.5
Model error .....	-.1	-.1
(inflow minus outflow)		

conditions and for hypothetical drought conditions. Drought conditions of a 30-percent decrease in the average recharge rate were simulated for 5 years.

The change in model-calculated water-table altitude from unstressed to stressed conditions for each of the flow cells is shown in table 17. The model-calculated decline in water-table altitude is largest near the center of the flow cells and diminishes toward the coast. The model-calculated average decline in water-table altitude

was 2.6 ft for the Eastham flow cell and 1.0 ft for the Wellfleet flow cell. Although the model-calculated decline in water levels in Eastham was nearly triple that of Wellfleet, the decline was 18 percent of the total relief of the water table in the Eastham flow cell and 14 percent of the total relief of the water table in the Wellfleet flow cell.

Model-calculated streamflow was decreased 30 percent and model-calculated coastal discharge by 28 percent in the Wellfleet flow cell (table 16) for the simulated drought conditions. In the Eastham flow cell, the model-calculated coastal discharge was decreased 25 percent. Although simulated recharge into the Eastham flow cell was decreased by 30 percent, the total decrease in outflow for the flow cell was about 25 percent. Water released from storage accounts for the additional source of water into the system in response to the simulated reduction of natural recharge. If the simulated drought conditions were continued until the groundwater system was in equilibrium (no change in storage) then the 30-percent decrease in recharge (inflow) would ultimately result in a 30-percent decrease in outflow.

### Limitations of the Numerical Modeling Analyses for the Cape Cod Basin

The Cape Cod flow models were developed to provide a regional assessment of the response of the ground-water-flow system to changing stress conditions. These flow models were not designed to provide detailed analyses of the effects of local stresses on specific areas in the flow system.

Four of the five flow models (not including Eastham) have uniform horizontal grid spacing of 1,320 by 1,320 ft with five to seven layers subdividing the system from the water table to the bedrock or freshwater-saltwater boundary. The discretized estimates of hydraulic properties and the contact between the unconsolidated deposits and bedrock were intended to provide an approximation of the actual flow system and should not be used to provide exact values of these parameters at specific locations in the flow cells.

Ground-water models developed for each of the flow cells assumed no-flow conditions in the underlying bedrock. As a result, the possibility of vertical saltwater

**Table 17.** Average measured water levels for selected wells, 1963-76, measured pond levels, and model-calculated water levels and pond levels for average recharge rates and for a 5-year drought for the Eastham and Wellfleet flow cells, Cape Cod Basin, Massachusetts

Well No. or Pond site	Model node			Average measured water level, in feet above sea level	Model-calculated water level, in feet above sea level		Decrease in model- calculated water levels between average and 30-percent decrease in recharge, in feet
	Layer	Row	Column		Average recharge conditions	30-percent decrease in recharge, after 5 years	
EASTHAM FLOW CELL							
Observation Well							
Town of Eastham							
EGS 49	1	29	20	16.9	15.6	12.6	3.0
EGW 50	2	29	20	16.9	15.4	12.4	3.0
EGW 51	4	29	20	17.2	15.4	12.4	3.0
EGW 46	1	35	33	17.7	18.4	15.0	3.4
EGW 47	2	35	33	17.6	18.4	15.0	3.4
EGW 48	3	35	33	17.6	18.4	15.0	3.4
EGW 32	1	49	48	12.8	13.4	10.7	2.7
EGW 36	1	48	44	13.9	15.3	12.3	3.0
EGW 37	1	75	17	8.2	8.3	6.4	1.9
EGW 39	1	65	33	13.9	14.3	11.5	2.8
EGW 40	2	55	55	8.6	9.2	7.3	1.9
Town of Wellfleet							
WNW 17	2	9	32	8.5	9.3	7.2	2.1
WNW 112	1	14	37	13.8	13.5	10.7	2.8
WNW 113	2	14	37	13.7	13.5	10.7	2.8
WNW 114	3	14	37	13.7	13.5	10.7	2.8
Pond							
Mill	1	81	37	10.2	8.1	6.3	1.8
Moll	1	65	38	13.2	13.6	10.9	2.7
Jemima	1	78	29	9.1	9.7	7.6	2.1
Briggs	1	59	23	15.5	15.4	12.4	3.0
Minister	1	64	36	12.6	12.0	9.6	2.4
Great	1	75	23	8.6	10.0	7.9	2.1
WELLFLEET FLOW CELL							
Observation Well							
Town of Wellfleet							
WNW 78	1	6	16	2.7	2.3	1.9	0.4
WNW 30	1	15	14	6.6	5.4	4.3	1.1
WNW 34	1	18	17	8.0	6.9	5.4	1.5
Town of Truro							
TSW 216	1	11	26	4.1	4.5	3.5	1.0
TSW 198	1	16	26	7.6	6.1	4.9	1.2

**Table 17.** Average measured water levels for selected wells, 1963-76, measured pond levels, and model-calculated water levels and pond levels for average recharge rates and for a 5-year drought for the Eastham and Wellfleet flow cells, Cape Cod Basin, Massachusetts--*Continued*

Well No. or Pond site	Model node			Average measured water level, in feet above sea level	Model-calculated water level, in feet above sea level		Decrease in model- calculated water levels between average and 30-percent decrease in recharge, in feet
	Layer	Row	Column		Average recharge conditions	30-percent decrease in recharge, after 5 years	
WELLFLEET FLOW CELL-- <i>Continued</i>							
Pond							
Town of Wellfleet							
Gull	1	19	16	6.0	7.7	6.0	1.7
Great	1	19	11	8.0	8.0	6.2	1.8
Long	1	18	13	8.0	7.9	6.1	1.8
Town of Truro							
Horseleech	1	21	19	6.0	7.3	5.7	1.6
Slough	1	20	19	6.0	7.3	5.7	1.6

intrusion in locations in the West Cape and East Cape flow cells, where freshwater extends to the top of the bedrock, can not be assessed.

In addition to hydraulic properties, streamflow and pumping well locations were controlled by model discretization. Streams in the Cape Cod ground-water-flow system are typically shallow and narrow. Representation of these streams results in coarse approximations in streambed conductance, streambed altitude and therefore, stream discharge. Pumping wells simulated in the flow models are assumed to be pumping at the center of each node and, therefore can only provide an approximation of the actual pumping locations.

Pumping and recharge rates also are approximations of the actual stresses on the ground-water-flow system. Three stress conditions were used to represent 71 years (1950-2020) of changing stresses on Cape Cod. This coarse representation resulted in periods of overestimated stresses from 1950 to 1974, 1982 to 1988, and 2005 to 2019, and underestimated stresses from 1976 to 1981 and 1990 to 2004. As a result of this temporal discretization, the effects of changing stress conditions for specific years are not possible. In-season and off-season stress periods were used to simulate seasonal fluctuations in pumping and recharge for the 1989 stress conditions. For the in-season stress condition, the summer pumping rate was assumed to occur from June through

August with the only recharge to the system from wastewater return flow. The off-season stress period was from September through May and winter pumping rates and all natural recharge and off-season wastewater return flow was assumed to occur. However, natural recharge is assumed to occur only from November through May (Barlow and Hess, 1993). Therefore, in order to accurately represent seasonal fluctuations in both pumping and recharge, monthly stress periods would have to be implemented.

Wastewater return-flow estimates also provide a coarse approximation of the percentage and location of the actual artificial recharge to the ground-water-flow system from wastewater-treatment facilities and domestic septic systems. The septic-system return-flow approximations were based on the total length of roads in each water district and does not account for housing/population density.

The limitations of the boundary condition representing the freshwater-saltwater interface for the West and East Cape freshwater-flow models are discussed in the section "Boundary Conditions." However, this boundary condition was based on the projected 2020 pumping rates discussed in the section "Ground-Water Use" and substantial changes in the projected pumping rates or well locations may produce results that are significantly different than those reported here.

The boundaries simulating the freshwater-saltwater interface in the Wellfleet and Eastham flow models were simpler than those used in the West Cape and East Cape flow models. The boundary used in the Wellfleet flow model was based on the freshwater-saltwater interface calculated by Guswa and LeBlanc (1985). The boundary separating the freshwater- and saltwater-flow systems in the Eastham model was assumed to coincide with the shoreline and extend to bedrock (Barlow, 1994). The freshwater-saltwater interface boundary for both flow models was assumed to be static and was not designed to account for increased stresses to the ground-water-flow system.

## **EFFECTS OF SIMULATED GROUND-WATER PUMPING AND RECHARGE ON MARTHA'S VINEYARD AND NANTUCKET ISLAND BASINS**

The analysis of the effects of pumping on the ground-water-flow systems of Martha's Vineyard and Nantucket Island Basins was completed using two-dimensional, finite-difference flow models that calculate changes (or drawdowns) in ground-water levels resulting from pumping. These "change models" do not calculate absolute water levels, nor were they calibrated against measured water levels in the basins. The models were used because available data were insufficient to construct three-dimensional, calibrated models that simulate flow in the basins. However, the use of the models is an improvement over the use of simple analytical models to calculate drawdowns resulting from pumping because (1) multiple pumping wells may be simulated simultaneously and (2) surface-water boundaries may be represented easily in the finite-difference models.

The change models assume that there is a linear relation between pumping rates and drawdowns. For linear flow systems, a change model produces valid results. In nonlinear systems, however, the effects of stresses cannot be calculated independently (Reilly and others, 1987); that is, the effect of a stress depends on all the conditions occurring when the stress is applied. The ground-water-flow systems simulated in this study are nonlinear because they include a water table and the transmissivity of the aquifer depends on the saturated thickness. Nevertheless, the change-model approach was used as an approximation to the response of the

basins to pumping. Although predicted changes will not be exact, they should provide a reasonable basis for evaluating effects of pumping and recharge on the simulated ground-water-flow systems.

The model of the Martha's Vineyard Basin consists of 70 rows and 74 columns and has a uniform grid spacing of 590 ft. The model of the Nantucket Island Basin consists of 30 rows and 36 columns with a uniform grid spacing of 810 ft. The grid spacing and model dimensions were selected arbitrarily to reference the location of the pumping wells and to cover a large enough area to minimize the effects of model boundaries on model-calculated drawdowns. Constant values of horizontal hydraulic conductivity and initial saturated thicknesses were used throughout the models. A horizontal hydraulic conductivity of 500 ft/d was used in the model of the Martha's Vineyard Basin and a horizontal hydraulic conductivity of 240 ft/d was used in the model of the Nantucket Island Basin. The initial water-table altitude was set at 0 ft in each flow model and a bottom altitude of -70 ft was set for the model of Martha's Vineyard (representative of the primary sand and gravel aquifer) and -250 ft was set for the model of Nantucket Island (representative of the shallow aquifer). These horizontal hydraulic conductivities and initial saturated thicknesses were assigned on the basis of average transmissivities of 35,000 and 60,000 ft<sup>2</sup>/d estimated from aquifer tests at pumping wells in the Martha's Vineyard and Nantucket Island Basins, respectively. A uniform value of 0.2 for specific yield was used for both models. Specified-head nodes with constant water levels of 0 ft were used at saltwater boundaries; no-flow boundaries were used to separate modeled from unmodeled areas of the flow basins. Simulations of each basin were made for conditions of 180 days of no recharge and pumping rates equal to those projected to occur in 2020 during summer (in-season) months.

Model-calculated changes in the altitude of the water table for the projected pumping rates and 180 days of no recharge are shown for the modeled areas of Martha's Vineyard and Nantucket Island Basins in figures 32 and 33, respectively. The changes in water-table altitudes were not superimposed on the current water-table maps (figs. 6 and 7) because of the limited number of observation wells used in the development of the maps for each basin. Maximum declines occur at pumping wells and decrease with distance from the wells. The largest model-calculated declines for the Martha's Vineyard



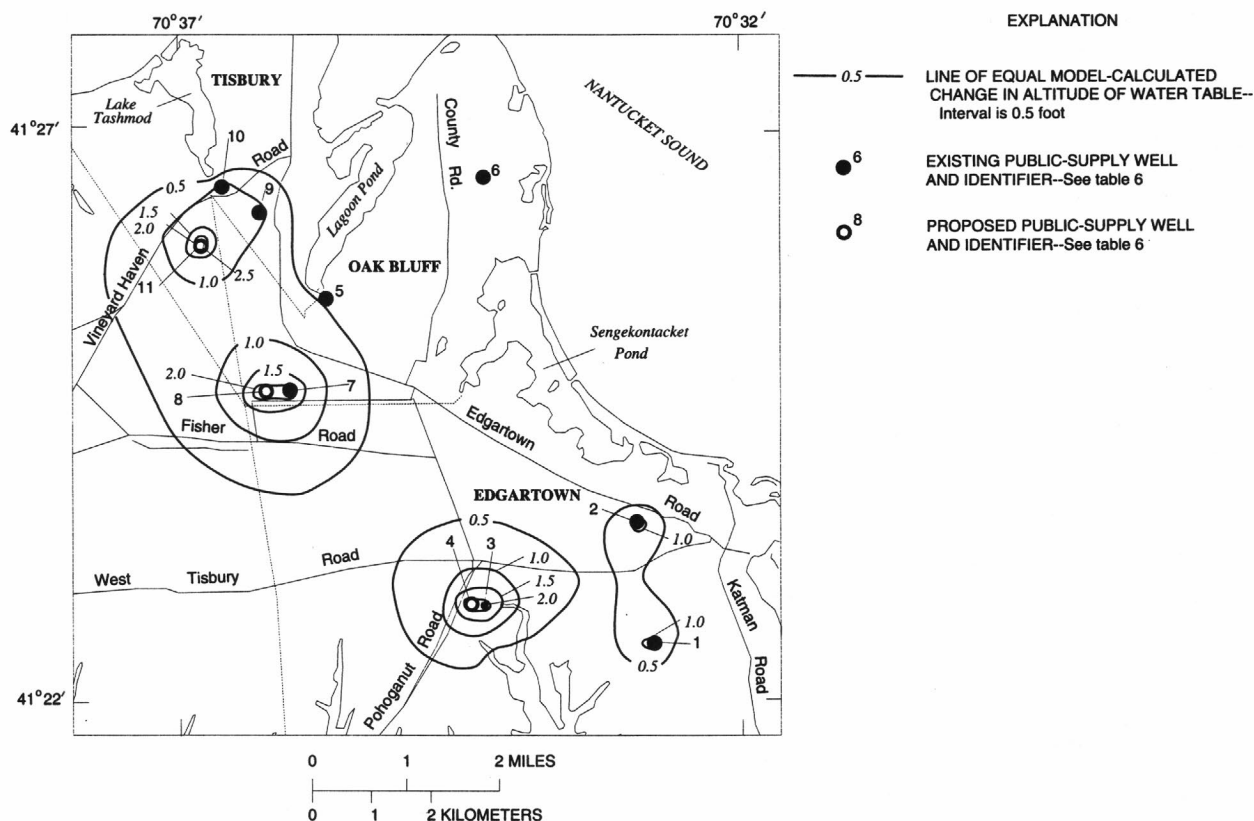


**Figure 32.** Model-calculated change in the altitude of the water-table configuration for projected 2020 summer pumping rates and 180 days of zero recharge in the Martha's Vineyard Basin, Massachusetts.

Basin were 2.7 ft near the proposed Manter site in Tisbury. The largest model-calculated declines for the Nantucket Island Basin were 1.6 ft near the proposed Wannacomet well. These maximum declines represent a small percentage of the total simulated saturated thickness in each flow basin.

Model-calculated changes in the altitude of the water table near Tisbury, Oak Bluffs, and Edgartown public-supply wells on Martha's Vineyard (fig. 32) show interference from nearby wells because of the proximity of the simulated pumping wells to one another and high (in-season) pumping rates simulated. Simulated well interference also occurs between the existing and proposed Wannacomet wells in the Nantucket Island Basin (fig. 33). Model-calculated declines are likely to be somewhat greater than those that would actually occur in the real flow basins because no-flow boundaries were simulated around the edge of each model. In the real flow basins, declines would be less at these boundaries than those calculated by the models

because of the availability of water to the wells from areas of the aquifers outside of the modeled areas. Also, the simulations indicate that pumping at the wells would cause a flow of water from surrounding saltwater boundaries to the flow basins. Although these results must be viewed in light of the limitations of the change-model approach, the possible movement of the interface between fresh water and salt water resulting from increased pumping from the flow basins should be considered in future evaluations of water-resource management options in the basins.

Metcalf and Eddy, Inc. (1972) estimated the total inflow to the Martha's Vineyard Basin aquifer system to be 58 Mgal/d. Total simulated in-season pumping from the aquifer in the year 2020 was 6.5 Mgal/d, or 11 percent of the estimated total inflow. Horsley Witten Hegemann, Inc. (1990) estimated the total inflow to the Nantucket Island Basin aquifer system to be 56 Mgal/d. Total simulated in-season pumping from the aquifer in the year 2020 was 2.4 Mgal/d, or 4 percent of total

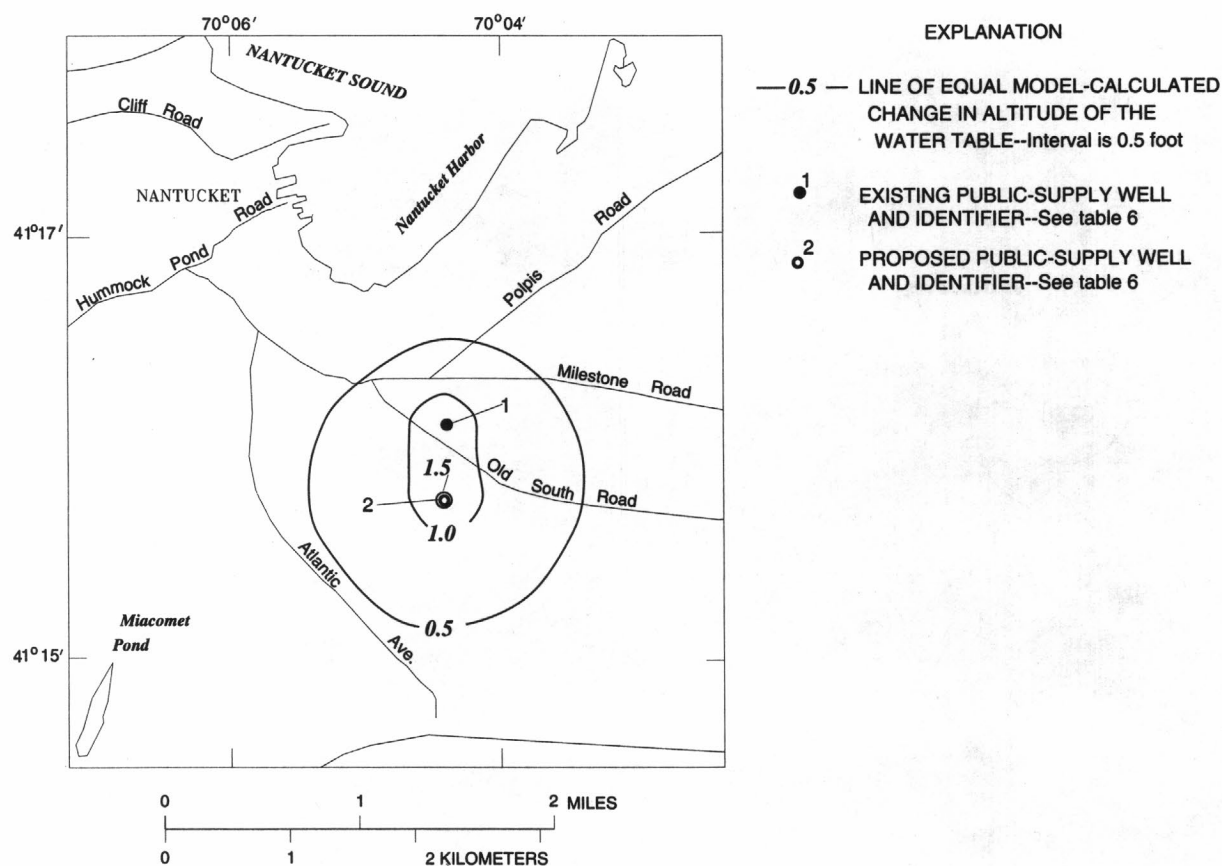


**Figure 33.** Model-calculated change in the altitude of the water-table configuration for projected 2020 summer pumping rates and 180 days of zero recharge in the Nantucket Island Basin, Massachusetts.

inflow. Most of the water pumped from the flow basins is returned to them as wastewater return flow through septic systems and wastewater-treatment facilities. Consequently, little water is actually lost from the flow basins through consumptive use. The analysis used in this investigation does not consider wastewater return flow as a source of water to the flow basins and therefore model-calculated changes in water-table altitudes are likely to be larger than if wastewater return flow had been included.

## SUMMARY AND CONCLUSIONS

The management and protection of water resources of Cape Cod, Martha's Vineyard, and Nantucket Island water-resource planning basins are of concern to Massachusetts State and local officials because ground water is the sole source of drinking water in the basins. Significant growth in the number of summer and

permanent residents has resulted in an increase in water use during the last 30 years and has placed stresses on the ground-water resources. In particular, there is concern over the extent and of long-term declines in ground-water and pond levels and in the quantity of streamflow, as well as in the possibility of saltwater intrusion from the surrounding ocean. Effects of simulated ground-water pumping and recharge on the ground-water-flow system were assessed for the Cape Cod, Martha's Vineyard, and Nantucket Island Basins. Five flow cells of Cape Cod Basin were assessed—the West Cape, East Cape, Eastham, Wellfleet, and Truro flow cells. These effects are reported as (1) changes in water-table altitudes in the three basins, (2) changes in pond altitudes and streamflow for selected ponds and streams of Cape Cod Basin, (3) changes in the sources and sinks of water in Cape Cod Basin, and (4) changes in the position of the freshwater-saltwater interface in the West Cape, East Cape, and Truro flow cells of Cape Cod Basin.

Cape Cod Basin consists of glacial deposits ranging in size from clay to boulders deposited during the glaciation of the Pleistocene Epoch. The glacial deposits overlie an igneous and metamorphic basement complex whose surface ranges in depth from 100 ft below sea level near Cape Cod Canal to more than 900 ft below sea level near Provincetown. The bedrock is overlain by a thin veneer of basal till, which is overlain in turn by thick deposits of fine sand, silt, and clay that were deposited in a pro-glacial lake. Extensive deposits of stratified drift were deposited on the fine-grained lake deposits by meltwater streams.

The coarse-grained stratified-drift deposits are generally highly transmissive to water and have high storage capacities. Horizontal hydraulic conductivity of the stratified drift ranges from about 40 ft/d for fine sand and silt to about 360 ft/d for medium to coarse sand and gravel. Estimates of the ratio of vertical to horizontal hydraulic conductivity range from 1:1 to 1:30 for all sediment classes except fine sand and silt, for which the estimated ratio is 1:50. There is a general increase in horizontal hydraulic conductivity with increase in grain size. Specific yield of the stratified drift, as estimated from 10 aquifer tests, ranges from 0.02 to 0.25, and is consistent with estimates made by previous investigators.

The Cape Cod ground-water-flow system consists of six flow cells that are hydraulically distinct under present-day hydrologic conditions. These flow cells are bounded laterally by saltwater bodies that include Cape Cod Bay, Nantucket Sound, and the Atlantic Ocean. Fresh water in the aquifers is separated from surrounding salt water by a zone of transition in which the two waters mix. The interface between freshwater and saltwater zones of the flow cells can move landward or seaward of its current position as a result of changes in the rate of recharge to the flow cells and changes in the rate of water pumped from the flow cells. There has been no known contamination of public-water supplies by saltwater intrusion due to ground-water pumping except where upconing of the freshwater-saltwater interface caused by ground-water pumping has been documented at the Knowles Crossing well field in Truro.

The flow cells are recharged by precipitation and wastewater return flow from such sources as septic systems and wastewater-treatment facilities. Estimates of precipitation recharge to the flow cells range from about 45 to 48 percent of annual precipitation, or from about

18 to 22 in/yr. Surface-water runoff is assumed to be negligible because of the highly permeable soils of Cape Cod.

The water-table configuration in the Cape Cod Basin is characterized by six oblong mounds, one in each flow cell, and water-table contours approximately follow the shape of the coast. Ground water flows radially from the center of the peninsula toward coastal discharge areas. The altitude of the water table fluctuates by a range of 0 to 7 ft because of seasonal changes in aquifer recharge and ground-water pumping.

Public-water supply systems have been in operation on Cape Cod since 1893. Average daily demand of water in 1989 in the West Cape and East Cape flow cells, the largest and most populated of the six flow cells of Cape Cod, was 24.2 and 11.4 ft<sup>3</sup>/s, respectively.

Transient, three-dimensional, finite-difference models were developed to simulate freshwater and saltwater flow in the West Cape, East Cape, and Truro flow cells. Results of simulations indicate little change in the position of the freshwater-saltwater interface in the West Cape and East Cape flow cells for pumping and recharge conditions similar to those that occurred in the basin from predevelopment flow conditions (assumed to have ended in 1950) to 1989, and for those anticipated to occur from 1989 to 2020. Possible reasons for the small displacement of the interface for the increased pumping and recharge rates are that (1) most pumping in the flow cells is more than 1 mi inland of the coasts and from the ground-water-flow system at depths less than 70 ft below sea level; (2) a large percentage of water withdrawn from the ground-water-flow system is returned through wastewater return flow from septic systems and at wastewater-treatment facilities and there is little consumptive use of the pumped water; (3) much of the wastewater return flow from septic systems is near the coasts.

Increases in pumping in the Truro flow cell also had a negligible effect on the position of the freshwater-saltwater interface except near the three areas of pumping in the cell. The most pronounced effect of pumping on the Truro flow cell occurred in response to a simulated 5-year (30 percent) decrease in natural recharge. The model-calculated water table responded rapidly to the increased stress and recovered quickly afterwards. The model-calculated freshwater-saltwater interface

responded more slowly to the drought stress than the water table, and subsequently recovered more slowly than the water table once the stress was removed.

Transient, three-dimensional, finite-difference models also were developed to simulate freshwater flow in the West Cape, East Cape, Wellfleet, and Eastham flow cells from predevelopment flow conditions to 2020. Locally, areas such as the Mary Dunn Pond in the West Cape flow cell are significantly affected by changes in pumping and recharge conditions. Total average declines in the water table at 32 observation wells in the West Cape flow cell and 19 observation wells in the East Cape flow cell are 1.8 and 2.9 ft, respectively, for the simulation period. Declines in the average water levels of ponds during the simulation period are less than those at observation wells because of the greater storage capacity of the ponds than of the surrounding aquifers. The average depletion in the rate of streamflow at the gaging points of eight of the largest streams in the West Cape and East Cape flow cells simulated in the models in 2020 was 14 percent of the model-calculated predevelopment streamflow in the streams.

Total sources and sinks of fresh water to the West Cape and East Cape flow cells calculated by the models increase from predevelopment flow conditions to 2020 because the total rate of simulated ground-water pumping and wastewater return flow to each system increases with time. The model-calculated source of the increased ground-water pumping from the flow cells is fresh water removed from storage in the flow cells and decreased rates of freshwater discharge to streams and saltwater boundaries of the flow cells. Sources and sinks of water to the Eastham and Wellfleet flow cells have not changed and are not projected to change significantly with time because there is no large-scale pumping in the flow cells for public supply.

The effects of fluctuations in seasonal pumping and recharge rates for 1989 stress conditions were determined for long-term average recharge rates and for a hypothetical, simulated 5-year (30 percent) decrease in natural recharge. Simulated seasonal fluctuations in stresses resulted in a model-calculated 2.0 and 1.7 ft average range in water-table altitudes at the observation wells for the West Cape and East Cape flow cells, respectively. Model-calculated fluctuations were

greatest near the top of the ground-water mounds and least near the coast where water levels are held nearly constant because of the ocean discharge boundary.

Numerical models developed for the Cape Cod Basin ground-water-flow cells provide information regarding regional-scale characteristic of the hydrology of the flow cells, including regional movement of the interface separating the freshwater- and saltwater-flow systems. Although detailed analyses of local hydrologic conditions were beyond the scope of the investigation, the flow models may serve as starting points for more detailed investigations of smaller areas of the flow cells. The results of the simulations are limited by the availability and accuracy of data on the hydraulic properties of the flow cells and streambeds; by the discretization of the models, which affects the representation of the geologic framework of the aquifer, of pumping wells, and of boundary conditions of the aquifers; and by the accuracy of available data and the temporal discretization of pumping and recharge stresses on the system.

Martha's Vineyard Basin consists of more than 600 ft of Cretaceous- and Tertiary-aged coastal-plain deposits that overlie crystalline bedrock and are mantled by Pleistocene glacial formations. The principal flow system of Martha's Vineyard consists of a primary and a secondary aquifer, both of which consist of glacial deposits within the upper 160 ft of saturated material.

Nantucket Island Basin consists of nearly 1,500 ft of Cretaceous- and Tertiary-aged coastal-plain deposits overlying crystalline bedrock. The coastal-plain deposits are mantled by 150 to 250 ft of sand and gravel deposited by Pleistocene-aged glaciers. The hydrologic system of Nantucket Island can be divided into a shallow and a deep aquifer. The upper 250 ft of sand and gravel outwash deposits of the shallow aquifer comprises the principal flow system. The thick wedge of fine sand, silt, and clay of the underlying coastal-plain deposits contain the deeper flow system, which is poorly understood. A wide range of hydraulic conductivity values for the coastal-plain deposits that are generally much lower than the overlying glacial deposits has been reported.

Martha's Vineyard and Nantucket Island Basins are surrounded by salt water that forms the outer boundary of the fresh ground-water-flow systems. Precipitation is the sole source of natural recharge to the basins. Precipitation recharge to the flow systems is estimated to be 22 in/yr in the Martha's Vineyard Basin and



19 in/yr in the Nantucket Island Basin. Ground water is the principal source of drinking water for the residents of Martha's Vineyard and Nantucket Island Basins.

Simulated effects of ground-water pumping on Martha's Vineyard and Nantucket Island Basins were analyzed by use of uncalibrated, two-dimensional, finite-difference flow models that do not calculate absolute ground-water levels. These simple flow models, called change models, were used to calculate the change in water-table altitude resulting from changes in pumping rates in the two basins. They were used because there was insufficient data available for the basins to construct three-dimensional, calibrated flow models: (1) the change models were used to calculate changes in the altitude of the water table in each basin resulting from 180 days of pumping at projected maximum (in-season) pumping rates for 2020, with no aquifer recharge, (2) calculated changes were largest at the pumping centers. The largest declines in the altitude of the water table for the Martha's Vineyard Basin were 2.7 ft near the proposed Manter site in Tisbury. The largest declines for the Nantucket Island Basin were 1.6 ft near the proposed Wannacommet well. The results of simulations made with the change models provide a preliminary estimate of the effects of ground-water pumping to the flow systems.

## REFERENCES CITED

- Barlow, P.M., 1989, Determination of aquifer properties from a thermal tracer experiment: EOS, v. 70, no. 15, p. 327.
- , 1994, Particle-tracking analysis of contributing areas of public-supply wells in simple and complex flow systems, Cape Cod, Massachusetts: U.S. Geological Survey Open-File Report 93-159, 68 p.
- Barlow, P.M. and Hess, K.M., 1993, Simulated hydrologic responses of the Quashnet River stream-aquifer system to proposed ground-water withdrawals: U.S. Geological Survey Water-Resources Investigations Report 93-4064, 52 p.
- Cape Cod Planning and Economic Development Commission, 1989, Truro/Provincetown aquifer assessment and ground-water protection plan: Barnstable, Mass., 65 p.
- Delaney, D.F., 1980, Water resources of Martha's Vineyard, Massachusetts: U.S. Geological Survey Hydrological Investigations Atlas 618, 2 plates.
- Dufresne-Henry, Inc., 1990, Report on prolonged pump test, well no. 4, Highwood Water Company, Mashpee, Massachusetts: Westford, Mass., 29 p.
- Essaid, H.I., 1990, The computer model SHARP, a quasi-three-dimensional finite-difference model to simulate freshwater and saltwater flow in layered coastal aquifer systems: U.S. Geological Survey Water-Resources Investigations Report 90-4130, 181 p.
- Farnsworth, R.K., Thompson, E.S., and Peck, E.L., 1982, Evaporation atlas for the contiguous 48 states: National Oceanic and Atmospheric Administration Technical Report NWS 33, 26 p.
- Garabedian, S.P., Gelhar, L.W., and Celia, M.A., 1988, Large-scale dispersive transport in aquifers: field experiments and reactive transport theory: Cambridge, Mass., Massachusetts Institute of Technology, Department of Civil Engineering, Ralph M. Parsons Laboratory Report 315, 290 p.
- Getzen, R.T., 1977, Analog-model analysis of regional three-dimensional flow in the ground-water reservoir of Long Island, New York: U.S. Geological Survey Professional Paper 708, 70 p.
- Guswa, J.H., and LeBlanc, D.R., 1985, Digital flow models of ground-water flow in the Cape Cod aquifer system, Massachusetts: U.S. Geological Survey Water-Supply Paper 2209, 112 p.
- Guswa, J.H., and Londquist, C.J., 1976, Potential for development of ground water at a test site near Truro, Massachusetts: U.S. Geological Survey Open-File Report 76-614, 22 p.
- Horsley Witten Hegemann, Inc., 1990, Nantucket water resources management plan: Barnstable, Mass. 147 p.
- Johnson, D.G., 1990, Use of ground-penetrating radar for water-table mapping, Brewster and Harwich, Massachusetts: U.S. Geological Survey Water-Resources Investigations Report 90-4086, 27 p.
- Kohout, F. A., Hathaway, J. C., Folger, D. W., Bothner, M. A., Walker, E. H., Delaney, D. F., Frimpter, M. H., Weed, E.G., and Rhodehamel, E. C., 1977, Fresh ground-water stored in aquifers under the continental shelf, implications from a deep test, Nantucket Island, Massachusetts: Water Resources Bulletin, v. 13, no. 2, p. 373-386.
- Kruseman, G.P., and de Ridder, N.A., 1983, Analysis and evaluation of pump test data: Bulletin 11, International Institute for Land Reclamation and Improvement, The Netherlands, p.104-107.
- LeBlanc, D.R., 1982, Potential hydrologic impacts of ground-water withdrawals from Cape Cod National Seashore, Truro, Massachusetts: U.S. Geological Survey Open-File Report 82-438, 62 p.

- LeBlanc, D.R., 1984a, Digital modeling of solute transport in a plume of sewage-contaminated ground water, *in* LeBlanc, D.R., ed., Movement and fate of solutes in a plume of sewage-contaminated ground water, Cape Cod, Massachusetts: U. S. Geological Survey Toxic Waste Ground-Water Contamination Program: U.S. Geological Survey Open-File Report 84-475, p. 11-45.
- \_\_\_\_\_, 1984b, Sewage plume in a sand and gravel aquifer, Cape Cod, Massachusetts: U.S. Geological Survey Water-Supply Paper 2218, 28 p.
- LeBlanc, D.R., Garabedian, S.P., Quadri, R.D., Morin, R.H., Teasdale, W.E., and Paillet, F.L., 1988, Hydrogeologic controls on solute transport in a plume of sewage-contaminated ground water, *in* Ragone, S.E., ed., Proceedings of the second technical meeting, Cape Cod, Massachusetts, October 21-25, 1985, U.S. Geological Survey Program on Toxic Waste—Ground-Water Contamination: U.S. Geological Survey Open-File Report 86-481, p. B-7 to B-12.
- LeBlanc, D.R., Guswa, J.H., Frimpter, M.H., and Londquist C.J., 1986, Ground-water resources of Cape Cod, Massachusetts: U.S. Geological Survey Hydrological Investigations Atlas 692, 4 pls.
- Letty, D.F., 1984, Ground water and pond levels, Cape Cod, Massachusetts, 1950-1982: U.S. Geological Survey Open-File Report 84-719, 81 p.
- Lindner, J.B., and Reilly, T.E., 1983, Analysis of three tests of the unconfined aquifer in Southern Nassau County, Long Island, New York: U.S. Geological Survey Water-Resources Investigations Report 82-4021, 46 p.
- Marsily, Ghislain de, 1986, Quantitative hydrogeology: Orlando Fla., Academic Press, 440 p.
- McCann, J.A., 1969, An inventory of the ponds, lakes, and reservoirs of Massachusetts, Barnstable County: Amherst, Mass., Water Resources Research Center, 102 p.
- McDonald, M.G., and Harbaugh, A.W., 1988, A modular three-dimensional finite-difference ground-water-flow model: U.S. Geological Survey Techniques of Water-Resources Investigations, book 6, chap. A1, 586 p.
- Metcalf and Eddy, Inc., 1972, Comprehensive water and sewerage plan for Martha's Vineyard: Wakefield, Mass., 120 p.
- Neuman, S.P., 1974, Effect of partial penetration on flow in unconfined aquifers considering delayed gravity response: Water Resources Research, v. 10, no. 2, p. 303-312.
- Oldale, R.N., 1969, Seismic investigations on Cape Cod, Martha's Vineyard, and Nantucket, Massachusetts, and a topographic map of the basement surface from Cape Cod Bay to the Islands, *in* Geological Survey Research 1969: U.S. Geological Survey Professional Paper 650-B, p. B122-B127.
- Oldale, R.N., 1984, Glaciotectonic origin of the Massachusetts coastal end moraines and a fluctuating late Wisconsinan ice margin: Geological Society of America Bulletin, v. 95, p. 61-74.
- Oldale, R.N., and Barlow, R.A., 1986, Geologic map of Cape Cod and the Islands, Massachusetts: U.S. Geological Survey Miscellaneous Investigations Series Map I-1763, 1 plate, scale 1:100,000.
- Palmer, C.D., 1977, Hydrogeologic implications of various wastewater management proposals for the Falmouth area of Cape Cod, Massachusetts: Woods Hole Oceanographic Institution Technical Report WHOI-77-32 (Appendix), 142 p.
- Perlmutter, N.M., and Geraghty, J.J., 1963, Geology and ground-water conditions in southern Nassau and southern Queens Counties, Long Island, New York: U.S. Geological Survey Water-Supply Paper 1613-A, 205 p.
- Perlmutter, N.M., and Lieber, Maxim, 1970, Dispersal of plating wastes and sewage contaminants in ground water and surface water, South Farmingdale-Massapequa area, Nassau County, New York: U.S. Geological Survey Water-Supply Paper 1879-G, 67 p.
- Reilly, T.E., Franke, O.L., and Bennett, G.D., 1987, The principle of superposition and its application in ground-water hydraulics: U.S. Geological Survey Techniques of Water-Resources Investigations, Book 3, Chapter B6, 28 p.
- Ryan, B.J., 1980, Cape Cod Aquifer, Cape Cod, Massachusetts: U.S. Geological Survey Water-Resources Investigations Report 80-571, 23 p.
- Socolow, R.S., Gadoury, R.A., Ramsbey, L.R., and Bell, R.W., 1991, Water resources data—Massachusetts and Rhode Island, water year 1990: U.S. Geological Survey Water-Data Report MA-RI-90-1, 260 p.
- Strahler, A.N., 1972, The environmental impact of ground-water use on Cape Cod, Impact Study III: Orleans, Massachusetts, Association for the Preservation of Cape Cod, 68 p.
- Thornthwaite, C.W., and Mather, J.R., 1957, Instructions and tables for computing potential evapotranspiration and the water balance: Centerton, N. J., Drexel Institute of Technology, Publications in Climatology, v. 10, no. 3, 331 p.
- Trescott, P.C., 1975, Documentation of finite-difference model for simulation of three-dimensional ground-water flow: U.S. Geological Survey Open-File Report 75-438, 30 p.
- Walker, E.H., 1980, Water resources of Nantucket Island, Massachusetts: U.S. Geological Survey Hydrologic Investigations Atlas 615, 2 pls.
- Wolf, S.H., 1988, Spatial variability of hydraulic conductivity in a sand and gravel aquifer: Cambridge, Mass., Massachusetts Institute of Technology, unpublished Engineers thesis, 118 p.









# United States Department of the Interior



GEOLOGICAL SURVEY  
Water Resources Division  
Massachusetts-Rhode Island District  
28 Lord Road, Suite 280  
Marlborough, MA 01752  
Tel. (508) 485-6360  
Fax (508) 490-5068

January 27, 1995

JAN 30 1995

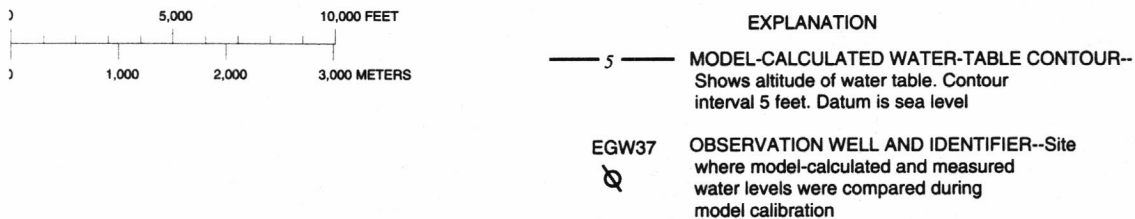
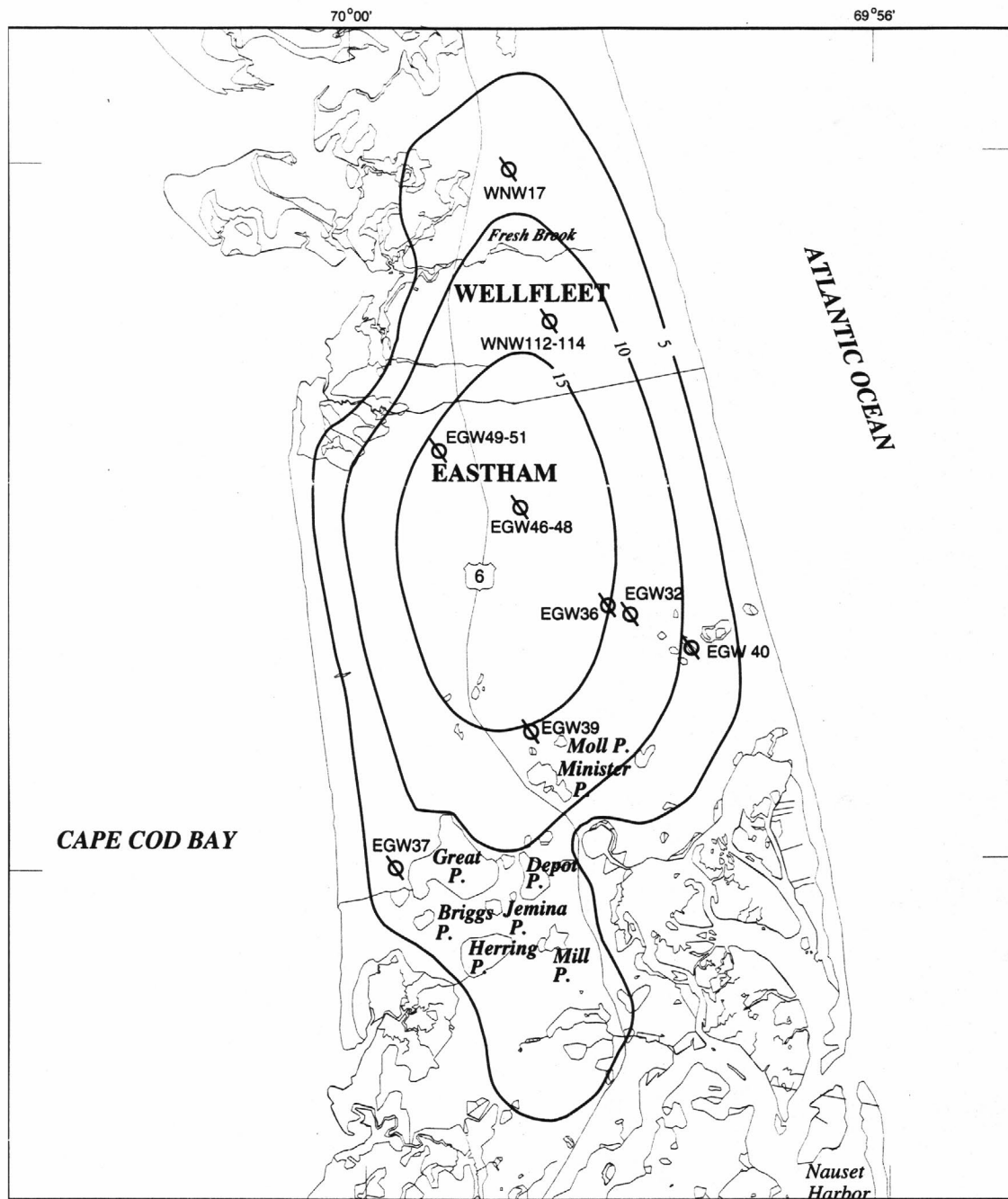
## ERRATA SHEET

Two errors were found in figure 30, page 69, of the recently published report, "Effects of simulated ground-water pumping and recharge on ground-water flow in Cape Cod, Martha's Vineyard, and Nantucket Island Basins, Massachusetts," by J.P. Masterson and P.M. Barlow (U.S. Geological Survey Open-File Report 94-316). The revised figure was done at the same scale as the report illustration and can be pasted into your report copy. The following corrections have been made:

- The contour interval has been changed from 2 ft to 5 ft.
- The locations of wells EGW49-51 and EGW32 have been corrected.

Enclosure





re 30. Model-calculated steady-state water-table configuration for the Eastham flow Cape Cod Basin, Massachusetts.

